Tu-Pos91

DILTIAZEM BLOCKS CONTRACTION AND DEPOLARIZATION INDUCED RELEASE OF RAPIDLY EXCHANGING Ca IN FROG SKELETAL MUSCLE.

((Brian A. Curtis)) Univ of Illinois College of Medicine at Peoria, Peoria, IL 61656

Diltiazem, (1μM) 5 min before and during a ^{45}Ca 190 K^+ contracture, reduced: tension (T) to 84±5 %, time-tension index (t-T) to 53±6% of control and Ca influx into Ca_{slow} from 3.9 to 3.2 pmol Ca. One hr later, (T) was reduced to 33±6%, (t-T) to 17±5% and Ca influx to 1.06 pmol Ca (resting). Like D600, Diltiazem uncouples depolarization and contraction but unlike D600, it also blocks voltage gated Ca entry and is effective during the first contracture. Diltiazem (as much as 10 μM) in ^{45}Ca repriming solution did not alter refilling the Ca_{fast} compartment. 1 μM Diltiazem during repriming reduced the subsequent contracture (T) to 62±6% and (t-T) to 44±7%; Ca_{fast} emptied only partially and $Ca_{transfer}$ was reduced. 10 μM Diltiazem during repriming blocked subsequent contraction and Ca_{fast} did not empty as it does when depolarization is linked to contraction. Diltiazem blocked tension development, $Ca_{transfer}$ and depolarization induced release of ^{45}Ca from Ca_{fast}. I suggest Ca_{fast} represents Ca known to be bound to the DHP receptor : Ca channel : e-c coupling voltage sensor moiety of the transverse tubular membrane (6-10 pmol Ca/fiber).

Supported by American Heart Association, Illinois Affiliate

Tu-Pos92

ACTION OF AMINOPHYLLINE ON CALCIUM CURRENT AND CONTRACTION OF MAMMALIAN SKELETAL MUSCLE FIBERS.

((Osvaldo Delbono, Adriana S. Losavio and Basilio A. Kotsias)). Dept. of Molecular Physiology and Biophysics, Baylor College of Medicine, Houston, TX and Inst. Inv. Médicas A. Lanari, Universidad de Buenos Aires, Argentina.

Twitches and K contractures were measured in the extensor digitorum longus muscle (EDL) of the rat and calcium currents (ICa) were recorded in single isolated cut fibers with the double Vaseline gap technique in in vitro conditions. The objective of this project was to determine the importance of the inward calcium current in the potentiating effect of aminophylline.

In 0.1mM aminophylline the mechanical activity was increased in comparison with the control values. The ICa currents were not affected by 0.1 nM aminophylline; with 1 mM of the drug the ICa amplitude significantly increased in the potential range of -20 and 20 mV with no modifications in the activation and inactivation time constants and in the charge movements: at 0 mV the maximum peak currents were (uA/uF): Control: -6.8 + 1.1 1 mM aminophylline: -8.1 + 1.6 (SD, n=6).

We suggested that the potentiating action of aminophylline is not related to an inward calcium current; the shift in the contraction threshold toward more negative values of the Vm promoted by aminophylline may play a role in the mechanism of action of this compound.

Tu-Pos93

PURIFICATION OF TWO ACTIVATOR AND TWO INHIBITOR PEPTIDES FROM BUTHOTUS SCORPION VENOM SPECIFIC FOR RYANODINE RECEPTORS.

((Jeffery Morrissette and Roberto Coronado)) Department of Physiology, University of Wisconsin, Madison, WI. 53706.

We previously reported purification through reverse-phase HPLC of a ~7 kDa activator peptide ($Buth_A$-1) from the venom of the scorpion *Buthotus hottentota*. $Buth_A$-1 specifically stimulated [^{3}H]ryanodine binding to ryanodine receptors of skeletal muscle with an ED_{50} of .5μg/ml (Biophysical Journal 61:A25). We now report the purification of an additional ~11 kDa activator peptide ($Buth_A$-2) that also stimulates [^{3}H]ryanodine binding to skeletal muscle ryanodine receptors with an ED_{50} of 10μg/ml. Two ~13 kDa inhibitor peptides ($Buth_I$-1 and $Buth_I$-2) were also purified, and found to inhibit [^{3}H]ryanodine binding with an ID_{50} of 390μg/ml and 90μg/ml respectively. Both of the activator peptides are able to release Ca^{2+} from heavy sarcoplasmic reticulum (HSR) vesicles as indicated by a shift in the flouresecence excitation spectrum of the Ca^{2+} indicator dye fura-2 from 380nm to 340nm. In contrast, the two inhibitor peptides are able to completely block the caffeine induced Ca^{2+} release from HSR vesicles in similar fura-2 studies. In addition, $Buth_A$-1 opens ryanodine receptor Ca^{2+} release channels incorporated into planar bilayers, whereas $Buth_I$-1 closes Ca^{2+} release channels. The four peptides were determined to be specific for the ryanodine receptor by their inability to effect the binding of [^{3}H]PN200-110, [^{3}H]IP_3, and [^{3}H]saxitoxin to skeletal muscle microsomes. The molecular characterization of these four peptides should prove useful in the understanding of the gating mechanisms of the ryanodine receptor Ca^{2+} release channel. (Supported by NIH, AHA, and MDJ)

Tu-Pos94

INHIBITION OF THE RYANODINE RECEPTOR CALCIUM RELEASE CHANNEL BY MEXICAN BEADED LIZARD VENOM.

((R. El-Hayek, J. Morrissette, R. Coronado, and L. Possani[#])) Department of Physiology, University of Wisconsin Medical School, Madison, WI 53706 and # Departamento de Bioquímica, Instituto de Biotecnologia, UNAM, Cuernavaca, Mexico.

Venom from *Heloderma horridum horridum* (Mexican beaded lizard) inhibited [^{3}H]ryanodine binding to ryanodine receptors from skeletal muscle, heart, and brain microsomes and inhibited the Ca^{2+} release channels fused into planar bilayers. In a standard assay containing 0.5 M KCl, 10 mM Na-PIPES, pH 7.2, 10 μM Ca^{2+}, and 10 nM [^{3}H]ryanodine, the venom had an IC_{50} ≈ 10 μg/ml. The effect of the venom was more pronounced in CHAPS-solubilized receptors than in native membranes. Decreased [^{3}H]ryanodine binding activity was observed at all [Ca^{2+}]. The venom was partially purified by reverse phase HPLC and at least 2 distinct inhibitory fractions were recovered. Mochca-Morales et al purified helothermine, a polypeptide component of the venom with an apparent mol. wt. of 25,500 (Toxicon, 1990, 28 (3); 299-309). Helothermine inhibited the ryanodine receptor calcium release channel with an IC_{50} ≈ 30 nM without affecting [^{3}H]PN200-110 binding. Phospholipase A_2, known to be present in this venom, could not account for the inhibitory effect of the venom. These findings suggest that the *Heloderma* venom contains polypeptide toxins capable of blocking the ryanodine receptor. The biochemical characterization of these peptides may be helpful in further studying the properties of the ryanodine receptor calcium release channel and in establishing its role in excitation-contraction coupling. (Supported by NIH, MDA, AHA., and HHMI)

Tu-Pos95

LONG-CHAIN ACYL CARNITINE AND ACYL COENZYME-A INCREASE THE SARCOPLASMIC RETICULUM Ca^{2+} PERMEABILITY BY OPENING RYANODINE RECEPTORS.

((R. El-Hayek, C. Valdivia, K. Hogan and R. Coronado)) Departments of Physiology and Anesthesiology. University of Wisconsin Medical School, Madison, WI 53706.

Long-chain acyl carnitine (C_{14}, C_{16}, C_{18}) and acyl CoA (C_{12}, C_{14}, C_{16}) in the range of 5 to 50 μM induced a massive release of $^{45}Ca^{2+}$ passively loaded in rabbit junctional SR. In rapid filtration experiments, release was dose-dependent, occured in nanomolar free Ca^{2+} plus 5 mM Mg^{2+}, proceeded with a lag of ~100 ms, and was partially blocked by neomycin (1mM) and ruthenium red (20μM). Neither 50 μM free fatty acid of chain length C_8 to C_{18}, free carnitine, nor free CoA, at room temperature or 36 °C, could release SR $^{45}Ca^{2+}$. There was a close correspondence between the increase in open ryanodine receptor probability induced by palmitoylcarnitine in planar bilayer recordings and the release of SR $^{45}Ca^{2+}$ suggesting that the lipid activation of the release channel could account for the increase in SR Ca^{2+} permeability. Palmitoylcarnitine and palmitoyl CoA also stimulated [^{3}H]ryanodine binding in the same concentration range as in single channel recordings and $^{45}Ca^{2+}$ fluxes suggesting a direct interaction of the acyl-metabolite with the ryanodine receptor. This newly identified lipid-ryanodine receptor interaction provides a mechanism by which muscle metabolism could influence intracellular Ca^{2+}, and may underlie the pathophysiology of disorders of β-oxidation such as carnitine palmitoyltransferase II deficiency. We propose that long-chain acyl carnitine accumulation in CPT II deficiency under conditions of increased metabolic demand leads to a severe increase in SR Ca^{2+} permeability and consequent muscle destruction by Ca^{2+} toxicity. (Supported by NIH, MDA, and AHA.)

Tu-Pos96

A SCORPION VENOM THAT ACTIVATES NORMAL AND INHIBITS MALIGNANT HYPERTHERMIA SUSCEPTIBLE PIG AND HUMAN RYANODINE RECEPTORS.

((K. Hogan, H. Valdivia, R. El-Hayek, D. Wedel, and R. Coronado)) University of Wisconsin, Madison, WI 53792

The venom of the scorpion *Buthotus hottentota* selectively increases [^{3}H]ryanodine binding and the mean open probability of ryanodine receptors (RYR1) from rabbit skeletal muscle (J Biol Chem;166:29:19135-19138, 1991). The main effect of the venom is to increase Bmax indicating a noncompetitive interaction with the binding site. Because RYR1 radioligand binding characteristics and single channel gating properties are altered in malignant hyperthermia (MH), we compared the effect of the scorpion venom on RYR1 isolated from normal and MH pig and human skeletal muscle. Methods. SR vesicles were isolated from 6 normal and 6 MH pigs by a modified microsome fractionation procedure, solubilized in 1% CHAPS, and [^{3}H]ryanodine binding assays carried out for 90 min at 36 °C in the presence and absence of 0-500 ug/ml venom (Latoxan, Rosans, FR). Porcine RYR1 were reconstituted in planar lipid bilayers using standard techniques. Muscle samples from 8 MH and 4 normal humans were homogenized in 0.3 M sucrose, 20 mM Hepes/pH 7.2 and solubilized in 1% CHAPS. Binding assay conditions were identical for the human and porcine RYR1. Results. *Buthotus* venom enhanced binding in normal porcine receptors 2.6 fold and increased Po from 0.21±0.05 to 0.48±0.08. In MH RYR1 the venom decreased [^{3}H]ryanodine binding by 60%, and inhibited Po from 0.19±0.04 to 0.06±0.02. In 7 of 8 MH humans venom inhibited binding by 75%. Binding was activated 2.8 fold in 3 of 4 normal individuals. The differential effect of *Buthotus* venom on MH muscle demonstrates that the MH RYR1 has a structurally altered gating domain which may be responsible for the hypersensitivity of the channel to Ca^{2+}, caffeine and halothane. (Supported by NIH, MDA and VA.)

Tu-Pos97

1,10-BIS-GUANIDINO-N-DECANE DIHYDROCHLORIDE (BISG10) BLOCKS THE CALCIUM RELEASE CHANNEL OF SKELETAL MUSCLE SARCOPLASMIC RETICULUM

((Le Xu and Gerhard Meissner)) Department of Biochemistry and Biophysics, University of North Carolina, Chapel Hill, NC27599-7260

The effects of BisG10, a blocker of the sarcoplasmic reticulum (SR) K^+ channel (Liu et al., 1992, Biophys J 61, 379a), on the ryanodine-sensitive Ca^{2+} release channel of rabbit skeletal muscle were examined by reconstituting the Chaps-solubilized, purified 30 S channel complex into planar lipid bilayers in a symmetric 0.25 M KCl medium. We found that addition of BisG10 to the trans (SR lumenal) but not to the cis (SR cytoplasmic) side of the bilayer reduced single channel K^+ currents at negative holding potentials. Block of Ca^{2+} release channel by BisG10 was weakly voltage-dependent and could be described by blocking (k_b), unblocking (k_{-b}) rates and dissociation constant (K_D) of 0.6 μM^{-1} ms^{-1}, 6 ms^{-1} and 10 μM, respectively.

Tu-Pos98

ENDOGENOUS SPHINGOSINE CONTROLS CARDIAC SR CA RELEASE.

((R. Betto, G. Salviati, C. Dettbarn, P. Palade, G. Jenkins and R. Sabbadini)) Institute of General Pathology, University of Padova Italy, Dept. of Physiology and Biophysics University of Texas Med. Branch, Galveston TX 77550, Dept. of Biology San Diego State University San Diego CA 92182.

Excitation contraction (EC) coupling involves the movement of calcium (Ca) through the Ca release channel of the sarcoplasmic reticulum (SR) membrane known as the ryanodine receptor (RyR). We have recently shown that the novel second messenger, sphingosine (SPH), can block Ca release from skinned skeletal muscle fibers and from isolated skeletal muscle SR membranes (Sabbadini et al., JBC 267:15475-15484, 1992). In this report, we demonstrate that SPH not only causes a significant reduction of cardiac myocyte beating behavior, but also inhibits Ca release from isolated canine cardiac SR membranes in the presence of APIII and PPi when release was induced by caffeine, doxorubicin or by Ca. SPH also prevents the augmentation of [3H]-ryanodine binding normally produced by caffeine, doxorubicin and Ca, which is consistent with a blocking action of SPH on the RyR Ca channel. SPH inhibits the extent of Ca-induced Ca release (CICR) and significantly shifts the threshold for CICR so that a higher level of trigger Ca is required to initiate CICR. HPLC analysis of cardiac SPH levels indicates that SPH is present in the cardiac cell at the same levels that would produce inhibition of Ca release. We hypothesize that sphingosine acts on the cardiac RyR by opposing the physiological stimulus (e.g. trigger Ca entering via the DHP receptor). We also propose that SPH is produced by the T-tubule membranes and that SPH is released into the protected intracellular environment of the T-tubule/SR junction to negatively modulate Ca release. Consequently, we propose that SPH could be a physiologically relevant regulator of Ca levels in the heart. Supported by NIH #HL42527 and from the CNR and Minestero della Pubblica Istruzione of Italy.

Tu-Pos99

CARDIAC SARCOPLASMIC RETICULUM CA RELEASE CHANNELS ARE ACTIVATED BY HALOTHANE, BUT NOT BY ISOFLURANE

((M. J. Frazer, C. Lynch III)) Department of Anesthesiology, Box 238, University of Virginia Health Sciences Center, Charlottesville, Virginia 22908

Canine ventricle was homogenized, centrifuged differentially on a sucrose gradient. Sarcoplasmic reticulum(SR) membrane vesicles enriched with Ca release channels (CaRCs) was defined by: 1. electrophoretic evidence of a ~450 kD protein consistent with CaRC; 2. > 5-fold enhancement of vesicular $^{45}Ca^{2+}$ uptake by ruthenium red (RR), which specifically blocks the CaRC and Ca efflux; 3. Ca-activated ^{3}H-ryanodine (RY) binding. Binding studies were performed in 25 mM Pipes (pH 7.4), 100 μM PMSF, 100 mM or 1M KCl, and 10 nM to 1 mM Ca^{2+} with an incubation time of 90 min at 37°C. Specific ^{3}H-RY binding, indicative of channel opening and activated by >0.5 μM Ca^{2+}, was maximal with ≥20 μM Ca^{2+} at 10-11 pmole RY/mg protein. Anesthetic enhancement of binding was studied at 5 μM Ca^{2+} where RY bound was 3-5 pmole/mg protein. [RY] from 5 nM-2 μM were used. In 1 M KCl medium, 0.75-1.5% halothane (H) enhanced ^{3}H-RY binding, while 2.5% isoflurane and 3.5% enflurane had no effect. A plot of bound/free vs. bound RY revealed a modest if any increase in binding affinity due to halothane, but rather a dose-dependent increase in the number of CaRCs which were opened and bound RY. Enhancement of RY binding by H was also present in 100 mM KCl. These results provide a molecular basis for the differing action of H and isoflurane on myocardial function. Increased RY binding in the presence of halothane corresponds to more open CaRCs and enhanced Ca^{2+} loss from SR, leaving less accumulated Ca^{2+} for release to activate contractions.
(Supported by NIH grant GM31144)

Tu-Pos100

DIFFERENT CALCIUM SENSITIVITY OF CALCIUM CHANNELS OF SARCOPLASMIC RETICULUM (SR) FROM FROG SKELETAL MUSCLE.

((R.Bull and J.J.Marengo)). Dept. Fisiología y Biofísica, Fac. Medicina, Univ. de Chile. Casilla 70005, Santiago 7, Chile. (Spon. by C.Hidalgo)

We have investigated the Ca^{2+} dependence of fractional open time (P_o) of calcium release channels of SR from frog skeletal muscle fused in bilayers. Two types of Ca^{2+} dependence were found: a) 25 out of 34 single channel experiments displayed a bell-shaped Ca^{2+} dependence with activation at micromolar concentrations and inhibition at millimolar concentrations. Maximal activation was achieved with 30 μM free Ca^{2+} (P_o=0.45±0.06; mean±S.E.M.). Data were fitted with an activation constant of 16 μM and an inhibition constant of 68 μM. Blocking effect was evident at 0.5 mM Ca^{2+} (P_o=0.218±0.03). b) 9 out of 34 channels displayed a sigmoidal Ca^{2+} dependence. No blocking effect was seen with Ca^{2+} up to 0.5 mM (P_o=0.74±0.05). Data were fitted with a Hill equation, obtaining an activation constant of 0.95 μM and a Hill coefficient of 2.4. Both blockable and non-blockable channels displayed low degrees of activation at resting levels of Ca^{2+} (0.1 μM) (P_o of 0.01 ± 0.01 and 0.08 ± 0.04, respectively; N.S.). However, a very significant difference was found at 3 μM Ca^{2+} (P_o of 0.18±0.02 and 0.71±0.05; $p<0.001$). Differences in Ca^{2+} sensitivity may correspond to the presence of two different types of calcium channels in frog SR. Alternatively, it could be the expression of two modes of activation by Ca^{2+} of only one population of channels. Supported by FONDECYT 1298-90.

Tu-Pos101

PHOSPHORYLATION OF THE SKELETAL MUSCLE CALCIUM RELEASE CHANNEL REMOVES BLOCK BY MAGNESIUM IONS.

((J.Hain+, H.Schindler+, S.Nath$, Sidney Fleischer$)) +:Biophysics, Univ. Linz, A-4040 Linz, Austria; $:Molec. Biol., Vanderbilt Univ., Nashville, TN 37235.

We investigated the paradox that reconstituted calcium release channels (CRC) are generally blocked by Mg at concentrations prevailing in the myoplasm. Typical CRC activity (after fusion of purified skeletal muscle microsomes to black lipid membranes) was abolished by 3mM Mg. Using a microdispensor, we applied about 1µl solution containing catalytic subunit of protein kinase A (PKA, kindly provided by J. Corbin) or calcium/calmodulin dependent kinase (CCPK, kindly provided by H. Schulman and T. Soderling) for a few minutes directly to the membrane. In most experiments, in 22 out of 25 using PKA and in 11 out of 15 using CCPK, CRC activity was recovered. Then application of protein phosphatase 1 (kindly provided by E. Lee) or potato phosphatase, reinstalled the block by Mg, which cyclically could be removed again by the protein kinases (see traces below). Activity of phosphorylated CRC with Mg present required ATP (0,5 mM used) at about 0,2 µM free Ca. Thus, Mg blocks the dephosphorylated CRC, while phosphorylation reverses the Mg block. We, therefore, propose that phosphorylation of skeletal muscle CRC is used *in vivo* for on/off regulation, and under some conditions may be fine-tuned by the ATP level. Supported by grant S45/07 of the Austrian Res. Fonds (H.S.), NIH HL32711 (S.F.), and NRSA Fellowship (S.N.).

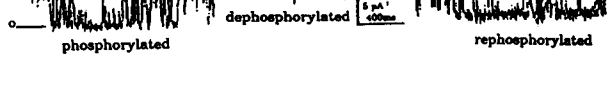

Tu-Pos102

CHARACTERIZATION OF Ca^{2+} RELEASE CHANNELS FROM DENERVATED RATS.

((Osvaldo Delbono*, Enrico Stefani* and Alice Chu+)). Dept. of Molecular Physiology and Biophysics* and Cardiovascular Sciences Section, Dept. of Medicine+, Baylor College of Medicine, Houston, TX 77030.

Faster and larger caffeine contractures have been previously observed after two weeks of denervation. It can be postulated that these changes are developed due to an increased affinity of the Ca^{2+} release channel to Ca^{2+} in the presence of caffeine. We proceeded to incorporate ryanodine-sensitive Ca^{2+} channels from normal and 14-day denervated fast rat muscle sarcoplasmic reticulum (SR) into lipid bilayers (PE:5, PC:3, PS:2), using Ca^+ as current carrier. The solutions contained 275/5 mM (*cis/trans*) $CaCH_3SO_3$ and symmetrical 10 mM HEPES (pH 7.4) and 8-10 µM free Ca^{2+}. The channel conductances for normal and denervated muscles were 503±15 pS and 509±22 pS (n=5) in symmetrical 275 mM Cs^+. Similarly, neither the affinity for [^{3}H]ryanodine nor the site density was changed between normal and denervated rat SR. Caffeine (0.1-5 mM) activation of single channel activity was studied in 10 µM free Ca^{2+}. At lower caffeine concentrations (0.1-0.2 mM), the time integral of the current increased in channels from denervated muscles, e.g., the ratio of the time integral of the current in denervated vs normal was increased to 2.3±0.7 at 0.1 mM caffeine, and was 1.1± 0.4 at 5 mM caffeine (n=10). Without caffeine, the same ratio was 0.5±0.08 in normal vs denervated muscles. Increased caffeine (0.5 mM) sensitivity was also observed in [^{3}H]ryanodine binding of denervated rat SR only; 25±7 fold (n=2) at pCa 5. The P_o-pCa relationship in channels from normal muscles (n=13) was similar to that reported for rabbit muscle, being bell-shaped. In contrast, the channels from denervated muscles (n=13) were not inactivated at higher Ca^{2+} concentrations (pCa 3.5-2). The lack of Ca^{2+} release channel inhibition by Ca^{2+} can explain the sustained and larger caffeine contractures after denervation. Supported by MDA, NIH and AHA-TX affil.

Tu-Pos103

Two Classes of Ca-release Channels in Cardiac Sarcoplasmic Reticulum and Excitation-Contraction Coupling in Heart.

((H. Cheng and W. J. Lederer)). Dept. of Physiology, Univ. of Maryland at Baltimore, School of Medicine, Baltimore, MD 21201.

Two classes of SR Ca-release channels in cardiac myocytes may exist: those in junction sarcoplasmic reticulum (JSR) and those elsewhere (in corbular SR and in longitudinal SR). During normal excitation-contraction (EC) coupling, the JSR channels, which face a restricted subsarcolemmal space, may sense a higher local triggering [Ca] than the other SR channels. Assuming that there are two functionally important classes of Ca-release channels, we have constructed a simple model of EC coupling in heart that provides an integrated explanation of the diverse and occasionally contradictory observations. (1) In response to I_{Ca} or step increases in [Ca] (that may be produced by photorelease of caged Ca), the model predicts families of graded Ca transients. (2) The model can provide an explanation of apparently "high gain" of CICR observed under some experimental conditions and also the "low gain" manifest in graded CICR. (3) The model predicts an SR Ca-release function with a prominent early peak and a sustained release phase that is in good agreement with recent experimental findings. (4) The intriguing observation that early termination of depolarizing voltage steps attenuate the peak Ca attainable is robustly reproduced in model simulation. (5) Deactiving Ca tail current (as may occur on repolarization) can trigger a sizable Ca transient despite the small Ca influx produced by the tail current. (6) Intracellular loading of a Ca chelator is shown in the model to slow down the kinetics of Ca release and to result in a more linear trigger-response relationship. In sum, a simple model of EC coupling in heart that assumes the existence of two classes of Ca-release channels in the SR, can accurately and robustly describe diverse experimental observations.

Tu-Pos104

REGULATION OF THE RYANODINE RECEPTOR/Ca^{2+} RELEASE CHANNEL OF SKELETAL MUSCLE SARCOPLASMIC RETICULUM BY LUMINAL CALCIUM.

((A. Herrmann-Frank)) Dept. of Applied Physiology, Universität Ulm, W-7900 Ulm, FRG

$^{45}Ca^{2+}$ flux and single channel measurements have shown that the Ca^{2+} release channel (CRC) of striated and smooth muscle sarcoplasmic reticulum (SR) is regulated by μM cytoplasmic (cis) Ca^{2+}. It is, however, not known if changes in luminal (trans) Ca^{2+} also affect the channel activity. In the experiments presented here, the isolated ryanodine receptor/Ca^{2+} release channel of rabbit skeletal muscle SR was reconstituted into planar lipid bilayers in the presence of symmetrical K^+-solutions. Using K^+ as the channel conducting ion, we were able to examine the effect of changes in trans Ca^{2+} in the μM to mM range. In the presence of μM cis Ca^{2+} and low [EGTA], the CRC was in a concentration-dependent manner activated and inactivated by trans Ca^{2+}. The inhibiting effect was antagonized by mM cis ATP or caffeine. Since increasing cis [EGTA] shifted the Po - trans Ca^{2+} relationship to higher trans [Ca^{2+}], it is assumed that trans Ca^{2+} is exerting its regulating effects by acting on binding sites accessable from the cytoplasmic site of the channel. These results favour the role of a Ca^{2+}-dependent component in EC-coupling of skeletal muscle.

Tu-Pos105

GATING OF SKELETAL MUSCLE RYANODINE RECEPTOR CHANNELS IN THE PRESENCE OF TRIADIN.

((D.M. Vaughan, H. K. Motoike*, N.R. Brandt*, A.H. Caswell* and R. Coronado.)) Department. of Physiology, University of Wisconsin Medical School, Madison, WI 53706; *Department of Molecular and Cellular Pharmacology, University of Miami School of Medicine, Miami, FL 33101.

We examined the effect of triadin, the dihydropyridine receptor/ryanodine receptor-binding protein, on the single channel activity of the Ca^{2+} release channel. Triads from rabbit skeletal muscle were solubilized in CHAPS and fractionated on hydroxyapatite by a modification of the procedure of Kim et al. (Biochemistry 29:9281, 1990). Fractions eluted in 0 mM KCl, 180 mM KP_i virtually lacked triadin (low triadin), while those eluted in 820 mM KCl, 180 mM KP_i contained triadin (high triadin). Low and high salt fractions retained [^{3}H]ryanodine binding activity (0.2-0.6 pmol/ml). Channels from each preparation were recorded in planar bilayers using standard techniques. The high triadin preparation displayed fewer conductance levels than the low triadin preparation, perhaps due to a regulatory role of triadin on the conductance or to a triadin-dependent difference in the aggregation of proteins. A conductance of 600 pS in cis and trans 820 mM KCl or 150 pS in cis 125 mM Tris(Hepes)$_2$ and trans 50 mM Ba-Hepes (+40 mV reversal potential) was common to both preparations. Channels from the high triadin preparations were more prone to close shortly after a negative voltage step than those from the low triadin preparations. These data suggest triadin changes the gating of the Ca^{2+} release channel in a manner that may be relevant to excitation-contraction coupling. (Supp. by NIH, AHA, and MDA.)

Tu-Pos106

HIGH AFFINITY [^{3}H]PN200-110 AND [^{3}H]RYANODINE BINDING TO RABBIT AND FROG SKELETAL MUSCLE HOMOGENATES.

((A. H. Cohn, K. Anderson, and G. Meissner)). Dept. of Biochemistry & Biophysics, Univ. of North Carolina, Chapel Hill, NC 27599.

In vertebrate skeletal muscle, the voltage-dependent mechanism of sarcoplasmic reticulum (SR) Ca^{2+} release, commonly referred to as excitation-contraction (E-C) coupling, is mediated by several integral membrane proteins located in the T-tubule and SR membranes. A T-tubule dihydropyridine (DHP) receptor which functions as a voltage-sensing molecule, is believed to effect SR Ca^{2+} release through a physical interaction with a SR ryanodine receptor/Ca^{2+} release channel. Scatchard analysis of [^{3}H]PN200-100 and [^{3}H]ryanodine binding to muscle homogenates indicated the presence of high-affinity sites with B_{max} values of 0.34 $\pm$ 0.14 and 0.30 $\pm$ 0.10 pmol/mg protein for rabbit muscle, and 0.09 $\pm$ 0.02 and 0.18 $\pm$ 0.04 pmol/mg protein for frog muscle, respectively. These B_{max} values correspond to a PN200-110/ryanodine binding ratio of 1.07 $\pm$ 0.27 and 0.49 $\pm$ 0.11 for rabbit and frog skeletal muscle, respectively. These results will be compared to measurements with membrane fractions and discussed in relation to our current understanding of the mechanism of E-C coupling in skeletal muscle.

Tu-Pos107

MEMBRANE TOPOLOGY OF THE RABBIT SKELETAL MUSCLE RYANODINE RECEPTOR AS DETERMINED BY SITE DIRECTED ANTIBODIES.

((Ron Grunwald, Robert Sealock, and Gerhard Meissner)) Department of Biochemistry and Biophysics, University of North Carolina, Chapel Hill, NC 27599-7260.

The ryanodine receptor (RyR) is a large (5037 amino acids) integral membrane protein of the sarcoplasmic reticulum (SR) which functions as a calcium release channel. Several folding models based on the deduced amino acid sequence have been proposed which predict as many as 10 membrane spanning segments in the channel forming domain. We have determined the orientation, with respect to the SR membrane, of several regions of the RyR using antibodies directed against the following peptide segments: residues 2804-2930, 4581-4640, 4941-5037. The membrane topology of the targeted epitopes was assessed by determining the relative binding affinity of the antibodies to closed SR vesicles (cytoplasmic-face out) and to vesicles permeabilized with 0.25% CHAPS, 0.25% Triton X-100, or elevated pH (8.5-10.5). Ab(2804-2930) bound with identical affinity to either closed or permeabilized vesicles, confirming the cytoplasmic location of this segment. This antibody also labeled the RyR in unfixed sections of rat skeletal muscle, consistent with an epitope which is exposed *in situ*. Ab(4581-4640) showed no significant binding to closed vesicles but bound well to permeabilized vesicles, supporting a lumenal location for this segment. Ab(4941-5037) bound significantly to closed vesicles, but binding was enhanced upon permeabilization. This confirms that at least part of the C-terminal domain is cytoplasmic, but suggests that some epitopes in this domain may be blocked by interactions which are disrupted by detergent or elevated pH. Ab(4941-5037) was not effective in labeling RyR *in situ*, consistent with blocked epitopes. The topological assignments of these segments are consistent with the topology models based on sequence analysis.

Tu-Pos108

MECHANISMS OF INHIBITION OF [^{3}H]-RYANODINE BINDING TO SKELETAL MUSCLE SARCOPLASMIC RETICULUM MEMBRANES BY NEOMYCIN, RUTHENIUM RED AND Mg^{2+}.

((J.P.Wang, D.H.Needleman, and S.L.Hamilton)) Dept. of Molecular Physiology & Biophysics, Baylor College of Medicine, Houston, TX 77030.

Neomycin, ruthenium red and Mg^{2+} are potent inhibitors of skeletal muscle sarcoplasmic reticulum (SR) Ca^{2+} release. In the present study, the binding of [^{3}H]-ryanodine is used to elucidate the mechanisms of inhibition. [^{3}H]-ryanodine has both high and low affinity binding sites in SR membranes. The inhibition of [^{3}H]-ryanodine binding is complete with Mg^{2+} and ruthenium red, but the inhibition with neomycin is not. Ruthenium red appears to inhibit [^{3}H]-ryanodine binding at both the high and low affinity sites, possibly by binding at the same sites as ryanodine. Neomycin appears to bind at a site distinct from the high-affinity [^{3}H]-ryanodine binding site. Both ruthenium red and neomycin slow the dissociation of [^{3}H]-ryanodine bound to SR membranes. The effect of neomycin on the dissociation of bound [^{3}H]-ryanodine is in the concentration range where it inhibits high affinity binding; the slowing of the dissociation by ruthenium red requires much higher concentrations than required for inhibition of [^{3}H]-ryanodine binding. Mg^{2+} does not slow the dissociation of bound [^{3}H]-ryanodine. Similar to ryanodine, ruthenium red, at concentrations which inhibit low affinity binding to SR membranes, also inhibits [^{3}H]PN200-110 binding to T-tubule membranes. Neomycin has no effect on [^{3}H]PN200-110 binding. A low affinity [^{3}H]-ryanodine binding site has been identified in t-tubule membranes, suggesting the possibly that other proteins can bind [^{3}H]-ryanodine with low affinity.

Tu-Pos109

RYANODINE SENSITIVE AMPLIFICATION OF Ca^{2+} SIGNALS IN SMOOTH MUSCLE CELLS. ((A. Guerrero, M.T. Kirber, J.J. Singer and F.S. Fay)) Dept. of Physiology and Prog. Mol. Med. UMMC. Worcester, MA 01605

We have employed a combination of fura-2 microfluorometry and patch-clamp techniques in single gastric smooth muscle cells to examine the role of ryanodine receptors in the release of calcium from internal stores. Application of 20 mM caffeine increased $[Ca^{2+}]_i$. This elevation was completely inhibited by ryanodine. Increases in internal $[Ca^{2+}]$ due to membrane depolarization strictly required Ca^{2+} influx through voltage operated Ca channels. Membrane depolarization induced increases in $[Ca^{2+}]_i$ were amplified by a ryanodine sensitive mechanism. This ryanodine inhibitable fraction of the $[Ca^{2+}]_i$ rise comprised as much as 50% of the voltage-induced increase in $[Ca^{2+}]_i$. Preliminary data indicate that most of the increase in $[Ca^{2+}]_i$ induced by stretch-activated Ca^{2+} permeable cation channels is also inhibited by ryanodine. These data suggest that calcium-induced calcium release is a general mechanism of amplification of the Ca^{2+} signal from different Ca^{2+} permeable channels in gastric smooth muscle cells.

Tu-Pos110

STOICHIOMETRY OF FK-506 BINDING PROTEIN TO THE RYANODINE RECEPTOR IN SKELETAL MUSCLE TERMINAL CISTERNAE OF SARCOPLASMIC RETICULUM. ((E.A.Freund#, A.P.Timerman#, T.Jayaraman*, G.Wiederrecht+, A.Marks*, and Sidney Fleischer#)). #Dept. Molecular Biology, Vanderbilt University, Nashville, TN 37235; *Brookdale Center for Molecular Biology, Mount Sinai School of Medicine, New York, NY 10029; +Dept. Immunology Research, Merck Research Laboratories, Rahway, NJ 07065.

The immunophilin FK-506 binding protein (FKBP-12) has been found to be associated with the ryanodine receptor of rabbit skeletal muscle terminal cisternae. (J. Biol. Chem. 267, 9474, 1992). We have evaluated the stoichiometry of FKBP to the ryanodine receptor in skeletal muscle terminal cisternae by two different methods: 1) densitometry of Western blot analysis using specific antibody to FKBP-12 and gel densitometry of Coomassie blue stained SDS-PAGE gels for the ryanodine receptor and 2) specific ligand binding of ^{3}[H] FK-816 (dihydropropyl derivative of FK-506) versus ^{3}[H] ryanodine. The stoichiometry is 2.4 to 1 by densitometry compared to 2.2 to 1 by ligand binding. FKBP was found in a sucrose gradient purified fraction of ryanodine receptor at a comparable ratio. The presence of FKBP on the ryanodine receptor has also been detected by Western blot analysis in porcine skeletal muscle terminal cisternae. These data indicate that the tight association of the FKBP with the ryanodine receptor of skeletal muscle may be a general phenomenon. Supported in part by grants from NIH HL32711 and Muscular Dystrophy Assoc. to S.F.

Tu-Pos111

CO-EXPRESSION OF RYANODINE AND DIHYDROPYRIDINE RECEPTORS IS NOT SUFFICIENT TO FORM A JUNCTION ((H. Takekura*, H. Takeshima*, S. Nishimura*, M. Takahashi*, T. Tanabe§, S. Numa*, V. Flockerzi*, F. Hofmann* and C. Franzini-Armstrong#)). *Univ. Penn.; §Kyoto Univ; *Univ. Munchen; #Yale Univ.

Ryanodine (RYR) and dihydropyridine (skDHPR) receptors are located at T-SR junctions (triads) of skeletal muscle and play a key role in e-c coupling. RYRs are the SR calcium release channels and their cytoplasmic domains form the feet, which span the gap between SR and T tubule membranes. skDHPRs are the voltage sensors of e-c coupling, they are located in the transverse tubules, and they probably compose the junctional tetrads. Clones of CHO cells were transformed with plasmids pRRS11 (for RYR); pCAs1 (for skDHPR), pCAS8 (for a card-skel DHPR chimera) and pCaS4; pCAS14; pCAS15 (for α_1, β and γ subunits of DHPRs). Clones RR, SKDHPR, CSK3, RR-SK, RR-CSK3 expressed the two proteins either alone or in combinations. RNA blot hybridizations gave positive results for all components. Immunoblots using monoclonal antibodies IIF7 and IIC12 against skDHPRs (from K.P. Campbell); monoclonal antibody RR1 against RYR and affinity purified antibodies CR2 against a c-terminal peptide of cDHPR confirmed expression of the three major components. The location and functional state of the expressed RYRs and DHPRs were determined by electrophysiology; Fura II signals; immunohistochemistry and electron microscopy. SK and CSK3 clones show calcium currents indicating some insertion of the expressed channels in the surface membrane, but CSK3 currents are much larger (K. Imoto, personal communication). Immunohistochemistry shows intense staining for DHPRs in the perinuclear region. Thus most DHPRs may be trapped in the endoplasmic reticulum (ER). Caffeine induces calcium release in RR cells, showing a functional RYR. In all RR cells, EM and immunohistochemistry show high density of RYR in orderly aggregates on flattened cisternae of the ER. RYR-rich membranes do not form junctions with either surface or other internal membranes in RR-CSK3 and RR-SK clones. Instead, the membranes face each other, forming double arrays of feet. We conclude that components other than RYRs and DHPRs are needed for the formation of triad-like junctions. Supp. by NIH HL15835 to PMI and Jap. Inst Phys. Chem. Res.

Tu-Pos112

ISOLATION OF A COMPLEX OF DIHYDROPYRIDINE RECEPTOR AND RYANODINE RECEPTOR FROM TRIAD JUNCTIONS OF SKELETAL MUSCLE.

((I. Marty[1], M. Robert[1], M. Villaz[1], Y. Lai[2], W.A. Catterall[2] and M. Ronjat[1])) 1 CENG-DBMS-BMC BP 85X F38041, GRENOBLE Cedex FRANCE. 2 Dept. Pharmacology, University of Washington, SEATTLE, WA 98195 USA. (Spon. by S. Crouzy)

The current model for excitation-contraction coupling proposes that a voltage-driven conformational change of the α1-subunit of the dihydropyridine (DHP)-receptor activates calcium release by the ryanodine receptor (RyR) through direct physical interaction.

Triad membrane vesicles showing a high binding capacity for azidopine (12 pmol/mg) as well as for ryanodine (30 pmol/mg) were solubilised in presence of CHAPS. The analysis of the sedimentation profile of solubilised proteins separated on a sucrose gradient shows that a fraction of the α1-subunit of the DHP receptors co-sediments with the 30S RyR. On the other hand, immunoprecipitation of the solubilised proteins with antibodies directed against the RyR, results in a co-precipitation of the RyR and the α1-subunit of DHP receptors. Both receptors were identified by immunoblotting and by specific binding of azidopine or ryanodine. These results demonstrate the existence of a complex involving both RyR and DHP receptor and therefore support the hypothesis of their direct physical interaction in excitation-contraction coupling in skeletal muscle.

Support: Association Française contre les Myopathies (AFM), American Heart Association.

Tu-Pos113

CRYO-ELECTRON MICROSCOPY OF FROZEN-HYDRATED ISOLATED TRIADS AND TERMINAL CISTERNAE FROM SARCOPLASMIC RETICULUM.

((T. Wagenknecht, R. Grassucci, J. Berkowitz, A.P. Timerman, and Sidney Fleischer)) Wadsworth Center for Laboratories & Research, New York State Dept. of Health, Albany, NY 12201 and Department of Molecular Biology, Vanderbilt University, Nashville, TN 37235.

Knowledge of the architecture of the triad junction is essential to understanding the mechanism of excitation-contraction coupling in muscle. Numerous studies by electron microscopy (EM) have not led to a consensus on the locations and configurations of the components comprising the triad, due in part to the limitations of conventional EM which requires dehydration, fixation, contrast enhancement with heavy metals and other treatments that affect preservation of the specimen. We have obviated these treatments by imaging native terminal cisternae vesicles derived from sarcoplasmic reticulum and associations of TC vesicles with transverse tubules (i.e. triads) that are embedded in a thin film of buffer by cryo-EM. Micrographs of TC clearly resolve the major components: calcium ATPase, foot structures (calcium release channels), and internal mass (presumably calcium binding proteins and bound calcium). Foot structures are faintly visible in the junctional gap of triads but additional components are also present which makes interpretation difficult. The junctional gap in some triads is up to 18 nm wide which is larger by several nanometers than most previous estimates. Frozen-hydrated TC and triads should be ideal specimens for high-resolution immuno-EM to provide detailed information on the identity and location of triad components. Such studies are in progress.

Supported by NIH HL32711 (SF) and NIH AR40615 (TW).

Tu-Pos114

LOCALIZATION OF ANTI-RYANODINE RECEPTOR ANTIBODY BINDING SITES IN VASCULAR AND ENDOCARDIAL ENDOTHELIUM AND SMOOTH MUSCLE. ((R. E. Lesh, A. R. Marks*, A. V. Somlyo, S. Fleischer# and A. P. Somlyo)) Dept. of Physiol., Univ. of Va. School of Medicine, Charlottesville, VA 22908; *Dept. of Mol. Biol., Mount Sinai School of Medicine, New York, NY, 10029; and #Dept. of Mol. Biol., Vanderbilt University, Nashville, TN, 37235.

Binding sites for an affinity-purified polyclonal antibody to a peptide sequence of the ryanodine receptor (Anti-RyR) were localized using laser scanning confocal microscopy. An intense fluorescent signal in endothelium (EN), both vascular and endocardial, was distributed nonhomogeneously throughout the cell, particularly in the perinuclear region. Northern blot analysis of cultured EN showed the presence of messenger RNA with homology to the cardiac RyR isoform, and Western blots confirmed the presence of RyR protein in freshly isolated human umbilical vein EN. The light microscopic distribution of antibody binding correlated with the extensive network of endoplasmic reticulum (ER) in the guinea pig aortic and endocardial EN visualized in electron micrographs of aortic and cardiac tissue postfixed with osmium ferrocyanide. Smooth muscle from guinea pig aorta and taenia coli also bound Anti-RyR antibody. There was a strong central fluorescent signal in aortic smooth muscle in contrast to taenia coli, where the signal was punctate and peripheral. The latter may represent the presence of RyR's present at surface couplings. We conclude that there are Anti-RyR binding sites in EN and in smooth muscle cells, and the distribution of these sites is different in the tonic (aortic) and phasic (taenia coli) smooth muscle. Supported by: PHS 1K11 AR01871, PHS 1PO1 HL48807, NIH HL32711, a grant-in-aid from New York Affiliate of AHA, and a Syntex Scholar Award.

Tu-Pos115

CYCLIC ADP-RIBOSE IS AN ENDOGENOUS REGULATOR OF THE CARDIAC ISOFORM OF THE RYANODINE RECEPTOR Ca-CHANNEL. L.G. Mészáros, J. Bak and A. Chu*, Dept. Physiol. Endocrinol., Med. Coll. Georgia, Augusta, GA 30909 and *Dept. Med., Cardiovasc. Sci., Baylor Coll. Med., Houston, TX 77030.

In sarcoplasmic reticulum (SR), the ryanodine receptor Ca^{2+} channel (RyRC) constitutes the major pathway for Ca^{2+} release. Although two mechanisms, i.e. a direct mechanical and a Ca^{2+} -triggered activation of the RyRC, have been put forward to explain the induction of *in vivo* Ca^{2+} release, their validity is still being assessed. In non-muscle cells, where the RyRC also contributes to Ca^{2+} signaling, the mechanism of their activation is unknown. Here we report that 10^{-7} M cyclic ADP-ribose (cADPR), which has been shown to be present in many mammalian tissues as a metabolite of NAD, activates the cardiac (but not the skeletal) isoform of the ryanodine receptor channel. This is shown in measurements of: i) Ca^{2+} release from isolated cardiac and skeletal SR as well as brain microsomes (the cardiac isoform of the RyRC is expressed in the latter), ii) [^{3}H]-ryanodine binding in cardiac and skeletal SR and iii) single channel conductance of the cardiac channel in lipid bilayers. The results suggest that cADPR might be an endogenous regulator of the cardiac isoform of the ryanodine receptor Ca^{2+} channel.

Tu-Pos116

CHANGES IN [INSP3] INDUCED BY Mg^{2+} IN MH SKELETAL MUSCLE ((C. Perez[1], J.R. Lopez[2], M. Alfonzo[1], P. D. Allen[2]))CBB, IVIC, Caracas Venezuela; [2]Dept of Anesthesia, Brigham and Women's Hospital, Boston, MA 02115

Malignant hyperthermia (MH) is a disorder of skeletal muscle triggered when susceptible subjects are exposed to volatile anesthetic agents and/or depolarizing muscle relaxants. We have reported experimental evidence suggesting that an alteration in metabolism of inositol trisphosphate (InsP3) in skeletal muscle may play an important role in the pathophysiology of MH. It is well known that the activity of the enzyme responsible for the first step in deactivation of InsP3, InsP3-phosphatase is [Mg^{2+}] sensitive. An increaser in $[Mg^{2+}]_i$ induces a reduction of $[InsP3]_i$. Experiments were carried out in 8 Yorkshire control swine, and 12 Pietrain MH susceptible swine. Anesthesia was induced and maintained with thiopental (25 mg/kg IV), nitrous oxide (66%) and oxygen (34%). In each animal a muscle biopsy was obtained from the intercostal muscle at the beginning of the experiment and again 10 min after the animals received a IV bolus of 150 mg/kg of $MgSO_4$. In each case muscle samples were divided in half, for electrophysiological and biochemical assays. The $[Ca^{2+}]_i$ measured with Ca^{2+} selective microelectrodes was 0.12 ± 0.01 µM (n=29) in the control muscle samples and 0.34 ± 0.02 µM (n=32) in the MH samples, prior the administration of Mg^{2+}. The $[Ca^{2+}]_i$ 10 minutes after the administration of $MgSO_4$ was 0.08 ± 0.01 µM (n=32) and 0.21 ± 0.02 µM (n=26) in control and MH skeletal muscles respectively. The $[InsP3]_i$ before the Mg2+ treatment was 58.3 ± 1.67 cpm/mg (n=29) in the control muscle and 267 ± 7.47 cpm/mg (n=22) in MH. The [InsP3] after Mg^{2+} was 36 ± 1.56 cpm/mg (n=26) and in MH was 115 ± 3.78 cpm/mg (n=31). These results provide new evidence for the relationship of InsP3 in the pathophysiology of MH. They also provide new evidence for the mechanism of the difference in clinical response and $[Ca^{2+}]_i$ during MH episode which we have previously observed in animals pretreated with Mg^{2+}. (Supported in part by Angelini Pharmaceuticals).

Tu-Pos117

AZUMOLENE BLOCKS THE LENGTH DEPENDENT EFFECTS OF INSP3 ON $[Ca^{2+}]_i$ ((J.R. Lopez)),CBB, IVIC, Caracas, Venezuela

We have reported that microinjection of inositol 1,4,5 trisphosphate (InsP3) into intact skeletal muscle fibers produced a transient increase in $[Ca^{2+}]_i$ which was length dependent (Biophy J 59:556a, 1991). Small bundles of intact fibers were isolated from the tibialis anterior muscle of a tropical amphibian Leptodactylus insularis and mounted horizontally in an experimental chamber. The ends of the fiber were fixed between two stainless steel forceps attached to two micromanipulators which allowed us to adjust the striation spacing (2.4 to 3.6 µm) using the laster diffraction technique. $[Ca^{2+}]_i$ was measured using Ca^{2+} selective microelectrodes. Lengthening of the muscle fibers produced an increment in $[Ca^{2+}]_i$ which was length-dependent. Microinjection of 0.5 mM InsP3 also induced increments in $[Ca^{2+}]_i$ which were length dependent. At 2.4 µm, microinjection of 0.5 mM InsP3 caused an increment of $[Ca^{2+}]_i$ from 0.12 ± 0.01 µM (n=12) to 0.52 ± 0.02 µM (n=10), at 2.8 µm $[Ca^{2+}]_i$ rose from 0.32 ± 0.01 µM (n=16) to 1.26 ± 0.18 µM (n=20), at 3.2 µm $[Ca^{2+}]_i$ rose from 0.51 ± 0.02 µM (n=15) to 1.86 ± 0.20 µM (n=13), and at 3.6 µm $[Ca^{2+}]_i$ rose from 0.91 ± 0.09 µM (n=21) to 3.10 ± 0.28 µM (n=14). Incubation of the muscle fiber in 10^{-6} M Azumolene, blocks the transient elevation of $[Ca^{2+}]_i$ associated with stretching the muscle and inhibits the the increase in $[Ca^{2+}]_i$ caused by InsP3 microinjection. Incubation of the fibers in 5 µM nitrendipine did not modify the increment in $[Ca^{2+}]_i$ associated with stretching or microinjection of InsP3. These results i) confirm previous findings about the influence of muscle length on resting $[Ca^{2+}]_i$, ii) that the effect of InsP3 on $[Ca^{2+}]_i$ in skeletal muscle is also length dependent; iii) that azumolene was able to block the effects of stretching on $[Ca^{2+}]_i$ at all the muscle lengths studied, and iv) that neither effect was modified by nitrendipine. (Supported by Angelini Pharmaceuticals).

Tu-Pos118

ENANTIOMERIC EFFECTS OF CHLOROPHENOXYPROPIONIC ACID ON MECHANICAL THRESHOLD IN RAT SKELETAL MUSCLE FIBERS. ((S.H. Bryant and D. Conte-Camerino)) Department of Pharmacology and Cell Biophysics, University of Cincinnati, Cincinnati, OH 45267-0575; Dipartimento Farmacobiologico, Facultà di Farmacia, Università di Bari, 70125 Bari, Italy.

The effects of the S(-) and R(+) enantiomers of 2-(4-chlorophenoxy)propionic acid (CPP), anthracene-9-carboxylic acid (9AC) and d-cis-diltiazem (DIL) were observed on the mechanical threshold (MT) of rat extensor digitorum longus fibers in vitro at 30° C. MT was determined by visualization of local contractions using a point 2-microelectrode voltage clamp in the presence of 3 µM tetrodotoxin. Neither the enantiomers of CPP nor 9AC produced any effect on MT at 100 µM in spite of the fact that these agents block chloride conductance at this concentration. This rules out any action of these compounds on the MT through a chloride conductance effect. At a concentration of 1 mM, however, the S(-) increased MT from a control of -59 mV to -49 mV, whereas the R(+) enantiomer decreased MT to -63 mV. Also the achiral compound, 9AC, at 0.5 and 1.0 mM lowered MT by 1 and 2 mV, respectively. DIL at 1 µM in normal ringer lowered MT by 6 mV and this was not affected by the presence of 1 mM R(+), but S(-) at 1mM completely antagonized the effect of DIL. The mechanism of interaction of the enantiomers with DIL is not clear although it suggests that a common receptor may be involved. We speculate that there is a stereospecific site for the CPP enantiomers on the dihydropyridine sensitive voltage sensor molecule of the rat skeletal muscle t-system. Supported by an MDA grant-in-aid, and Italian CNR Grants 89-4116 and MPI-89 (DC-C); and NIH Grant HL-22619-IIb (SHB).

Tu-Pos119

PRODUCTION AND REMOVAL OF INOSITOL (1,4,5) TRISPHOSPHATE IN FROG SKELETAL MUSCLE. ((M.Angélica Carrasco, Jimena Sierralta and Silvia Figueroa)) Dept. Fisiol. Biofis., Fac. Med., U. de Chile, Casilla 70005, Santiago, and C.E.C.S.(Spon. by M.T. Nuñez)

We have studied IP_3 production by hydrolysis of phosphatidylinositol 4,5 bisphosphate (PIP_2) by phospholipase C (PLC), and IP_3 conversion to inositol 1,4 bisphosphate and inositol 1,3,4,5 tetrakisphosphate in membrane and cytosolic fractions isolated from frog skeletal muscle.

PLC activity was determined with exogenous [^{3}H]-PIP_2 presented as a sonicated mixture with PS and PE (2:1:1). PLC activity membrane bound was found in triads and T-tubules but not in sarcoplasmic reticulum. Soluble activity represented 20% of the total obtained in homogenate. Correcting for the T-tubules present in triads (10%), the hydrolysis rates were 0.76 ± 0.29 nmol/mg/min at pCa 7 and 2.53 ± 0.33 nmol/mg/min at pCa 5 with 0.1 mM substrate. This activation increased up to pCa 4, was also obtained in a soluble fraction and was not replaced nor inhibited by magnesium.

Removal of IP_3 was studied with [^{3}H]-IP_3 separating the formed inositol phosphates by anionic exchange chromatography. IP_3 kinase activity studied in cytosolic fraction (60 % of the activity in total homogenate) presented an optimum pH of 8, was activated by calcium in the physiological range and its Km for IP_3 was 0.5 to 1 µM. The study of the metabolism of IP_3 by phosphatase and kinase activities in total muscle homogenate under physiological conditions gave comparable values of 8.6 ± 3.8 and 6.4 ± 2.6 pmol/mg/min respectively. Therefore both routes would be equally important in IP_3 removal. Supported by FONDECYT 91-1116 and by DTI 3200.

Tu-Pos120

INOSITOL (1,4,5) TRISPHOSPHATE STIMULATES CA^{2+} RELEASE IN MECHANICALLY PEELED SKELETAL MUSCLE FIBERS WHEN APPLIED BY IONTOPHORESIS OR PRESSURE MICROINJECTION. ((S.K. Donaldson and D.A. Huetteman)) U of MN, Minneapolis, MN 55455.

Single rabbit adductor magnus fibers were peeled (sarcolemma removed) and pretreated as follows: 1) 10mM bath caffeine, 2) bath pCa 5.6; 4mM EGTA, 3) bath pCa 6.5; 20µM EGTA. Other bathing solution components were either depolarizing (66mM Cl^-, 4mM K^+) or polarizing (4mM Cl^-, 66mM K^+) for sealed TT in this preparation (Donaldson et al., PNAS, 85:5749, 1988). Ca^{2+} release from the SR was measured as Fluo-3 fluorescence. For depolarized fibers, stimulation was microinjection of 1nl of either a 1µM IP_3 or a 10mM caffeine solution (depolarizing solution solvent). IP_3 elicited a faster rate of release than caffeine; some IP_3 Ca^{2+} releases peaked ≤1.0 sec. In contrast, the tension response of pieces of the same fibers microinjected with 1.0µM IP_3 (in depolarizing solution) was up to 10X slower. For polarized fibers, microinjection of 1nl of depolarizing solution elicited a localized Ca^{2+} release which peaked in 3-5 seconds. In paired data experiments of polarized fibers, the addition of 1.0µM IP_3 to the depolarizing injectate always elicited a larger and equal/faster Ca^{2+} release. Iontophoresis of IP_3 (10µM in H_2O) also elicited large, although slow (delayed onset ≥1.0 sec), releases of Ca^{2+} in depolarized fibers, again demonstrating that the injectate volume is not the stimulus (Donaldson et al., BBA, 927:92, 1987). Supported by USPHS, NIH (AR 35132).

Tu-Pos121

HEME IS NOT A PLANAR OSCILLATOR WHEN IT ACTS AS ACCEPTOR OF RADIATIONLESS ENERGY TRANSFER FROM TYPRTOPHAN IN HEMOPROTEINS. ((Z.Gryczynski, J.Kusba, and E.Bucci)) UMAB, Baltimore, MD (Spon. by Z. Gryczynski)

We measured the linear dichroism of deriva-tives of metalloporphyrin IX (Fe^{+++}, $Fe^{++}CO$, Mg^{++}, Zn^{++}) in stretched polyvinyl alcohol (PVA) films. The linear dichroism was wavelength dependent, indicating a high complexity of the transition moments. Deconvolution in terms of Gaussian components of the Soret region of the spectrum for all four derivatives gave three components between 380-450 nm and only one in the 300-380 nm region. In this region the linear dichroism of the single transition was constant and suggested a 60° orien-tation from the alpha-gamma meso-axis of the heme moiety. Gaussian deconvolution of the Soret spectra of oxy-, deoxy-, and carbon monoxy-hemoglobin gave very similar results, suggesting a similar orientation of the single transition in the 300-380 nm region. This is the region of the overlap which regulates the energy transfer from tryptophan to heme. Therefore, it appears that heme is not a planar oscillator when it acts as acceptor of energy from the excited states of try-ptophyl residues in hemoproteins. This implies a much larger sensitivity of the transfer to the reciprocal position of heme and tryptophan.

Tu-Pos122

Resonance Raman spectroscopy probes two different conformations of Ni(II)-octaethylprophyrin in CH_2Cl_2.

((W. Jentzen, W. Dreybrodt and R. Schweitzer-Stenner)), Inst. of Exp. Physics, University of Bremen, 2800 Bremen 33, Germany (Sponsored by A. Mayer-Heinricy)

Recently experimental evidence was provided that a ruffled and a planar conformation of Ni(II)-octaethylporphyrin (NiOEP) may coexist in solution (Alden et al, JACS, 111, 2070, 1989). To check whether this can be proven further we first measured the Raman spectra of NiOEP in CH_2Cl_2 with high resolution (2-4cm^{-1}) at excitation wavelengths between 441nm and 528nm. The 'core size marker' lines ν_2, ν_{10} and ν_{16} were decomposed into two different sublines (SL)(i.e.ν_2: 1517 and 1521cm^{-1}; ν_{10}: 1594 and 1604cm^{-1}; ν_{16}: 1650 and 1658cm^{-1}). Following Alden et al. we attribute the SLs at the lower frequencies to the ruffled conformation. Second we measured the temperature dependence of the SLs intensities between 300 and 190 K. By fitting their intensity ratios I(ruffled)/I(planar) to a Boltzman equation we found that the ruffled conformation is stabalized by approximately 0.8 KJ/mol. Moreover we observed that the frequencies of all SLs increase linearly with temperature thus indicating to anharmonic coupling with low frequency modes (Asher and Murtaugh, JACS 105,7244,1983). Third we measured the resonance excitation profiles of the ν_{16}-SLs and found that the Q_0-resonance of the ruffled molecule is red shifted by 180cm^{-1} with respect to that of the planar conformation, in accordance with theoretical predictions (Shelnutt et al., JACS,113,4077,1991).

Tu-Pos123

VIBRATIONAL ENERGY DYNAMICS IN IRON-CONTAINING PORPHYRINS ((M. C. Schneebeck, L. E. Vigil, P. A. Gurule, M. R. Ondrias)) Dept. of Chemistry, Univ. of New Mexico, Albuquerque, NM, 87131.

Absorption and rapid (<10 ps) non-radiative decay can deposit a large excess of vibrational energy in the ground electronic state of iron porphyrins. Intra- and intermolecular vibrational energy dynamics may influence the subsequent reactive pathway of these species. We have used transient resonance Raman spectroscopy to investigate this phenomenon. The corrected ratio of anti-Stokes to Stokes scattering intensities yields direct information about vibrational level populations. A steady state, non-Boltzmann vibrational energy distribution has been observed in deoxyhemoglobin and in protoporphyrin IX 2-methyl imidazole during high intensity, nanosecond pulsed excitation. These results are compared to those obtained from cytochrome c and the model compound Fe-octaethyl porphyrin. In addition, the $\lambda_{excitation}$ dependence of this behavior is explored.

Supported by the NIH (GM33330). M. C. S. is a Howard Hughes Predoctoral Fellow.

Tu-Pos124

AN OPTICAL, ESR, AND TRANSIENT RESONANCE RAMAN INVESTIGATION OF THE INTERACTION OF Cu(II) PROTOPORPHYRIN IX WITH AQUEOUS MICELLAR SYSTEMS.

((Bryan S. Wicks, Eric W. Findsen)) Department of Chemistry, University of Toledo, Toledo, OH 43606.(Spon. by B. Wicks)

Membrane bound metalloporphyrins play important roles in biological processes such as electron transport and photosynthesis. Micellar media are among the simplest models of membrane environments and can be used as models to study the effects of charged surfaces, interfacial polarities, and other physiochemical properties of microheterogenous systems on the spectroscopic properties of solubilized molecules. We report the results of ESR, transient resonance Raman, and UV-VIS studies which have characterized CuPP in aqueous (0.1 M NaOH) solutions containing cationic(CTAB), anionic(SDS) or neutral(Triton X-100) surfactants. The results of UV-VIS studies clearly demonstrate that the micellar environment has a significant effect on the degree of porphyrin solubilization. We have assigned a g ~ 1.93 signal in the room temperature ESR spectrum to the monomeric species, for which the nitrogen hyperfine splitting and intensity of this resonance are strongly dependent on the properties of the micelle. Resonance Raman spectra of CuPP exhibited little or no sensitivity to the porphyrin monomer ⇌ dimer equilibrium in contrast to the behavior of Cu uroporphyrins reported by (Shelnutt et al.).

Tu-Pos125

SOLVENT EFFECTS ON FIVE-COORDINATE FERRIC PORPHYRINS. ((R.E. Nalliah, E.W. Findsen)) Department of Chemistry, University of Toledo, Toledo, OH 43606.

The characterization of solvent effects upon iron porphyrins is a promising tool in probing the environment of hemeproteins. In order to initially characterize the behavior of ferric porphyrins in different environments, UV-VIS absorption spectra of these compounds were obtained in ten non-coordinating solvents. Solvent $E_T(30)$ is an empirical parameter of solvent polarity based upon the wavelength of a charge-transfer band of a pyridinium N-phenoxide betaine dye. Results of absorption studies indicate the average of the Soret and alpha band energies (the Gouterman A_{1g}' parameter) for the 5-coordinate iron porphyrins decreases with increasing solvent $E_T(30)$. It was also observed that the A_{1g}' parameter decreases with increasing solvent refractive index. The A_{1g}' parameter for Fe(III)PPDME(Cl) correlates significantly better to solvent refractive index than to solvent $E_T(30)$, while the opposite behavior was found for Fe(III)OEP(Cl). A two-parameter linear least squares fit of the absorption data with both the solvent $E_T(30)$ values and refractive index has been determined to provide the best overall correlation (R = 0.94) with A_{1g}'. These results, when compared to those obtained with Ni porphyrins (Findsen et.al.) suggest that the solvent parameter $E_T(30)$ reflects solvent interactions with the porphyrin electronic structure primarily through metal-porphyrin interactions, while solvent refractive index reflects solvent interactions through the macrocycle HOMO and LUMO orbitals.

Tu-Pos126

STRUCTURE AND LIGAND BINDING PROPERTIES OF NONPLANAR, MESO-SUBSTITUTED NICKEL(II) OCTAETHYLPORPHYRINS: A POSSIBLE MODEL FOR COFACTOR F_{430}

((J. D. Hobbs[1], S. A. Majumder[1,2], L. Luo[3], G. H. Allen-Sickelsmith[3], J. M. E. Quirke[3] and J. A. Shelnutt[1,2])) [1]*Fuel Science Department 6211, Sandia National Laboratories, Albuquerque, NM 87185.* [2]*Department of Chemistry, University of New Mexico, Albuquerque, NM 87131,* [3]*Department of Chemistry, Florida International University, Miami, Fl 33199.*

Molecular mechanics calculations, UV-visible absorption and resonance Raman spectra are presented for mono-, 5,15-di-, 5,10-di-, tri-, and tetra-substituted Ni(II) octaethyl-meso-nitroporphyrin in coordinating and non-coordinating solvents. We find that Ni(II)octaethyl-tetra-nitroporphyrin (NiOETNP) readily binds even weak field ligands such as methanol. The increased ligand affinity of NiOETNP is probably a result of the strong electron-withdrawing character of the four NO_2 groups. These result suggest that NiOETNP is a potential model for ligand binding in cofactor F_{430} which, due to its highly reduced macrocyclic ring, can assume a nonplanar structure and has a higher affinity for axial ligands than most nickel porphyrins. Further, molecular mechanics calculations for NiOETNP also predict a highly distorted, nonplanar structure similar to that found for Ni(II) octaethyl-tetra-phenylporphyrin (NiOETPP). Our interpretation of absorption and resonance Raman spectra suggest that the sterically induced nonplanarity of the porphyrin, and not the electronic effect of nitro-substitution, dominates the observed spectral frequency shifts. Supported by U.S. DOE Contract DE-AC04-76DP00789 (JAS) and Associated Western Universities Fellowships (JDH and SAM).

Tu-Pos127

STRUCTURAL HETEROGENEITY OF OCTAETHYLPORPHYRINS PROBED BY RESONANCE RAMAN SPECTROSCOPY

((K. K. Anderson[1,2], J. D. Hobbs[1], L. Luo[3], K. D. Stanley[3], J. M. E. Quirke[3] and J. A. Shelnutt[1,2])) [1]*Fuel Science Department 6211, Sandia National Laboratories, Albuquerque, NM 87185.* [2]*Department of Chemistry, University of New Mexico, Albuquerque, NM 87131,* [3]*Department of Chemistry, Florida International University, Miami, Fl 33199.*

The importance of nonplanar macrocyclic conformations in the biological function of tetrapyrrole containing proteins has become increasingly evident. In this work, UV-visible absorption and resonance Raman spectra (RRS) are presented for nickel(II), cobalt(III) and copper(II) derivatives of octaethylporphyrin (OEP) and mono-substituted octaethyl-meso-nitroporphyrin (OEMNP) in CS_2 solution. The RRS of NiOEP in solution has been shown to be consistent with the presence of an equilibrium mixture of planar and nonplanar conformers. Structural heterogeneity in the vibrational spectra for both OEP and OEMNP is observed to decrease with increased metal size (Ni < Co < Cu) as a result of the disappearance of the nonplanar conformers. The width of ν_{10}, which has been shown to be sensitive to porphyrin planarity, is observed to decrease by 9 cm^{-1} for the OEP series and by 13 cm^{-1} for the OEMNP series as metal size increases. For NiOEMNP, the data also indicate that, in contrast to NiOEP, that the nonplanar structure dominates the equilibrium. This shift in the equilibrium is probably due to steric interactions between the NO_2 group and the adjacent pyrrole ethyl groups. Further, the Raman modes ν_3, ν_2, and ν_{10} shift to lower frequencies consistent with an increase in macrocyclic core size induced by the larger metal. Supported by U.S. DOE Contract DE-AC04-76DP00789 (JAS) and Associated Western Universities Fellowships (KKA and JDH).

Tu-Pos128

RESONANCE RAMAN SPECTROSCOPY OF NICKEL PORPHYRINS IN DIFFERENT ENVIRONMENTS AS MODELS FOR FERROCHELATASE

((S.A. Majumder[1,2], J.D. Hobbs[1], G.C. Ferreira[3], M.R. Ondrias[2], and J.A. Shelnutt[1,2])) [1]*Fuel Science Department 6211, Sandia National Laboratories, Albuquerque, NM 87185.* [2]*Department of Chemistry, University of New Mexico, Albuquerque, NM 87131.* [3]*Department of Biochemistry and Molecular Biology, University of South Florida, Tampa, Fl 33612.*

UV-visible absorption and dual-channel resonance Raman spectroscopies have been used to determine the conformations of Ni protoporphyrin IX (NiPP) and Ni mesoporphyrin IX (NiMP) in protein and solvent environments to model the structural properties of the active site of ferrochelatase. Ferrochelatase catalyzes the insertion of Fe(II) into protoporphyrin. Ferrochelatase function has been proposed to involve a nonplanar distortion of free base protoporphyrin IX. Purification and catalytic activity measurements usually involve the presence of sodium cholate detergent. Consequently, Ni-porphyrin interactions with micelles of cetyltrimethyl ammonium bromide (CTAB) and sodium cholate and Ni-porphyrin binding to bovine serum albumin (BSA) have been investigated. Resonance Raman spectra were simultaneously obtained for NiPP in CTAB and NiPP in sodium cholate and for monomeric NiPP in one of the detergents and NiPP bound to BSA. Changes in the NiPP absorption bands and Raman vibrational lines for the cases of the BSA-bound and the sodium cholate solution suggest that nonplanar conformers of the porphyrin macrocycle are stabilized over the planar conformer when compared with NiPP in CTAB. Similar results were obtained for NiMP. Supported by the U.S. DOE Contract DE-AC04-76DP00789 (JAS), NSF MCB9257656 (GCF), NIH GM33330 (MRO), and Associated Western Universities (SAM, JDH).

Tu-Pos129

BIOMIMETIC ISOPENTANE HYDROXYLATION CATALYZED BY NONPLANAR DODECA-SUBSTITUTED IRON PORPHYRINS.

((K. E. Erkkila, S. L. Martinez, C. J. Medforth, K. M. Smith, J. A. Shelnutt)) Fuel Science Department 6211, Sandia National Laboratories, Albuquerque, NM 87185 and University of California, Davis, CA 96616.

Nonplanarity of the porphyrin macrocycle may affect the catalytic activity of iron porphyrins in alkane partial oxidation reactions that mimic the action of cytochrome P450. Consequently, we have measured rates for oxidation of isopentane to the tertiary, secondary and primary alcohol products for a series of dodeca-substituted Fe(III)-porphyrin catalysts using iodosylbenzene as oxidant. As an example, for a series of tetra(perfluorophenyl)porphyrins with either alkyl or phenyl substituents at the β-carbons of the pyrrole rings, the activity was found generally to correlate with the electron-withdrawing ability of the substituents (as measured by the sum of the Hammett σ constants of the substituents). A similar activity dependence on the electron-withdrawing capacity is noted for planar porphyrin analogs. However, the catalytic activity appears to be enhanced for nonplanar porphyrins over planar porphyrins with equal Σσ's. For example, Fe(Cl) dodecaphenylporphyrin-F_{20} (DPP) has a slightly lower (1.56 versus 1.64) $\Sigma\sigma_p$ than Fe(Cl) tetraphenylporphyrin-F_{20} (TPP), but DPP-F_{20}, which is highly nonplanar, has higher activity. The higher activity of DPP could result either from the nonplanarity or the steric properties of the cavity formed by the phenyl substituents; selectivity differences for °1, °2, and °3 alcohols among the porphyrins suggest the latter.

This work is supported by the U.S. DOE Contract DE-AC04-76DP00789 and Associated Western Universities (KEE).

Tu-Pos130

SOLUTION CONFORMATIONS OF DODECASUBSTITUTED PORPHYRINS DETERMINED FROM COBALT (II) PARAMAGNETIC NMR SHIFTS.

((C. J. Medforth, L. D. Sparks, M. R. Rodriguez, K. M. Smith, J. A. Shelnutt)) Fuel Science Department 6211, Sandia National Laboratories, Albuquerque, NM 87185 and Department of Chemistry
University of California, Davis, CA 95616

Recent structural studies have indicated that dodecasubstituted porphyrins adopt extremely nonplanar saddle conformations. Because several of these porphyrins also possess cavities formed by the pyrrole substituents, it is of interest to determine whether the orientation of the substituents is a result of the crystal packing forces or if they are determined by the molecular structure. We have investigated the feasibility of using cobalt(II) paramagnetic NMR shifts for the protons on the porphyrin substituents to determine the orientations of these substituents in solution. NMR shifts are calculated using structures obtained from molecular mechanics calculations and compared to the experimental NMR shifts. Our results indicate that the observed paramagnetic shifts are largely dipolar in nature and that useful structural predictions can be made. The solution conformations of several dodecasubstituted porphyrins have been determined using this technique. Supported by Department of Energy Contract DE-AC0476DP00789 (JAS), National Science Foundation Grant CHE-90-01381 (KMS) and the Associated Western Universities (LDS, CJM).

Tu-Pos131

HIGH RESOLUTION SOLUTION STRUCTURE OF REDUCED HORSE HEART CYTOCHROME C

((P. X. Qi#, R.A. Beckman§, D.L Di Stefano§ & A.J. Wand#§)) §Institute for Cancer Research, Philadelphia, PA 19111, #Department of Biochemistry, University of Illinois at Urbana-Champaign, Urbana, IL 61801

The solution structure of reduced horse cytochrome c has been determined by a combination of high resolution NMR spectroscopy and restrained simulated annealing. Two- and three-dimensional NOE spectra were used to obtain over 2000 distance constraints. Further geometric constraints were derived from analysis of amide NH-CαH spin-spin coupling constants. Prochiral assignments were obtained for over a third of Cβ centers using the floating chirality method. A family of 128 structures has been obtained with no violations over 0.5 A and an average main chain r.m.s.d. from the mean structure of better than 0.6 A. The general solution structure of the protein is similar to the crystal structure. However, subtle local differences in hydrogen bonding and other short range interactions exist between the solution and crystal structures. The significance of these and other observations will be discussed.

Tu-Pos132

HIGH RESOLUTION X-RAY CRYSTAL STRUCTURE OF CYTOCHROME *C* AT LOW IONIC STRENGTH.

((Mark H. Walter)) Department of Biochemistry, Molecular Biology and Cell Biology, Northwestern University.

Tuna ferricytochrome *c* has been crystallized at an ionic strength of 45 mM, an X-ray data set, 89% complete to 1.89 Angstrom, has been recorded, and the initial phases obtained by the molecular replacement method are being refined by the least squares procedure of PROLSQ. After 320 cycles of refinement with manual adjustments of the model and addition of over 300 water molecules the R value has reached 22.0%. A comparison is being made between this high resolution structure at an ionic strength of 45 mM and the high resolution structure at an ionic strength of 9.5 M (Takano and Dickerson (1981) *J. Mol. Biol.*, 153, 95-115). As predicted by UV-Raman and visible absorption spectroscopy a weakening of the heme proprionate hydrogen bonds and the methionine 80 - Sulfur coordination is observed at low ionic strength. As indicated by variation in phi/psi angles, the flexible protein regions present at high ionic strength are present at low ionic strength. Additional flexible regions are observed at low ionic strength, specifically near tryptophan 33, tyrosine 67 and tyrosine 74.

Tu-Pos133

QUALITATIVE RESONANCE RAMAN SPECTRAL ANALYSIS OF CYTOCHROME C

((Songzhou Hu and Thomas G. Spiro))
Department of Chemistry, Princeton University, Princeton, NJ 08544.

Resonance Raman spectra with both the Soret (413.1 nm) and Q-band (520.8 and 530.9 nm) excitations are obtained for yeast iso-1 cytochrome c and its *meso*-d_4, pyrrole-^{15}N, 2,4-di(α-d_1) and 2,4-di(β-d_2) isotopomers. These specifically labeled molecules are synthesized from apocytochrome c and hemes by use of cytochrome c heme lyase. Based upon the isotopic shifts and the depolarization ratios, we have unraveled the complex spectra and assigned observed bands to the heme skeletal in-plane, out-of-plane and substituent vibrations. Most infrared-active E_u vibrations are located in the resonance Raman spectra, and splitting of some E_u modes into two bands is observed. The doublet bands in the low frequency region are attributed to the C_β-C_1-C_2 bending vibrations of 2,4-substituents and 6,7-propionic acid group. The structural implication of these results will be discussed.

Tu-Pos134

STRUCTURAL CHARACTERIZATIO OF ISOLATED MITOCHONDRIAL CYTOCHROME C_1

((Bih-Show Lou[1], J. David Hobbs[1], Yeong-Renn Chen[2], Linda Yu[2], Chang-An Yu[2] and Mark R. Ondrias*[1])) [1]Department of Chemistry, University of New Mexico, Albuquerque, NM 87131; [2]Department of Biochemistry, Oklahoma State University, Stillwater, OK 74078
(Spon. by M. Ondrias)

Resonance Raman spectroscopy (RRS) has been employed to characterize cytochromes c_1 isolated from bc_1 complexes of beef heart mitochondria and R. Sphaeroides. The data obtained in this study extend the physical characterization of cytochromes c_1 and focus on the effects of the local protein environment on the heme active site. While the general characteristics of these cytochromes c are similar to those of smaller soluble cytochromes c, the behavior of several core-size and ligation sensitive heme modes reveal that significant systematic differences exist between those species. These, most likely, result from changes in the heme axial-ligand interactions.
This work is supported by grants from the NIH. (GM 33330 and GM 30721).

Tu-Pos135

SIMULATION OF ELECTRON TRANSFER SELF-EXCHANGE IN CYTOCHROMES C AND B5. ((Sedonia M. Andrew, Kathryn A. Thomasson and Scott H. Northrup)) Dept. of Chemistry, Tennessee Technological University, Cookeville, TN 38505

Brownian dynamics (BD) has been employed to simulate the kinetics of the electron transfer self-exchange reactions of trypsin-solubilized bovine liver cytochrome *b5* (*cytb5*) and horse heart cytochrome *c* (*cytc*). A structurally robust BD method simulating diffusional docking and electron transfer was employed to compute bimolecular rate constants, which were then compared with experiment. BD provides a detailed description of the collision stage of the process, determined by the atomic scale irregularity of the proteins (steric factors) and mutual electrostatic interactions. A realistic two-parameter model of the electron transfer unimolecular rate constant was employed which is exponentially varying over donor-acceptor distance. BD theory successfully reproduces the ionic strength dependence of the reaction. By fitting BD-generated rate constants to experimental and using Marcus theory, we extracted a reorganization energy λ and distance decay factor β for both self-exchange reactions. Values obtained were λ = 1.06 and 0.69 eV for *cytb5* and *cytc* systems, respectively, and $\beta = 0.9$ A^{-1} was obtained for both systems. For the first time BD was used in the limit where reaction is activation controlled rather than diffusion-influenced. This was facilitated by a model that explicitly couples diffusion and chemical dynamics. Direct calculation of the entropy cost of forming docked protein-protein complexes was performed by tallying the potential of mean force versus heme-heme distance.

Tu-Pos136

A MODEL OF THE CYTOCHROME b_L/b_H MODULE OF THE bc_1 COMPLEX ((R.S. Farid, D.E. Robertson, J.S. Keske, P.L. Dutton)) Johnson Research Foundation, University of Pennsylvania, Phila, PA 19104 (spon. by D. Tiede)

The two *b*-type cytochromes of the bc_1 complex act to separate charge following oxidation of hydroubiquinone at site Q_o. The protein structural determinants for ligation and solvation of the hemes and for the intervening medium are of paramount importance to the study of electron-transfer mechanism within this structural motif. We have therefore constructed a testable model incorporating the two ligand-containing helices. Use of membrane helical predictions plus a further refinement based upon helix termination preferences from the *Rhodopseudomonas viridis* reaction center crystal structure allowed the prediction of helix lengths for the two transmembrane helices containing the invariant histidines. Predicted α-helical ϕ and ψ angles are also based on the 11 transmembrane helices of *R. viridis*. Rotamer searching of histidines in helices from Protein Data Bank structures and further consideration of the steric constraints on χ_1 and χ_2 values for histidines in helices that ligate hemes has led to the development of a general principle of heme-histidine ligation. These searches indicate that helix-histidine ligands invariably form an H-bond between the histidine δ-N and the i-4 backbone carbonyl of the helix. Combining this information obtained from known protein structures with molecular modeling calculations, we have constructed a model which defines the interheme distance and geometry as well as ligand geometry and possible electrostatic contributions for control of heme electrochemistry. Using the model we have successfully predicted the EPR *g*-values of the two hemes based upon the geometrical relationships between the planes of the histidines and the non-bonding orbitals of the heme Fe. Supported by NIH 27309.

Tu-Pos137

RATIONAL DESIGN OF A TWO-HEME, TWO-HELIX CYTOCHROME *b* ((D.E. Robertson, R.S. Farid, W.F. DeGrado, R. Pidikiti and P.L. Dutton)) Johnson Research Foundation, University of Pennsylvania, Phila., PA 19104

The factors that control direction, rate and efficiency of electron transfer between redox centers are determined by ligation, electrostatics and intervening protein structure. To better understand these factors, we have constructed a 62-amino acid, water-soluble, heme-binding peptide based upon structural features gleaned from modelling of the charge separating motif of the transmembrane cytochrome *b* of cyt bc_1 complex (Farid, Robertson, Keske, Dutton, preceding abstract). A 31-amino acid peptide was synthesized using FMOC chemistry with cysteine at the N-terminus, followed by three non-helix forming glycines, followed subsequently by 27 residues designed to form α-helix. A tryptophan was placed at residue 7, phenylalanine at 17, histidines at positions 10 and 24 and an arginine at 27. The peptide was constructed such that α-helix formation would result in leucines predominating in the interhelical packing region and glutamates and lysines would be solvent exposed. Oxidizing the cysteines leads to formation of a homodimer with parallel helical dipoles. The heme binding pockets of the dimer are assymmetric in that one pocket is near the N-terminal connecting loop while the second is near the helical C-termini. CD experiments indicate 90%α-helix, as modelling predicted. Titration of the peptide with ferroprotoporphyrin IX indicates that two hemes bind selectively, i.e., the first heme binds to the site nearest the tryptophan at the N-terminus and the second heme to the site near the C-terminus. Both sites bind with high affinity. Optical and EPR spectra confirm *bis*-histidine ligation and the formation of two six-coordinate, low-spin *b*-type hemes. Redox titrations indicate the electrochemical assymmetry of the hemes, showing two Em values of -210mV and -95mV. The -210mV heme is the first heme into the peptide at the C-terminus. Supported by NIH 27309 and 41048.

Tu-Pos138

THE REACTION OF CYTOCHROME c OXIDASE WITH O_2 PROBED BY FLOW-FLASH MULTICHANNEL TRANSIENT ABSORPTION SPECTROSCOPY. ((Ólöf Einarsdóttir, Katy E. Georgiadis, Timothy D. Dawes and Nam-In Jhon)) Department of Chemistry and Biochemistry, University of California, Santa Cruz, CA 95064

Multichannel transient absorption spectroscopy has been used to study the reduction of O_2 by cytochrome c oxidase. The reaction was studied using the flow-flash method in which carbon monoxide is photodissociated from the fully reduced enzyme in the presence of O_2. The multichannel method allows simultaneous collection of spectra over a wide spectral range on timescales of nanoseconds to milliseconds. The transient difference spectra in the Soret region have been modeled by the spectra of oxidized-, reduced-, and oxy-derivatives of the enzyme. The Soret region transient difference spectra and transient double difference spectra show at least two processes in the first 100 μs, including the binding of O_2 to cytochrome a_3^{2+} and the oxidation of cytochrome a. The oxidation of cytochrome a occurs with a half-life of ~20 μs, followed by a slow phase between 100 μs and 20 ms attributed mostly to the oxidation of cytochrome a_3. These results are in agreement with previous single wavelength transient kinetic measurements and time-resolved resonance Raman results. Flow-flash multichannel transient absorption studies in the visible region are in progress.
Supported by ACS-PRF grant #222478-G3 and NIH grant R 29 GM4588.

Tu-Pos139

INTRAMOLECULAR ELECTRON TRANSFER IN CYTOCHROME c OXIDASE. ((K.E. Georgiadis, N.-I. Jhon, T.D. Dawes and Ó. Einarsdóttir)) Department of Chemistry and Biochemistry, University of California, Santa Cruz, CA 95060

The intramolecular electron transfer in cytochrome c oxidase has been studied following photolysis of CO from the mixed-valence enzyme (cytochrome a_3^{2+}-CO Cu_B^+ cytochrome a^{3+} Cu_A^{2+}) by multichannel time-resolved optical absorption spectroscopy on timescales of nanoseconds to milliseconds. The transient absorption difference spectra show a large absorbance increase on a microsecond timescale ($t_{1/2}$ ~2 μs) centered at ~ 520 nm in the visible region. One-third of the absorbance increase at 520 nm can be attributed to the reduction of cytochrome a. The other two-thirds may at least partially reflect a charge transfer involving Cu_B^{2+} formed upon electron transfer to cytochrome a (PNAS, 89:6934-6937, 1992). In the Soret region, the transient difference spectra show a large increase centered around 390 nm and an absorbance decrease at 443 nm on the microsecond timescale ($t_{1/2}$ ~2 μs) suggestive of both reduction of cytochrome a and oxidation of cytochrome a_3. Simultaneously, there is an absorbance increase at ~675 nm attributed to the oxidation of cytochrome a_3. An absorbance decrease is observed in the near-infrared 830 nm band on a later timescale, $t_{1/2}$ ~ 50-100 μs, reflecting the reduction of Cu_A^{2+}. A new band of unknown origin is observed around ~310 nm upon photodissociation of CO from the mixed-valence enzyme. These results indicate that Cu_A^{2+} is the primary acceptor of electrons from cytochrome c in the forward direction and that cytochrome a is the electron donor to the binuclear center. Supported by ACS-PRF grant #222478-G3 and NIH grant R 29 GM4588.

Tu-Pos140

CONFORMATIONAL EFFECTS OF HYDROGEN PEROXIDE BINDING TO CYTOCHROME C OXIADSE. ((R. W. Larsen and D. H. Omdal)) Department of Chemistry, University of Hawaii at Manoa, 2545 The Mall, Honolulu, HI 96822.

It is now widely believed that the first two electrons transferred to the dioxygen reduction site in cytochrome c oxidase (CcO) are not coupled to proton translocation. The activation of the pump correlates with the formation of catalytic intermediates of dioxygen reduction at the binuclear center. A possible mechanism of pump activation which is consistent with existing data involves a conformational transition associated with ligand binding to cytochrome a_3 that activates the proton pump. In order to investigate this possibility we have examined the effects of hydrogen peroxide binding to CcO using optical absorption and circular dichroism spectroscopy. Previous studies have demonstrated that the addition of low concentrations of hydrogen peroxide to fully oxidized CcO results in binuclear center exhibiting spectroscopic properties analogous to those observed during oxidation of fully reduced CcO by dioxygen. Our results indicate that the addition of low concentrations of hydrogen peroxide to fully oxidized CcO produces perturbations in the near UV region of the optical spectrum consistent with an overall conformational transition within the enzyme. Our results will be discussed in the context of current proton pump models of this functionally important enzyme.

Tu-Pos141

RESONANCE RAMAN SPECTRA OF CYTOCHROME C OXIDASE WITH Q-BAND EXCITATION

Bih-Show Lou[a], Randy W. Larsen[b,c], Sunney I. Chan[b], and Mark, R. Ondrias[a]
[a]Department of Chemistry University of New Mexcio, Alberquerque, NM, 87131; [b]Arthur Amos Noyes Laboratory of Chemical Physics, California Institute of Technology, Pasadena CA 91125; [c]Present address: Department of Chemistry of University of Hawaii

While cytochrome oxidase has been extensively studied using resonance Raman scattering (RRS) the vast majority of these investigation utilized B-band excitation. In the present study resonance Raman spectroscopy with Q-band excitation (λ=595 nm) was employed to investigate the equilibrium heme structures of cytochrome c oxidase at room temperature. Resonance Raman spectra (RRS) were obtained in oxidation-state marker, core-size marker and middle-frequency regions for fully oxidized, two-electron reduced (mix-valenced), three electron reduced and fully reduced species to determine the influences of Cu_A and cytochrome a_3 redox-state upon the heme a vibrational spectrum. These spectra reveal that Q-band scattering is dominated by heme a modes. The behavior of these modes is consistent with the known equilibrium properties of heme a.

Time-resolved RRS using both Q- and B- band excitation were also obtained on ns to ms timescales following CO photolysis from partially reduced species. These data will be discussed within the context of current views of electron transfer dynamics in Cco.

Supported by NIH (GM33330 to MRO and GM22432 to SIC).

Tu-Pos142

TIME-RESOLVED RAMAN STUDIES OF PHOTOINDUCED ELECTRON TRANSFER IN UROPORPHYRIN-CYTOCHROME c.

((Y. Zhou, B. Fan, J. Wang, and M. Ondrias)) Department of Chemistry, University of New Mexico, Albuquerque, NM 87131 (Spon. L. Sparks)

Time-Resolved resonance Raman spectroscopy has been employed to monitor the dynamics of photoinduced electron transfer in electrostatic complexes of uroporphyrin (UroP) and cytochrome c (cyt c). In this system, the photogenerated uroporphyrin triplet state is quenched via electron transfer to ferri-cyt c (Zhou et al., *J. Am. Chem. Soc, 112,* 5074). Resonance Raman spectroscopy can be used to monitor both the kinetics and structural dynamics associated with electron transfer. Our preliminary results confirm that rapid electron transfer ($K > 10^6$ S^{-1}) occurs from UroP* to cyt c. However, the low yields require the addition of sacrificial oxidants or reductants to the solution in order to probe structural dynamics on sub-millisecond timescales. Supported by the NIH (GM 33330).

Tu-Pos143

MULTIPLE FE-CO STRETCHING MODES IN TERMINAL OXIDASES.

((J. Wang, Y.-c. Ching, & D. L. Rousseau))
AT&T Bell Laboratories, Murray Hill, NJ 07974.

The resonance Raman spectra of CO-bound bovine cytochrome *c* oxidase and bacterial quinol oxidase reveal multiple Fe-CO stretching modes. In the mammalian enzyme the lines are located at 494 and 520 cm^{-1}. In cytochrome *bo* from *E. coli*, the lines are found at 496 and 521 cm^{-1} confirming a prior report [Uno, *et al., J. Biol. Chem.* **260**, 6755 (1985)] of the resonance Raman spectra of the CO-bound form of this bacterial enzyme. The pH dependence of the intensity of these lines and the ease of photodissociation of them in each type of protein was also studied and it was found that the behavior in the two proteins was very different. To account for these data, distal interactions with the bound CO and properties of the proximal ligand bond are considered. An analysis of the data from the mammalian enzyme indicates that the proximal ligand may not be a histidine in the CO-bound derivative or if it is histidine the iron-imidazole bond has unique properties. Based on these data the possibility of ligand exchange on cytochrome a_3 is put forth as a mechanism for redox linkage to proton translocation. (Supported by a NIH grant GM-39359 (JW).)

Tu-Pos144

RESONANCE RAMAN STUDIES OF THE REACTION OF YEAST CYTOCHROME *C* PEROXIDASE WITH OXYGEN.

((J. Wang**, D. L. Rousseau**, H. Anni*, &T. Yonetani*)) *University of Pennsylvania Medical School, Department of Biochemistry and Biophysics, Philadelphia, PA 19104-6089 and **AT&T Bell Laboratories, Murray Hill, NJ 07974.

The reaction of yeast cytochrome *c* peroxidase (CcP) with oxygen was studied with the flow-flash-probe technique by mixing the carbon monoxide-bound ferrous enzyme with oxygen-saturated buffer and photodissociating the CO to initiate the reaction. CO-photolysis control experiments were done to measure the time of CO recombination. The reaction of oxygen with the ferrous enzyme occurred much faster than CO recombination. Within 100 μs, a reaction product was obtained that had a resonance Raman spectrum characteristic of compound ES. Evidence for other earlier intermediates was not found on this time scale. The data on CcP, compared to those obtained on horseradish peroxidase under similar conditions, reflect the different protein environment in the two peroxidases suggesting the contribution of more "active" or "labile" endogenous donors in CcP. (Supported by grants from NSF 76-16796, NIH HL-14508 (TY); Research foundation of the University of Pennsylvania 3-71501 (HA); and NIH GM-39359 (JW).)

Tu-Poe145

^{1}H-NMR STUDIES OF PROTEIN-PROTEIN ASSOCIATION AND FERRICYTOCHROME *c* EXCHANGE DYNAMICS IN COMPLEXES BETWEEN CYTOCHROME *c* PEROXIDASE AND VARIOUS FERRICYTOCHROMES *c*, Qiang Yi, Yihong Ge, James D. Satterlee and James E. Erman Departments of Chemistry, Washington State University, Pullman, WA 99164-4630 and Northern Illinois University, DeKalb, IL 60115

Cytochrome *c* peroxidase(CcP)/Ferricytochrome *c* (ferri- Cyt.*c*) complexes have been used as models for studying electron transfer in biology. Knowing the structure, stoichiometry and dynamics of protein-protein interactions is essential to understanding this type of long-range electron transfer. ^{1}H-NMR spectroscopy has been used to examine the stoichiometry and exchange dynamics of CcP/ferriCyt.*c* complexes and CcP-CN/ferriCyt.*c* complexes. Changes in ferriCyt. *c* ^{1}H hyperfine shifts when titrated by either CcP or CcPCN indicate the formation of binary complexes between these two heme proteins, and extensive experiments reveal the stoichiometry of the complexes as 1:1. The simul- taneous detection of both free and bound forms of yeast-iso1 ferriCyt.*c* further reveals a slow exchange process on the NMR time scale. This has enabled us to use dynamic NMR techniques, such as inversion transfer, to study the exchange process in this system. Numerical analysis of the data from inversion transfer experiments, analyzed using the McConnell-modified Bloch Equations, has given estimates of 1--4ms for the life-time of the complex under various conditions of temperature and concentration (ranging from ~1 mM to ~200 μM in total protein).

Tu-Poe146

UNUSUAL REACTIVE-SITE DYNAMICS OF A82-CYTOCHROME C PEROXIDASE STUDIED BY 1D AND 2D PROTON NMR SPECTROSCOPY, James D. Satterlee, Steve Alam, James E. Erman[1], J. Matt Mauro[2], Thomas L. Poulos[3] Departments of Chemistry, Washington State University, Pullman, WA 99164-4630, [1]Northern Illinois University, DeKalb, IL 60115; [2]Center for Advanced Research in Biotechnology, 9600 Gudelsky, Drive, Rockville, MD 20850; and [3]Department of Molecular Biology/ Biochemistry, University of California, Irvine, CA 92717

Yeast cytochrome *c* peroxidase is a 34 kDa ferriheme enzyme that has become a paradigm for studying redox-related protein-protein association and long-range electron transfer. An approach that we are pursuing in attempting to dissect the mechanism of this enzyme's function is through use of site specific mutants designed to probe "second sphere" interactions. The mutations made are for testing potentially significant structure/function relationships, but ones that are removed by one molecular layer from the enzyme's heme active-site. One locus for mutations is primary sequence position 82 (N in wild-type enzyme) where the peptide carbonyl acts as a hydrogen bond acceptor from the functionally critical "distal histidine". Two mutants have been studied so far, D82N and A82N. The latter produces proton NMR spectra at 500 MHz that is characteristic of two enzyme forms. These are detected by splitting of proton hyperfine-shifted resonances. The two enzyme forms are interconvertible by temperature so that the equilibrium and kinetics exchange dynamics for the interconversion have been quantitated by both 1D and 2D proton NMR spectroscopy.

Tu-Poe147

CHARACTERIZATION OF PROTEIN CONFORMATIONS BY SPECTRAL HOLE BURNING. ((J. Fidy, J. M. Vanderkooi, J. Zollfrank and J. Friedrich)) Semmelweis Medical Univ., Budapest, Hungary; Dept. Biochem. Biophys., Univ. Penn., Philadelphia PA; Physikalisches Institute, Univ. Bayreuth, Germany. (spon. J. R. Williamson)

The substituted fluorescent enzyme, mesoporphyrin (MP) horseradish peroxidase, was studied by spectral hole burning, performed in fluorescence excitation mode. Spectral holes with a width of about 0.1 cm^{-1} were burnt into the 0,0 bands of selected tautomeric forms of MP which are stabilized by interactions with the protein. Following burning at 1.5 K and atmospheric pressure, the spectrum of the burnt line/hole was measured under increasing pressure (Δp) up to 2 MPa, and the shift and broadening of the hole were observed. The changes were totally reversible within the pressure range studied. The line shift, Δν, was a linear function of Δp, and Δν/Δp was linear with the burn frequency. By using the theoretical model of Laird and Skinner (J. Chem. Phys. 1989, 90:3274), the heme crevice and the protein conformation could be characterized by the protein induced shift of the electronic transition energy and the isothermal compressibility of the protein molecule, respectively. The binding of a H-donor near the porphyrin in the enzyme induced a significant gross conformational change in the protein shown by a compressibility increase from 0.14 to 0.4 GPa^{-1} for the complex. pH changes also lead to compressibility changes, and new tautomeric forms of MP were found stabilized in the heme crevice when changing the pH from 5 to 8. (Supported by NSF DM88-15723, NATO grant 210103 and by DAAD).

Tu-Poe148

FLUORESCENCE LINE NARROWING STUDIES OF MESOPORPHYRIN-SUBSTITUTED CYTOCHROME C PEROXIDASE AND ITS COMPLEX WITH CYTOCHROME C.
((H. Anni, J.M. Vanderkooi, S.C. Hopkins, T. Yonetani and J. Fidy)) University of Pennsylvania, Medical School, Department of Biochemistry and Biophysics, Philadelphia, PA 19104-6089.

Fluorescence emission spectra of mesoporphyrin-substituted cytochrome c peroxidase (MP-CcP) were measured in 50 % glycerol at 77 K and were further resolved when obtained at liquid helium temperature. With excitation at the higher vibronic S_1 levels, interconverting emission lines in the fluorescence line narrowing spectra at 5 K have been detected in MP-CcP, originating from the four possible positions of the two inner-porphyrin hydrogens. The tautomerization reaction was then used to follow conformational changes of MP-CcP with pH in the range pH5-8. In comparison with the earlier data in MP-horseradish peroxidase (Fidy et al., Biophys. J. 1992, 61, 381-391) the fluorescence energy selection spectra in MP-CcP under the same conditions are significantly altered, reflecting the different protein environment in the two peroxidases. Our fluorescence line narrowing data imply ionic strength-dependent changes in the tautomeric distribution of MP-CcP when complexed with its native redox partner, ferrous cytochrome c, in a ratio of cyt c:MP-CcP = 1 or 2. (Supported by NSF grants DM 88-15723 (JMV), DMB 76-16796 (TY), and NIH grant HL-14508 (TY).

Tu-Poe149

PHOTOREDUCTION DYNAMICS OF NATIVE AND MUTANT CYTOCHROME c PEROXIDASE.
((J. Wang,[a] M. Miller,[b] Y. Zhou,[a] B. Fan, F. Gao, and M. Ondrias[a])) [a]Department of Chemistry, University of New Mexico, Albuquerque, NM 87131; [b]Department of Chemistry, University of California at San Diego, La Jolla, CA 92093 (F. Allen)

The photodynamics of ferric cytochrome c peroxidase (CCP) have been characterized by using time-resolved resonance Raman spectroscopy. At alkaline pH (>8.5), the heme of ferric CCP undergoes a ligation and spin-state change predicated upon large-scale changes in protein conformation. Concurrent with these changes, native CCP exhibits reversible protoreduction. The 235N mutant of CCP displays appreciable photoreduction even at neutral pH, while 191F CCP does not. These results will be discussed within the context of current theories of electron transfer in CCP. Supported by the NIH (GM 33330).

Tu-Poe150

TIME-RESOLVED RESONANCE RAMAN SPECTROSCOPY OF CHLOROPEROXIDASE INTERMEDIATES ((A.M. Sullivan, C.M. Hosten, V. Palaniappan, M.M. Fitzgerald and J. Terner)) Dept. of Chemistry, Virginia Commonwealth University, Richmond, VA 23284-2006

Chloroperoxidase is a heme enzyme which contains a thiolate ligated heme in common with the cytochrome P-450 enzymes. The intermediates known as compounds I and II are among the least stable of the known peroxidase intermediates. Compounds I and II are two and one oxidizing equivalents above the ferric resting enzyme. We have obtained resonance Raman spectra of these labile intermediates by generating the intermediates with a Ballou four jet mixer, and interrogating the resulting sample jet with low powered laser excitation from several of the near ultraviolet lines of krypton and argon ion lasers. Polarization measurements have been used to determine band assignments. Of interest is the observation that the resonance Raman frequencies for chloroperoxidase compound I are somewhat different from those that we had previously reported for horseradish peroxidase compound I [1]. Nevertheless, the directions and magnitudes of the resonance Raman frequency shifts for compound I relative to compound II are substantially the same for both chloroperoxidase and horseradish peroxidase, supporting $^2A_{1u}$ radical types for both of the respective compound I forms.

[1] V. Palaniappan and J. Terner (1989) J. Biol. Chem. 264, 16046-16053.

Tu-Pos151

HALOPEROXIDASE ACTIVITY OF *PHANEROCHAETE CHRYSOSPORIUM* LIGNIN PEROXIDASES H2 AND H8.*

((S. Farhangrazi, R. Sinclair, I. Yamazaki, L. Powers)) National Center for the Design of Molecular Function, Utah State University, Logan, Utah 84322-4630.

Most haloperoxidases, like lactoperoxidase, bromoperoxidase, and horseradish peroxidase, have higher pH optima for the oxidation of I^- than for Br^-. From the results of our study, pH-activity curves for the oxidation of both electron and hydrogen donors by lignin peroxidases (isozymes, H2 and H8) revealed pH optima of 2.5 for I^-, Br^-, hydroquinone and guaiacol. In general, the oxidation of hydrogen donors such as hydroquinone and phenols by peroxidase systems is favorable near neutral pH, while oxidation of electron donors such as ascorbate, halides, and veratryl alcohol is at acidic pH. The results of our study lead us to conclude that, the haloperoxidase activity of lignin peroxidases is controlled by a kinetic factor such as protonation of the enzyme rather than a thermodynamic factor. Lignin peroxidases are therefore atypical and could be called acid peroxidases. The catalytic activity of peroxidases will be discussed in terms of thermodynamic and kinetic factors.

* Supported in part by NIH-1 P41 RR06030

Tu-Pos152

OXIDATION OF REDUCED YEAST FLAVOCYTOCHROME b_2 BY TRIPLET STATE FREE FLAVINS AND SUBSEQUENT INTRAMOLECULAR ELECTRON TRANSFER

J. T. Hazzard, C. A. McDonough, G. Tollin. Dept. of Biochemistry, Univ. of Arizona, Tucson, AZ. 85721.

We have studied the redox changes occurring within S. cerevisiae flavocytochrome b_2, Flcyt b_2, (lactate dehydrogenase) following its rapid in situ oxidation using the triplet state of lumiflavin or 5-deazariboflavin, (^3F). Initial oxidation of the enzyme occurs at the heme site. The second-order rate constant for this process is 5.0×10^8 M^{-1} s^{-1} for lumiflavin and $\geq 1 \times 10^9$ M^{-1} s^{-1} for deazariboflavin. Re-reduction of the Flcyt b_2 heme occurs by two different processes, depending upon the free flavin used. With lumiflavin, re-reduction occurs predominately by a rapid (2.7×10^7 M^{-1} s^{-1}) bimolecular reaction with reduced flavin generated by the initial oxidation reaction. With 5-deaza-riboflavin, a slow (~ 11 s^{-1}) re-reduction of the b_2 heme occurs which is independent of enzyme concentration. We interpret this to be due to intramolecular reduction of the heme by the enzyme bound FMN. The results are consistent with those reported previously by our laboratory for the intramolecular electron transfer within a one-electron reduced enzyme.

Work supported by a grant from N.I.H. (D.K. 15057 to G.T.).

Tu-Pos153

A MECHANISM FOR NADPH INHIBITION OF CATALASE COMPOUND II FORMATION. ((A. Hillar and P. Nicholls)) Dept. Biol. Sci., Brock University, St. Catharines, Ontario, L2S 3A1, Canada. (Spon. by B.C. Hill)

Mammalian catalase has a nucleotide binding site, each tetramer binding four NADPH molecules. Catalase-bound NADPH both prevents and reverses the accumulation of inactive catalase compound II. A previous scheme for catalase-NADPH interaction involved a role for NADPH in one electron reductions from compound I to compound II and compound II to ferricatalase with free radical forms of NADPH as intermediates (Kirkman,H. N.; Galiano, S. and Gaetani, G.F. (1987) J. Biol. Chem., Vol **282**, 660-666). But NADPH effectively prevents accumulation of bovine liver catalase compound II generated by 'endogenous' donors under conditions of steady H_2O_2 formation without reacting rapidly with either compound I or compound II. It thus differs from both 2-electron donors of the ethanol type, and 1-electron donors of the ferrocyanide/ascorbate type. NADPH also inhibits compound II formation induced by the exogenous one-electron donor ferrocyanide. A catalase reaction scheme is proposed in which the initial formation of compound II from compound I involves production of a neighbouring radical species. NADPH blocks the final formation of stable compound II by reacting as a 2-electron donor to compound II and to this free radical, located in the protein between the NADPH binding site and the catalytic site. The proposed radical behaviour resembles that of labile free radicals formed in cytochrome *c* peroxidase and myoglobin. Such radical migration patterns within heme enzymes are an increasingly common motif. Supported by Canadian NSERC grant #A-0412 to PN.

Tu-Pos154

SITE-DIRECTED MUTANTS OF HPII CATALASE FROM *E. COLI*. ((P. Nicholls*, B. Tattrie*, A. Hillar*, J. Switala & P. Loewen)) Dept. Microbiology, Univ. Manitoba, Winnipeg, Man., and *Dept. Biol. Sci., Brock Univ., St. Catharines, Ont., Canada.

Wild-type and mutant *E. coli* HPII catalases contain haem d or protohaem as determined by relative absorbances at 630-660nm & 715-750nm or by pyridine haemochromogen. Wild-type has nearly all haem d, H128N & H128A nearly all protohaem. N201A & N201Q have haem d with a little protohaem, N201H protohaem with a little haem d. Wild-type and N201 mutants show ligand-binding and catalytic activity; H128 mutants are inactive and do not bind ligands. N201A, H, & Q show much lower activities than wild type, but titrations with peroxide in presence of azide indicate essentially all haems remain active at the lower level. Azide and cyanide binding are biphasic with N201 mutants and wild type enzyme, indicating high- and low-affinity haem populations. In the case of N201A & H titrations show almost equal amounts of these two haem 'types' while absolute spectra suggest only small quantities of a second haem (proto or d). There must be conformational differences between subunits of HPII, probably a hexamer, as well as >1 haem type, complicating interpretation of functional change consequent upon single residue substitution. We conclude that the putative distal histidine H128 is essential for both inhibitor(HCN) and substrate(peroxide) binding. N201, a conserved distal asparagine, stabilises ligands or HOOH in the haem pocket but is not essential. Mutation of either can modify haem-binding or haem-modification specificity so that protohaem incorporation/retention is preferred over that of haem d. Supported by NSERC (Canada) operating grants to PN and to PL.

Tu-Pos155

A CATALASE GENE FROM ALKALIPHILIC *BACILLUS FIRMUS* OF4 IS PRECEDED BY A *FUR* SEQUENCE. ((P.G. Quirk, T.A. Krulwich, and D.B. Hicks)) Dept. of Biochemistry, Mount Sinai School of Medicine of CUNY, New York, NY 10029.

A fragment of *B. firmus* OF4 DNA isolated from a genomic library contained an incomplete ORF comprising the first 449 aa of a protein with 67% identity to *E. coli* catalase HP-II, and designated katA. The GenBank accession number is LO2551. A chlorin-containing catalase protein of 83 kDa was purified from the alkaliphile and shown by N-terminal sequence analysis to be the product of this ORF. Upstream of the ORF was a 19 bp region of dyad symmetry, AAAAATGGTCATCATTTTC, of which 14 of the bases are identical to the consensus *E. coli fur* sequence, a transcriptional regulator of genes involved in iron metabolism (1). A similar sequence has been detected upstream of a *L. seeligeri* catalase gene (2). The function of such a regulatory system in the alkaliphile might be to allow increased production of catalase at more alkaline pH, where respiration produces increased amounts of toxic oxygen radicals.

(1) De Lorenzo et al. (1987) J. Bacteriol. 169:2624-2630.
(2) Haas et al. (1991) J. Bacteriol. 173:5159-5167.

Tu-Pos156

AMINOLEVULINATE SYNTHASE: A POSSIBLE DUAL ROLE FOR THE PYRIDOXAL 5'-PHOSPHATE BINDING LYSINE RESIDUE.

(G.C. Ferreira and U. Vajapey) University of South Florida College of Medicine and Institute of Biomolecular Science, Tampa, FL 33612. (Spons. by G.C. Ferreira)

5-Aminolevulinate synthase (ALAS) (E.C. 2.3.1.37) is the first enzyme of the heme biosynthetic pathway in non-plant higher eukaryotes. ALAS catalyzes the condensation of glycine with succinyl-CoA to yield 5-aminolevulinic acid. It requires pyridoxal 5'-phosphate (PLP) as an essential cofactor and is functional as a homodimer. Murine erythroid ALAS has been recently purified from an *Escherichia coli* overproducing strain. In addition, murine erythroid ALAS lysine-313 was identified as the residue involved in the Schiff base linkage between the cofactor and the enzyme.

Site-directed mutant variants of ALAS, in which lysine-313 (K-313) was replaced by alanine, histidine, arginine or glycine, bind PLP and form external aldimines with the incoming substrate (glycine), although they do not exhibit enzyme activity. Spectroscopic and catalytic characterization of the K-313-directed mutants in relation to the wild-type enzyme led us to propose a dual role for the lysine-313: in formation of an internal aldimine with the PLP cofactor and in catalysis.

Supported by grants from NSF (MCB-9206574), AHA (92GIA/829) and ACS Junior Faculty Award (JFRA-401).

Tu-Pos157

SULFUR CONTAINING COBALAMINS: EXAFS AND CYCLIC VOLTAMETRIC CHARACTERIZATION.

((E. M. Scheuring[1], I. Sagi[2], M. R. Chance[1])) [1]Albert Einstein Col of Med, Bronx, N.Y. 10461; [2]Weizmann Institute of Science, Rehovot 76100, Israel

Sulfur containing cobalamins are thought to have a special role in the intracellular conversion of cyanocobalamin (CN-Cbl or vitamin B_{12}) to its coenzyme forms through a Co(I) intermediate. Glutathionylcobalamin (GS-Cbl) is especially interesting as a possible precursor of cobalamin coenzymes (*Ann. NY Acad. Sci., 1969, 112,* 580). Pezacka and co-workers show (*Biochem. and Biophys. Res. Comm., 1990, 169,* 443) that the formation of adenosylcobalamin (Ado-Cbl) from GS-Cbl was accelerated compared to Aq-Cbl using cell extracts. Decyanation of CN-Cbl results in sulfitocobalamin (HSO_3-Cbl) and requires the presence of reduced glutathione. Intracellular CN-Cbl must first undergo a CN-elimination reaction followed by GS-Cbl formation that serves as an intermediate in the biosynthesis of methyl-Cbl and Ado-Cbl.

In this study three sulfur containing cobalamin derivatives (GS-Cbl, HSO_3-Cbl and cysteinylcobalamin) have been characterized by Extended X-ray Absorption Fine Structure (EXAFS) analysis. The Co-S bond distance for Cys-Cbl was found to be 2.33Å while the distance from Co to the axial base was 2.13Å. The distances have been compared to those obtained from the Cambridge Crystallographic Structural Database. GS-Cbl has been selected for cyclic voltametric studies to examine the redox behavior of sulfur containing cobalamins using CN-Cbl as reference. We have found that under the same experimental conditions GS-Cbl can be reduced more easily than CN-Cbl. This result is very important in the understanding of the physiological significance of sulfur cobalamins. This research is supported by USDA/NRICGP-CSRS Program in Human Nutrients #91-37200-6180.

Tu-Pos158

LASER PHOTOLYSIS OF ALKYL-COBINAMIDES: MODELS FOR HOMOLYTIC AND HETEROLYTIC COBALAMIN ENZYMES

((A.M. Brownawell, E. Chen, M.R. Chance*)) Georgetown University and *Albert Einstein College of Medicine, Bronx, NY 10461

Vitamin B_{12} coenzymes are essential cofactors in enzymatic reactions of mammalian metabolism, including the conversion of methylmalonyl-CoA to succinyl-CoA (homolytic cleavage) and the synthesis of methionine from homocysteine (heterolytic cleavage). It is well established that the cobalt-carbon bond of many B_{12} enzymes is cleaved homolytically (forming radical species) upon interaction with enzymes in vivo, such enzymes generally have a 5'-deoxy-adenosylcobalamin cofactor. We have developed an in vitro method to study the homolytic cleavage of this bond in an attempt to better understand the structural and kinetic features of the cleavage mechanism. Methylcobalamin dependent enzymes involve methyl transfer and a heterolytic cleavage of the cobalt-carbon bond. Our study used photolysis to induce homolysis. By synthesizing various alkylcobalamins and alkyl-cobinamides (five coordinate complexes where the axial base is absent) that induce strain and destabilize the Co-C bond based on the bulk of the alkyl group, we observe the influence of the axial ligands on reactivity.

We have determined the quantum yields of photolysis for methylcobinamide (0.42 ± 0.01) and ethylcobinamide (0.41 ± 0.01). Photolysis was performed using a CW HeCd laser and changes in the optical spectra due to photolysis are followed. The quantum yields of photolysis of the cobinamides are compared with those for the analogous cobalamins obtained previously. In this manner we hope to elucidate the mechanism of homolytic cleavage. This work has been supported by a grant from NRICGP-CSRS, USDA Program in Human Nutrients # 91-37200-6180.

SPECTROSCOPIC STUDIES (FLUORESCENCE) II

Tu-Pos159

STRUCTURES OF MELANOTROPIN PEPTIDES IN MODEL LIPIDS BY TRYPTOPHAN FLUORESCENCE STUDIES. ((A.S.Ito* and A.G Szabo**)) *Inst. de Física, Universidade de São Paulo, C.Postal 20516, 01498 São Paulo, Brazil and **Inst. for Biological Sciences, NRC Canada.

Steady-state and time-resolved fluorescence spectroscopy was employed in the study of α-MSH (alpha-melanocyte stimulating hormone) and analogues. In the presence of charged lipid vesicles, increase in fluorescence intensity and in fluorescence anisotropy, and blue shift of maximum emission, indicated incorporation of the peptides into the liquid-crystalline phase, above the phase transition temperatures. The association constants for lipid-peptide interactions were determined using binding isotherms corrected for electrostatic interactions through Gouy-Chapman potentials. The constants are higher for analogues showing increased potencies and prolongation of response, as compared to the native hormone. Fluorescence decay of peptides obeys a tri-exponential process. The pre-exponential terms in the lipid-peptide complex are different from the values in aqueous phase, indicating structural modifications of the peptides. It is suggested that the hormones accumulate near the surface of the vesicles through electrostatic interaction and incorporates into the lipid phase due to hydrophobic interactions and/or conformational changes.

Financial support: FAPESP and USP-BID agreement.

Tu-Pos160

DETECTION OF WATER PROXIMITY TO TRYPTOPHAN RESIDUES IN MEMBRANE PROTEINS BY SINGLE PHOTON RADIOLUMINESCENCE ((S. Bicknese, D. Zimet, A.N. van Hoek, S.B. Shohet and A.S. Verkman)) UCSF, CA

We recently developed a *Single Photon Radioluminescence* (SPR) technique to measure submicroscopic distances of up to 100 nm in biological samples (Bicknese *et al*, and Shahrokh *et al*, Biophys. J. 63: Nov. 1992). *SPR* is based on the ability of a fluorophore to "capture" the energy dissipated by a ^3H beta electron as it interacts with the environment. To detect very small SPR signals, we have constructed a sample compartment consisting of a truncated ellipsoidal mirror containing the sample vial at one focus, and the quartz window of the cooled PMT housing at the second focus. Cut-on filters were used to reduce Bremsstrahlung background signal. This arrangement gave a 4-fold increase in photon collection efficiency and a >5-fold improvement in measurement precision.

To determine the accessibility of water to membrane protein tryptophans, the tryptophan SPR signal produced by ^3H_2O decay was measured by photon counting and multi-channel discrimination. Background signal produced by extramembrane water was determined from the tryptophan SPR signal produced in an equivalent sample containing ^3H-methylglucose (^3HMG). Measurements were carried out on erythrocyte KI-IOVs, where the majority of tryptophan fluorescence arises from band 3, water channel CHIP28 vesicles, and vesicles containing lens protein MIP26. KI-IOV's (10 mg/ml protein), MIP26 vesicles (2.5 mg/ml) and CHIP28 vesicles (0.6 mg/ml) were suspended in 10 mM Na phosphate (pH 7.4) containing ^3H_2O or ^3HMG (65 to 250 μCi/ml). SPR signals (mean ± SE [cps/mg/μCi] n=3-7) were 0.087 ± 0.005 (^3H_2O) and 0.070 ± 0.004 (^3HMG) for KI-IOVs, 0.86 ± 0.02 (^3H_2O) and 0.88 ± 0.02 (^3HMG) for MIP26 vesicles, and 0.38 ± 0.03 (^3H_2O) and 0.27 ± 0.03 (^3HMG) for CHIP28 vesicles. SPR signals for ^3H_2O were greater than for ^3HMG water channel CHIP28 vesicles, indicating water > methylglucose proximity to tryptophan residues. These results demonstrate the ability to detect weak SPR signals from protein tryptophans and provide a novel method to establish accessibility of water to putative aqueous channels traversing proteins.

Tu-Pos161

PARAMAGNETIC QUENCHING IN NATIVE AND MODEL MEMBRANES: CORRELATION BETWEEN FLUORESCENCE LIFETIME AND STERN-VOLMER QUENCHING CONSTANT.

((B.V. Nguyen, C.F. Valenzuela, and D.A. Johnson)), Div. of Biomed. Sci. and Depart. of Neurosci., U.C., Riverside, CA 92521. (Spon. by E.A. Nothnagel)

The quenching by paramagnetic compounds in lipid membranes is generally assumed to occur at the diffusion limit; consequently, fluorophores with fluorescence lifetimes (τ) below 10-15 ns are thought to be poorly quenched by dynamic mechanisms. However, recent studies have demonstrated that paramagnetic quenching in aqueous solutions is not diffusionally dependent but rather a distance-dependent (15-20Å center-to-center) electron-exchange process. To contribute to this issue for membrane-partitioned fluorescent probes, we examined the time-resolved and steady-state quenching of five hydrophobic fluorophores by the nitroxide radical TEMPO in cyclohexane, *Torpedo* electroplax plasma membranes (TEPM), and egg PC bilayers. The probes studied were perylene, DPH, triphenylene, phenanthrene, and pyrene with fluorescent lifetimes in TEPM of 4.4, 9.1, 33, 45, and ~200 ns, respectively. Our results indicated that: (1) The intrinsic quenching efficiencies (γ) in cyclohexane varied between 0.3–2.8. (2) Within a factor of 5, no correlation was observed between the fluorescent lifetimes of the probes (with $\tau \leq 45$ ns) and the steady-state or the lifetime Stern-Volmer quenching constants. (3) Significant lifetime quenching was detected with all probes. The existence of significant lifetime quenching of probes with a $\tau < 10$ ns suggests that short range non-translational or orientational processes (rotational, wobbling, etc.) produce lifetime quenching in lipid membranes. (Support: NSF grant BNS-8821357)

Tu-Pos162

A GENERAL MODEL OF DYNAMIC QUENCHING: REVISITED.

((J. Carrero & E. Gratton)) Univ. of Illinois at U-C, Laboratory for Fluorescence Dynamics, Dept. of Physics, 1110 W. Green St., Urbana, IL 61801.

Gratton et al. (1984) outlined a model for dynamic quenching of a fluorophore in the protein interior. This model reconciled the apparent contradiction resulting when the classical Stern Volmer analysis, which can be applied to a free fluorophore in solution, is used for the analysis of the quenching behavior of internally buried fluorophores of proteins (Vaughn & Weber 1970, Lackowicz & Weber 1973). Gratton et al. proposed that, for internally buried fluorophores with single exponential decays, the presence of quencher molecules leads to doubly exponential decay times. These decay times or rates are eigenvalues that encompass the acquisition rate of the quencher by protein, the migration rate of the quencher in the protein interior, and the exit rate from the protein. Longer lifetime probes necessitate less quencher concentration and will respond to the acquisition rate of the quencher by the protein. Shorter lifetime probes, due to the greater quencher concentration needed to cause quenching, will respond to the migration rate of the quencher within the protein. These rates, having different orders of magnitude, result in different quenching behavior. In this study, the quenching by O_2 of Zinc Protoporphyrin IX reconstituted Horse Skeletal myoglobin (ZNPPIXGLOBIN) is monitored using frequency domain lifetime acquisition in the MHz frequency range at two emission wavelengths as a function of temperature. The advantage of the ZNPPIXGLOBIN system is the presence of two distinct lifetimes that are present at zero quencher concentration. Selection of emission wavelengths allows the study of each lifetime individually on the same sample. According to the model, the two lifetimes (2.9ns @ 595nm, 5ns @ 630nm) of the ZNPPIXGLOBIN will highlight the migration rate of the quencher within the protein to different degrees. Comparison of the data with the aforementioned model will be made. [Gratton, Jameson, Weber & Alpert, 1984, *Biophysical J.* 45:789-794; Vaughn & Weber, 1970, *Biochemisrty* 9:466-473; Lackowicz & Weber, 1973; *Biochemistry.* 12:4171-4179.] Supported by NIH RR03155.

Tu-Pos163

CHARACTERIZATION OF TWO HUMAN MONOCLONAL ANTIBODIES BY CIRCULAR DICHROISM AND FLUORESCENCE SPECTROSCOPY.
((Joseph E. Curtis, Christy A. Sasiela, and Sam L. Helgerson)) Baxter Biotech Group, Immunotherapy Division, Duarte, CA 91010

Two human monoclonal antibodies directed against *Pseudomonas* flagellar protein antigens were studied using spectroscopic methods. The two IgG antibodies, mAb-A and mAb-B, have kappa and lambda light chain variable regions, respectively. Circular dichroism and fluorescence spectroscopies are being used to characterize the native protein structure and lot-to-lot uniformity of these mAb preparations. Both antibodies had similar deep ultraviolet circular dichroism spectra (260 -182nm), with CD intensity values of -1.35 $\Delta\varepsilon$ at 217 nm, 1.7 $\Delta\varepsilon$ at 201 nm and zero crossings at 208-209 nm and 190-192 nm. The extinction coefficients at 280 nm were determined to be 1.60 $(cm[mg/mL])^{-1}$ for mAb-A and 1.55 $(cm[mg/mL])^{-1}$ for mAb-B. This corresponds with the similar tryptophan contents of mAb-A (12 trp) and mAb-B (11 trp) determined from the cDNA sequences of the IgG variable regions and by assuming conserved tryptophan contents for the constant regions. However, the intrinsic fluorescence emission for the native proteins was significantly different. The relative fluorescence emission intensity of mAb-A (Emax 340 nm) was 45% less than that of mAb-B (Emax 335 nm). When the proteins were denatured in 6 M guanidine hydrochloride, the fluorescence intensity of mAb-A (E max 352 nm) was 8% greater than mAb-B (Emax 352 nm) as expected from their tryptophan content. The lower fluorescence intensity from mAb-A was not due to increased solvent exposure of its tryptophan residues relative to mAb-B. This was shown by the effect of adding an ionic fluorescence quencher, potassium iodide (0.3M KI), which lowered the emission intensity by less than 15% for both mAb-A and mAb-B. Also, the polarization of the fluorescence emission was constant from 310-380 nm with anisotropy values of 0.35 for mAb-A and 0.37 for mAb-B, independent of the addition of KI. In order to determine the reason for differences in the native protein fluorescence, Fab fragments are being isolated and characterized. Near-ultraviolet circular dichroism and fluorescence spectra of these preparations will localize the tryptophan residues responsible for the observed fluorescent properties.

Tu-Pos164

CHARACTERIZATION OF AFFINITY AND STOICHIOMETRY OF ANTIGEN-ANTIBODY INTERACTION USING A HOMOGENEOUS FLUORESCENCE QUENCHING ASSAY. ((M.M.Lopez. ;M.V.Alvarez. P.Lillo ;U.Acuña)) Consejo Superior de Investigaciones Cientificas. Madrid (SPAIN).

We have developed a methodology to study the heterodimer GPIIb/IIIa (fibrinogen receptor in human platelets) in a homogeneous phase using monoclonal antibodies (IgG (M6)) which have bound Fluorescein-Isotiocianate (FITC).This technique is easy to implement,inexpensive and fast and its sensitivity allows measurement of dissociation constants in the range 1x10-7 - 5x10-10 M when the molar probe/protein ratio is one.Using the quenching of fluorescence intensity,we have been able to determine the stoichiometry (n) and the dissociation constants for the interaction of M6/FITC with GPIIb under equilibrium conditions,and in different levels of biological organization: plasma membrane of human platelets Kd = (1.3±0.2)x10-8 M , and in whole platelet Kd = (2.2±0.2)x10-8 M. So the homogeneous fluoroassay has allowed us to: 1) determine the quantity of GPIIb in lysate of platelets (1.7% of the total protein in platelet) and the number of molecules of GPIIb exposed in the surface of the platelet (88±20)x103 molecules of GPIIb/platelet; 2) observe changes in the conformation of GPIIb depending on whether it was isolated in solution or as GPIIb/IIIa,or in the membrane or in the whole platelet; and 3) design an antigenic map taking into account the competition between M6/FITC and another monoclonal antibody such as anti-GPIIIa or anti-GPIIb whose epitopes have been determined before in the sequence of the glycoproteins.(This work was supported by Proyecto SEUI PB 86-0629 and PM 88-022).

Tu-Pos165

TIME-RESOLVED ANISOTROPY OF FLUORESCEIN BOUND TO THE ANION CHANNEL AND CYTOPLASMIC DOMAIN OF BAND 3 IN ERYTROCYTE MEMBRANES. ((B.J-M. Thevenin, N. Periasamy, S.B. Shohet and A.S. Verkman)) Dept. Lab. Med., UCSF, San Francisco, CA 94143.

To examine the influence of pH and other potential effectors on band 3 conformation, two strategic sites on band 3 were selectively labeled by fluorescein maleimide in stripped erythrocyte membranes: *site 1*, the cysteine cluster next to the hinge in the cytoplasmic domain (cdb3), and *site 2*, cys 479 in the anion channel membrane domain. Carbonic anhydrase (CA) was labeled as a control. Labeling specificity was demonstrated by SDS-PAGE, and time-resolved fluorescence was measured by parallel acquisition frequency-domain microfluorimetry. All samples had a single component fluorescein lifetime of ~ 4 ns. Multifrequency phase and modulation data (5-200 MHz) fitted well to a two-component hindered rotator model for anisotropy decay, but not to a one component model. At *site 1*, the two correlation times were 150 ps (fraction ~ 0.7) and 4 ns; corresponding r_∞ values decreased sharply (0.12 to 0.02, fast rotation; 0.31 to 0.04, slow rotation) as pH increased from 6 to 10. A similar pH-dependence was also obtained after chymotryptic release of cdb3. Ionic strength, 2,3-DPG, Ca^{++} and glycolytic enzyme binding weakly influenced fluorescein rotation at *site 1*. At *site 2*, r_∞ values at pH >7.5 were greater than at *site 1* (fast: ~ 0.10, slow: ~ 0.19) and not significantly pH-dependent; both r_∞ increased below pH 7.5. Similar results were also obtained with cdb3-cleaved samples and intact membranes. Ionic strength and 2,3-DPG binding significantly altered fluorescein rotation at *site 2*. The anisotropy of control CA was not pH-dependent. Thus, *a)* probe rotation at *site 1* becomes restricted at low pH when cdb3 structure is most compact, and *b)* the environment at *site 2* is crowded, yet structurally sensitive. These results support the utility of time-resolved anisotropy to examine physiological changes in band 3 structure.

Tu-Pos166

TIME-RESOLVED FLUORESCENCE MEASUREMENTS OF CALCIUM-CHELATING PROBES: QUANTITATION OF CATION BINDING ((K.M.Hirshfield, D.Toptygin, B.Z.Packard*, and L.Brand)) Dept. of Biology, The Johns Hopkins University, Baltimore, MD 21218; *Division of Cytokine Biology, CBER, FDA, Bethesda, MD 20892.

Steady-state fluorescence enhancements and fluorescence lifetime changes associated with cation binding to calcium-chelating probes, e.g. Quin-2 and Calcium Green, have been described. Previous work from our lab showed that free Quin-2 and the calcium and magnesium Quin-2 complexes have unique fluorescence decay times(Wages et al., 1986, Biophys. J., 51, 284A). We have used these changes to quantitate ion concentrations and determine dissociation constants. We describe a single frequency phase/modulation approach to assess the fraction of cation bound and the K_d. This technique has been applied to systems with two or more states, e.g. Quin-2 titration with calcium in the absence or in the presence of magnesium. Nanosecond time-resolved fluorescence spectroscopy offers additional information to that of steady-state since it is highly sensitive to probe heterogeneity. As these probes are used extensively in cellular measurements where a high degree of heterogeneity is likely to exist, we explore the possibilities of using single frequency phase/modulation measurements in Quin-2 loaded cells.[Supported by NIH Grant GM11632, NSF Grant DIR 8721059 and a gift from the W.M. Keck Foundation to The Institute for Macromolecular Assemblies].

Tu-Pos167

GLOBAL TARGET ANALYSIS OF SPECTROSCOPIC BINDING DATA. ((D.Toptygin and L.Brand)) Department of Biology, The Johns Hopkins University, Baltimore, MD 21218.

Spectroscopic methods are often utilized in studies of binding equilibria of biological macromolecules. Although complex binding models are often inferred the treatment of spectroscopic data is frequently oversimplified by assuming that for every chemical interaction, a spectroscopic "observable" can be selected that will reflect only the fractional completion of that interaction. In fact spectroscopic data such as absorption spectra or fluorescence spectra or decay curves may depend on the concentrations of the species involved in more than one interaction. A family of spectra and/or decay curves obtained during the course of multiple titrations can be decomposed into basic components in an infinite variety of different ways. Straight forward application of the mathematical method known as singular value decomposition yields components that may not be associated with actual chemical species. In this report we describe a data analysis program, SPECTRABIND. The model equilibrium equations are used as constraints in the analysis of the entire data set. No assumption of the parametric form of the component spectra and/or decays is made. The program evaluates the binding constants and provides the resolved spectra and/or decays associated with the actual species. The conditions necessary and sufficient for the existence of a unique solution are considered. (Supported by NIH grant No. GM11632).

Tu-Pos168

STUDY OF INTRAMOLECULAR INTERACTIONS OF LIPIDS BY FREQUENCY-DOMAIN FLUORESCENCE SPECTROSCOPY.
((L.I. Liu, K.H. Cheng and P. Somerharju)) Texas Tech University, Lubbock, TX 79409 and University of Helsinki, Helsinki, Finland.

The intramolecular interactions among the acyl chains at different depths of the lipid layers in the gel (Lβ), liquid crystalline (Lα) and inverted hexagonal (HII) phases were investigated. Upon incorporating a small amount (0.1%) of dipyrenyl labeled lipids of different chain lengths (4, 10 and 14) into DMPC and DOPE lipids, the frequency-domain intensity decays of the monomer and excimer fluorescence of dipyrenyl lipids were measured as a function of temperature. Using a 3-state kinetics model, the effective concentration (C) and the intramolecular excimer formation rate constant (Kdm) of the intramolecular pyrene moieties of dipyrenyl lipids were determined. The values of C were found to increase abruptly at the Lβ-Lα and Lα-HII phase transitions of DMPC and DOPE, respectively. The values of Kdm were not sensitive to the Lβ-Lα transition, but decreased abruptly at the Lα-HII transition. The extent of the above changes depended on the chain length of the dipyrenyl lipids. We concluded that the 3-state kinetics model provides more detailed information about the intralipid acyl chain interactions than does the classical 2-state (or Birks) kinetics model.

Tu-Pos169

CYTOPLASMIC VISCOSITY NEAR THE CELL PLASMA MEMBRANE: MEASUREMENT BY EVANESCENT FIELD FREQUENCY-DOMAIN MICROFLUORIMETRY. ((S. Bicknese, N. Periasamy, S.B. Shohet and A.S. Verkman)) U.C.S.F., CA.

The purpose of this study was to determine whether the unique physical environment just beneath the cell plasma membrane influences the rheology of aqueous-phase cytoplasm. Cytoplasmic viscosity was evaluated from the picosecond rotation of the small fluorophore BCECF by parallel-acquisition Fourier transform microfluorimetry (Fushimi & Verkman, J. Cell Biol. 112:719-725, 1991). Information about viscosity within ~200 nm of cell plasma membranes was obtained by selective excitation of fluorophores in the evanescent field by total internal reflection (TIR) of impulse-modulated s-plane polarized 488 nm laser illumination at a glass-aqueous interface. Measurements of fluorescence lifetime and time-resolved anisotropy were carried out in aqueous solutions containing 140 μM fluorescein or BCECF at known viscosities or monolayers of BCECF-loaded Swiss 3T3 fibroblasts and MDCK cells. Specific concerns associated with time-resolved fluorescence measurements in the evanescent field were examined theoretically and/or experimentally, including variations in lifetime due to fluorophore proximity to the interface and the use of s- and p-polarized excitation. In aqueous solution of fluorescein studied with s-plane polarized light, there was a 5-10% decrease in lifetime (3.8 to 3.6 ns) with TIR compared to trans (subcritical) illumination, but no significant change in rotational correlation time (~100 ps/cP); these findings are in agreement with theory predictions. Lifetimes measured with s- or p-polarized TIR illumination did not differ, whereas anisotropy measurements could be obtained only with s-polarization. Intracellular BCECF had a single-component lifetime of 3.7 ± 0.1 ns near the cell plasma membrane. Apparent aqueous-phase viscosity near the cell plasma membrane was 1.1 ± 0.2 cP (fibroblast) and 1.0 ± 0.2 cP (MDCK), not significantly different from the viscosity measured in bulk cytoplasm far from the plasma membrane. These results establish methodology for measurement of time-resolved fluorescence in the evanescent field, and indicate that the unique physical milieu in cytoplasm near cell membranes has little effect on aqueous-phase viscosity.

Tu-Pos170

ROTATIONAL AND TRANSLATIONAL DYNAMICS OF METABOLITE-SIZED MOLECULES IN THE MITOCHONDRIAL MATRIX. ((James R. Abney,[1] Bethe A. Scalettar[2] and A. S. Verkman[1])), [1]Cardiovascular Res. Institute & [2]Dept. of Biochemistry and Biophysics, UCSF, S.F., CA 94143.

It has been proposed that metabolite diffusion in the mitochondrial matrix is severely impeded due to the high concentration (several hundred mg/ml) of matrix protein. Here this idea was directly tested by introducing metabolite-sized fluorophores (carboxyfluorescein or BCECF) into the matrix of rat liver mitochondria and measuring rates of fluorophore rotation and translation as a function of osmotically induced changes in matrix protein concentration. Rotational dynamics in the matrix was studied using frequency-domain microfluorimetry. Differential phase angles and modulation amplitude ratios were collected at 40 frequencies between 5 and 200 MHz; data were best fit by a two-component isotropic rotator model, demonstrating the presence of unbound (more rapidly rotating) and bound (more slowly rotating) fluorophore. At the highest matrix protein concentrations, ~ half of the fluorophores are bound and the rotational correlation time of unbound fluorophore is < 2-fold that in water. As matrix protein concentration is lowered, fluorophore binding and the rotational correlation time of unbound fluorophore both decrease. Translational dynamics in the matrix was studied experimentally, using FRAP, and theoretically, using a molecular model developed to describe the diffusion of small solutes in concentrated media. The results show that rates of long-range translation of metabolite-sized fluorophores in the matrix are as much as 30-fold slower than in dilute solution. Obstruction of fluorophore motion by protein obstacles and, to a lesser extent, fluorophore binding to protein and increased matrix viscosity produce this slowing of translation. These data suggest that over long time and distance scales motion in the matrix is relatively hindered, but that over short time and distance scales it is not.

Tu-Pos171

SYNTHESIS AND CHARACTERIZATION OF A SOLVATOCHROMIC, LIPOPHILIC FLUORESCENT OXAZONE ((Todd Brugel[a] and Brian Wesley Williams[b])) [a]Chemistry Dept., Muhlenberg College, Allentown, PA and [b]Chemistry Dept. Bucknell University, Lewisburg, PA 17837.

Fluorescent probes such as PRODAN, LAURODAN, and Nile Red have increasingly been used to characterize membrane, protein and micelle properties. For Nile Red, a perceived limitation has been the lack of an acyl chain substituent enhancing solubility in lipid membranes. By analogy to Nile Red, we have recently begun exploration of the synthesis of solvent sensitive oxazones possessing acyl chain substituents. In particular, the simple reaction

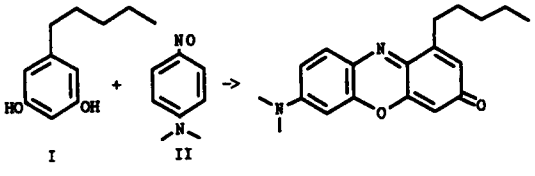

between olivetol (I) and 4-nitroso-N,N-dimethylaniline (II) has been used to produce the 1-pentyl-7-dimethylamino-3H-oxazone. Data relating to the fluorescence emission of this compound in pure solvents and in lipid vesicles will be presented. (Supported by NSF-REU, Bucknell Univ.).

Tu-Pos172

INTERACTION OF THE ANTIMALARIAL DRUG PRIMAQUINE WITH HEMOGLOBIN. ((Samira Barghouthi)). Department of Chemistry and Physics, Southeastern Louisiana University, Hammond, LA 70402.

In our research we are studying the interaction of some selected antimalarial drugs such as Primaquine diphosphate and Quinacrine dihydrochloride with hemoglobin. Fluorescence spectrophotometry is used to monitor changes in emission spectra upon binding of any of these ligands to hemoglobin. Since antimalarial drugs are believed to be capable of reversing the multidrug resistance developed by tumors, we are investigating the synergism (if any) of the binding of both cancer chemotherapeutics and antimalarial drugs to hemoglobin. By studying individual ligands and comparing chemical and thermodynamic behavior of compounds we hope to gain a better understanding of the mechanism of action of these drugs.

Tu-Pos173

COMPARISON OF CALCIUM RECEPTOR BINDING AND CYTOTOXICITY OF CISPLATIN WITH CARBOPLATIN ((E.G. Thompson and R.G. Canada)) Department of Physiology & Biophysics, Howard University College of Medicine, Washington, D.C. 20059.

Terbium (Tb^{3+}) luminescence was used to investigate the calcium receptor binding of cisplatin and carboplatin in Chinese Hamster Ovary (CHO-K1) cells. The quenching of the Tb^{3+}-CHO/K1 intensity by cisplatin and carboplatin was used to determine their equilibrium binding constants. Cisplatin and carboplatin noncompetitively quenched the intensity of the Tb^{3+}-CHO/K1 complex, decreasing I_{max} without affecting K_d. The quenching of Tb^{3+}-CHO/K1 intensity by cisplatin was significantly greater than the quenching caused by carboplatin. The K_d's for cisplatin and carboplatin were very similar to their respective K_d, obtained by Stern-Volmer quenching analysis (K_d=2.2mM for cisplatin and K_d=4.8mM for carboplatin). The cytotoxicity of cisplatin (ID_{50}=14.3μM) was greater than the cytotoxicity of carboplatin (ID_{50}=87.3μM). The dissimilarities between the ID_{50} and K_d values for each drug are due to the relatively large population of spare receptors. The data suggests that the different cytotoxicities of cisplatin and carboplatin are because of their distinct affinities for the terbium binding protein. This research was supported by the MBRS Grant Program, NIH, Grant No. 2S06GM08244-05.

Tu-Pos174

ENGINEERING A PROTEIN FOR HIGH SENSITIVITY TIME-RESOLVED FLUORESCENCE IMMUNOASSAYS.

((J. P. MacManus*, I. D. Clark*, A. G. Szabo* and D. Banville#)) National Research Council of Canada, *Institute for Biological Sciences, Ottawa, Ontario K1A 0R6, and #Biotechnolgy Research Institute, Montreal, Quebec H4P 2R2. (Spon.: I. D. Clark).

The CD loop of the Ca^{2+}-binding protein, oncomodulin, was replaced by a high affinity sequence that was found to reverse the order of fill of the two sites in the protein (MacManus *et. al.* (1990) *J. Biol. Chem.* **265**, 10358-10366; Hogue *et al.* (1992) *J. Biol. Chem.* **267**, 13340-13347). In this study, a cysteine was placed at position 7 of this sequence i.e. DKNADGCIEFEE, and this mutant named construct 3 (C3). The cysteine allowed covalent attachment of chromophores to the loop that could subsequently be tested for their ability to sensitize the luminescence of Tb^{3+} or Eu^{3+} bound in the loop. The probes examined were: *N*-(1-pyrene)iodoacetamide (PIA), 1-pyrene methyliodoacetate (PMIA), 4,4'-dimaleimidylstilbene (DIMS), benzophenone-4-iodoacetamide (BPIA), 4-iodoacetamidosalicylic acid (IASA) and 7-diethylamino-3-((4'-iodoacetylamino)phenyl)-4-methylcoumarin (DCIA). DCIA was the most efficient Eu^{3+} sensitizer studied, consistent with a mechanism of energy transfer that involves the triplet state of the donor. IASA was the most efficient Tb^{3+} donor tested. Levels of lanthanide ion and labelled C3 could be detected as low as 5×10^{-10} moles/l.

Tu-Pos175

ADVANCED PHOTOPHYSICAL APPLICATION OF CYCLODEXTRINS

Rezik A. Agbaria and David Gill

Departments of Physics, Ben-Gurion University, Beer-Sheva 84105, Israel.

ABSTRACT

Cyclodextrins are shown to have useful properties in photophysical studies of luminescent molecules. Host-guest inclusion complexes of these oligosacharides with biophysical fluorescent probes are formed in aqueous solutions. Crystalline solids are formed when the aqueous inclusion complexes are let to dry. These crystalline solids are shown to have molecular photophysical properties similar either to those at low temperature glass water matrices or in the gas phase.

This novel approach, when applied to $1,N^6$-ethenoadenosine (εAdo), supports evidences that there are at least two fluorescent singlet states. Both singlets and their correspondent triplets play major role in the photophysics of εAdo. We assign these singlets to $S_{\pi\pi^*}$ and a low lying $S_{n\pi^*}$.

The method is not limited to εAdo and particularly can be applied to those luminescent compounds which decompose in the gas phase.

Tu-Pos176

SPECTROSCOPIC STUDIES OF DIPYRIDAMOLE DERIVATIVES IN HOMOGENEOUS SOLUTIONS. ((Christiane P.F. Borges, Marcel Tabak)). Instituto de Física e Química de São Carlos-USP, C.P. 369, 13560-970, São Carlos-SP, Brasil.

Electronic absorption and fluorescence spectra of three different dipyridamole (DIP) derivatives, RA 39, RA 14 and RA 25, were monitored in aqueous solution as a function of pH in the range 2-13. These derivatives of DIP have different effects upon the transport of adenosine and phosphate in red blood cells, so we expect to be able to correlate their chemical structure, spectroscopic properties and biological activity as a vasodilator. Quantum yields, extinction coefficients and fluorescence lifetimes are similar to those obtained for DIP (BBActa 1116 (1992) 241). Excitation of the longer wavelength band 415nm for RA 39 and RA 14 and 370nm for RA 25 gave an intense fluorescence emission, strongly dependent upon the pH. Fluorimetric titration gave pK values of 5.8 and 12.5 for RA 39, similar to DIP, an unique pK of 5.8 for RA 14 and pKs of 2.25, 5.8 and 12.1 for RA 25. Below pH 6.0 both fluorimetric and spectrophotometric titrations evidentiate the changes in fluorescence quantum yield implying the involvment of the π-conjugated system of the pyrimido-pyrimidine ring. Preliminary experiments of interaction of DIP derivatives with bovine serum albumin suggest that the substituents are very important for an effective binding.

Support: CNPq, FAPESP, FINEP.

Tu-Pos177

PHOTOCHEMICAL ISOTOPE EXCHANGE AT AROMATIC CARBONS IN TOMAYMYCIN. ((Qi Chen and Mary D. Barkley)) Chemistry Department, Louisiana State University, Baton Rouge, LA 70803.

Tomaymycin is a pyrrolo[1,4]benzodiazepine antibiotic that binds covalently and specifically at guanine-N2 in the minor groove of the DNA double helix. It also serves as a fluorescent probe of rapid internal bending motions in DNA. The fluorescence properties of tomaymycin in different solvents and in DNA adducts have been investigated using both steady-state and time-resolved techniques. The quantum yields and lifetimes in alcohol solutions and DNA adducts are much higher than in aqueous solution and very close to the low temperature values. The quantum yield and lifetime are 1.5-fold greater in D_2O than H_2O. Photo-induced H-D exchange was detected at C6 and C9 of the benzene ring in methanol-d_4 solution by ^1H NMR. To our knowledge, this is the first report of photochemical exchange of aromatic protons in the absence of a strong proton donor, such as H^+ or ammonium group. The H-D exchange is quenched efficiently by the fluorescence quencher KI. The Stern-Volmer quenching constant for H-D exchange is 8.6 M^{-1}, which is much faster than the fluorescence quenching constant of 1.2 M^{-1}. These results suggest a fluorescence quenching process involving excited-state proton transfer followed by an H-D exchange process, both occurring in the excited singlet state. A mechanism is proposed and used to interpret and predict the fluorescence lifetimes of tomaymycin in different types of DNA adducts.

Tu-Pos178

EXCITED STATES OF MATRIX ISOLATED GUANINE: ABSORPTION, FLUORESCENCE, AND LIFETIME MEASUREMENTS*. ((Krzysztof Polewski and John C. Sutherland)) Biology Department, Brookhaven National Laboratory, Upton, NY 11973. (Spon. G. Hind)

Ultraviolet synchrotron radiation from station U9B at the National Synchrotron Light Source was used to excite guanine molecules isolated in low temperature (< 15°K) argon and nitrogen matrices. Fluorescence emission spectra for four different excitation wavelengths correspond to the features resolved in the absorption spectrum are similar in peak wavelength and shape. From fluorescence excitation spectra measurements we have obtained four well resolved peaks corresponding to the features observed in the absorption spectrum, but the bands are more clearly resolved. In addition to four distinct components, the fitting program indicated a fifth band at about 300 nm. The fluorescence decay lifetimes determined for excitation at each resolved band could be fit with a single exponential with a lifetime of between 9.5 and 10.1 ns, except for excitation at 305 nm where two exponentials are required with one of the lifetimes near 9 ns and the other 1.76 ns. Our results for the major transitions are consistent with an photo-physical mechanism in which all emission is from a single excited state. *Research sponsored by the Office of Health and Environmental Research, USDOE. The NSLS at BNL supported by the Office of Energy Research, USDOE.

Tu-Pos179

FLUORESCENCE SPECTROSCOPIC EVIDENCE FOR DIFFERENCES IN SUBSTRATE BINDING CAPACITY BETWEEN OCTAMERIC AND DIMERIC MITOCHONDRIAL CREATINE KINASE ((M. Gross, R. Furter, H.M. Eppenberger, T. Wallimann)) Swiss Federal Institute of Technology, Institute for Cell Biology, CH-8093 Zurich, Switzerland

Mitochondrial creatine kinase (Mi-CK) usually forms octamers consisting of four stable homodimers. The enzyme is confined to the mitochondrial intermembrane space, where it is bound to the inner membrane and supposed to participate in contact site formation. Based on enzyme kinetics and chemical labeling experiments, some evidence for limited active site accessibility in the octamer and slight differences in enzyme activity between octameric and dimeric Mi-CK have been reported. In the present study a 30% decrease in tryptophan fluorescence during the time course of octamer dissociation by the transition state-analogue complex (Cr+Mg^{2+}+nitrate+ADP) is demonstrated, and is shown to be due to enhanced quenching of an active site trp residue by the nucleotide substrate. This suggests a higher substrate binding capacity for the Mi-CK dimer in comparison to the octamer. The fluorescence decrease can be described by a biexponential decay law, indicating at least two slow steps during octamer dissociation. Upon removal of ADP by the use of apyrase, reoctamerization can also be followed on-line by monitoring a biphasic fluorescence increase. The individual dissociation and reassociation rate constants represent useful parameters for mechanistic studies on the octamer-dimer transition and for the systematic comparison of Mi-CK mutants. Dissociation rates of mutated proteins are presented and correlated with enzyme kinetical parameters. Both slower and faster decaying mutants have been investigated.

Tu-Pos180

INTERACTIONS OF RETINOIDS WITH INTERPHOTORECEPTOR RETINOL-BINDING PROTEIN ((Y. Chen and N. Noy)) Division of Nutritional Sciences, Cornell University, Ithaca, NY 14850.

Interphotoreceptor retinol-binding protein (IRBP) is a large retinol-carrying glycoprotein which is found primarily in the interphotoreceptor matrix of the retina between the retinol pigment epithelium (RPE) and the rod cells (ROS). The equilibrium constants for binding of several retinoid species IRBP were measured by fluorescence titrations. The rate constants of the dissociation of retinoids from IRBP were determined by monitoring the transfer of the retinoids between the protein and synthetic unilamellar vesicles. The transfer reactions were followed by using a stopped-flow fluorescence method. The results of these studies have implications for the movement of the retinoids involved in the visual cycle.

Tu-Pos181

EFFECT OF LIPID-PROTEIN AND LIPID-LIPID INTERACTIONS ON LIPID DYNAMICS AND LIPID PHASES IN RENAL APICAL MEMBRANES. ((Moshe Levi, Dave Jameson, Paul Wilson, and Jay Cooper)) U of Texas Southwestern Med Ctr and VAMC, Dallas, TX and U of Hawaii, Honolulu, HI.

Steady-state and time-resolved fluorescence measurements with 1,6-diphenyl-1,3,5-hexatriene (DPH) and the phase sensitive probe 6-dodecanoyl-2-dimethylaminonaphthalane (Laurdan) indicate that at the physiological temperature of 37°C the renal apical brush border membrane (BBM) lipids have a relatively low fluidity and that approximately 40% of the lipids are in a gel or liquid-ordered (rather than liquid crystalline) phase. The purpose of the present study is to determine the potential effect of lipid-protein, lipid-sphingomyelin and lipid-cholesterol interactions on the lipid dynamics and phase characteristics of BBM lipids. DPH and Laurdan lifetime and DPH rotational diffusion measurements indicate that lipid-cholesterol (a major effect), lipid-sphingomyelin and lipid-protein (a moderate effect) interactions are largely responsible for the low fluidity of BBM lipids. In addition, generalized polarization of Laurdan fluorescence as a function of temperature indicates that in BBM 41.1%, in BBM lipids depleted of proteins 36.9%, in BBM lipids depleted of sphingomyelin 23.1%, and in BBM lipids depleted of cholesterol 11.4% of lipids are in the gel or liquid-ordered phase. Thus, lipid-cholesterol > lipid-sphingomyelin > lipid-protein interactions play an important role in determining the lipid dynamics and phase characteristics of BBM lipids at 37°C.

PROTEIN STRUCTURE AND FUNCTION I

Tu-Pos182

THERMAL DENATURATION OF GIUCOSE OXIDASE AT THE PRESENCE OF DODECYL TRIMETHYL AMMONIUM BROMIDE

A.A.Moosavi-Movahedi, M.R. Housaindokht, Institute of Biochemistry and Biophysics, University of Tehran, Tehran, Iran.

The thermodynamic parameters of interaction of glucose oxidose and dodecyl trimethyl ammonium bromide (DTAB) were obtained by equlibrium dialysis and U.V. temperatures scanning (Gilford) and have compared the chemical and thermal stability of the enzyme. Using the Wyman theoretical potential and Pace model to obtain all thermodynamic parameters at wide range of temperatures.
The chemical and thermal stability of glucose oxidose is very high and denaturation of glucose oxidase is very hard. Among this study we found that the DTAB because of cationic group is very successful denaturant for denaturation of glucose oxidase.

Tu-Pos183

TEMPERATURE-INDUCED CHANGES IN THE SECONDARY STRUCTURE OF CAPRINE α_{S1}- AND β-CASEINS AS DETERMINED BY FTIR. ((A. Mora-Gutierrez, T.F. Kumosinski, D.M. Curley and H.M. Farrell, Jr.)) Prairie View A&M Univer., Prairie View, TX 77446 and USDA, ERRC, Philadelphia, PA 19118

Although caprine casein micelles have been studied as a prototype for understanding mechanisms of electrostatic and hydrophobic interaction in bovine casein micelles, the structural and functional properties of its four casein components (α_{s1}-, α_{s2}-, β-, and κ-) have remained elusive. We have studied the secondary structure of purified caprine α_{s1}- and β-caseins at 5 and 23°C in an attempt to correlate temperature-induced conformational changes of individual caseins with submicelle and micelle formation. The results of Fourier-transform infrared (FTIR) experiments indicate that in aqueous solution and at 23°C the caprine β-casein has a low content of α-helical conformation but contains a significant amount of β-sheet. Under the same experimental conditions caprine α_{s1}-casein has a larger tendency toward α-helix formation. Moreover, the data present the first direct spectroscopic evidence of turns in caprine α_{s1}- and β-caseins.

Tu-Pos184

MODELING ELECTROSTATIC INTERACTIONS IN PROTEINS WITH THE FINITE DIFFERENCE METHOD. ((H. Oberoi & N. M. Allewell)) Department of Biochemistry, University of Minnesota, St Paul, MN 55108

Electrostatic interactions in proteins have been modeled extensively with various forms of the Poisson-Boltzmann equation [Sharp & Honig *Ann. Rev. Biophys. Biophys. Chem 19,* 301 (1990)] The Finite Difference method has been used to calculate titration curves for lysozyme [Bashford & Karplus *Biochemistry 29,* 10219 (1990)]. While several calculated $pK_{1/2}$ values agree with experiment to within one pH unit, there are large differences in the calculated $pK_{1/2}$ and experimental pK_a values for several sites. One reason for the difference between experiment and calculation may be errors in the estimation of terms that enter into the calculation of charges at individual sites.

The intrinsic proton association standard free energy of a charge at site i, ΔG_{int} may be defined as $\Delta G_{int} = \Delta G_{Born} + \Delta G_{prot}$ where ΔG_{Born} is the Born solvation energy of the charge and ΔG_{prot} is the interaction energy of the charge with the nontitrating charges in the protein with all other sites neutral. The Finite Difference approximation introduces large errors in the calculated values of ΔG_{Born} and ΔG_{prot} unless one uses grid sizes of the order of 0.2-0.1 Å. The standard approach to reduce the error is to use fine grids at the site and coarse grids elsewhere. This approach however gives large errors for ΔG_{prot}.

We have developed a multigridding method which reduces the error for the Born and background terms without requiring fine grids. This approach will allow modelling of significantly larger proteins than has been previously possible.

pK_a values for 21 of the 32 titrating sites in lysozyme have been determined experimentally. 17 of the calculated $pK_{1/2}$s are within 0.4 pH units of the experimental values while the other 4 are within 1.5 pH units.

Tu-Pos185

LINKAGES BETWEEN SINGLE SITE MUTATIONS, ELECTROSTATIC EFFECTS AND THE FUNCTIONAL PROPERTIES OF E. COLI ASPARTATE TRANSCARBAMYLASE. ((X. Yuan, H. Pan and N.M. Allewell)) Dept. of Biochemistry, University of Minnesota, St. Paul, MN 55108. (Spon. by N.M. Allewell)

The conformational change of E. coli aspartate transcarbamylase (ATCase) induced by substrate binding has been interpreted in terms of the T and R states of the MWC model of allosteric regulation [Monod *et al.* (1965) J.M.B. 12:88-118; Howlett *et al.* (1977) Biochem. 16:5091-5099; Ke *et al.* (1988) J.M.B. 204:725-747]. Mutant ATCase enzymes have been classified as T or R state based on catalytic activity and substrate affinity. We find that the pH dependencies of the catalytic parameters, V_{max} and $[S]_{0.5}$, of T state mutants differ markedly from the wild type enzyme, while the pH dependencies of these parameters for R state mutants are similar to the wild type. Y165F, which is mutated at the c1-c4 interface of the holoenzyme, appears to be a particularly interestingT state mutant. This mutant shows the most extreme differences from the wild type enzyme in terms of the pH dependence of its functional parameters, suggesting global changes in its electrostatic properties. While the catalytic activity and substrate affinity of the mutant holoenzyme are reduced by approximately a factor of 5 relative to the wild type enzyme, the catalytic parameters of the mutant catalytic subunit are similar to the wild type holoenzyme. Similarly, the bisubstrate analog PALA activates the mutant holoenzyme to a much greater extent (a factor of 10) than it does the wild type holoenzyme. Differential scanning calorimetric data interpreted in terms of the model of Brandts [Brandts *et al.* (1989) Biochem. 28:8588-96] indicate that the free energies of the c:r interactions in this mutant are more negative than in the wild type enzyme. These results suggest that Y165F is deeply locked in the T state, but can be unlocked from this state by PALA or by removing the regulatory subunits. Supported by NIH grant DK-17335.

Tu-Pos186
STRUCTURAL THERMODYNAMIC PARAMETRIZATION OF THE ENERGETICS OF PROTEIN-CARBOHYDRATE INTERACTIONS.
((Gabrielle Bains, Dong Xie, Renji Wang and Ernesto Freire)) Departments of Biology and Molecular Biophysics Program. The Johns Hopkins University, Baltimore, MD 21218

The binding thermodynamics of eight protein-carbohydrate complexes for which high resolution structural information is available have been analyzed. These complexes involve the following proteins: wheat germ agglutinin, lysozyme, concanavalin A and the arabinose binding protein. As in the case of protein-protein interactions, the experimental enthalpy and heat capacity contributions to the Gibbs free energy of binding can be expressed in terms of the accessible polar and apolar surface area differences between the protein-carbohydrate complex and those of the isolated components free in solution. The resulting parametrization has allowed us to dissect the magnitude of the polar and apolar contributions to the binding energetics. In all cases the binding process is characterized by small (<100 cal $K^{-1}mol^{-1}$) negative heat capacity changes. At 25°C the main contribution to the binding enthalpy arises from polar van der Waals and hydrogen bonding contributions. This stabilizing contribution is partially offset by the positive enthalpy contribution arising from the burial of apolar groups. This same burial of apolar groups provides a stabilizing contribution to the binding entropy that partially compensates the negative entropy due to the loss of configurational degrees of freedom. Supported by the National Institutes of Health (RR04328, GM37911, and NS24520).

Tu-Pos187
THERMODYNAMIC INVESTIGATION OF THE INTERFACIAL FORCES RESPONSIBLE FOR ANTIBODY STABILITY
((J. R. Livingstone, M. L. Rodrigues, P. J. Carter, S. J. Shire, and R. F. Kelley)) *Department of Protein Engineering, Genentech, Inc., South San Francisco, CA 94080*

Protein-protein association is dominated by noncovalent forces (e.g. hydrogen bonding, hydrophobic effects) which mediate the specificity and stability of the complexes which are formed. Protein engineering can be used to probe the individual contributions of amino acid residues important in the production of biologically important complexes. Antibodies are composed primarily of two chains, linked together by multiple disulfide bridges, which form an extensive protein-protein interface. We have investigated the thermodynamic consequences of mutating key interfacial residues to the thermodynamics of chain-chain association in the hu4D5v8 antibody by using noncovalently linked antibody fragments (F_V, Fab*, C_H/C_{L1}). The enthalpic and entropic contributions to the Gibbs free energy, and changes in heat capacity for denaturation were measured using differential scanning calorimetry. The thermodynamics of chain-chain association were determined from the concentration dependencies of the thermodynamics of denaturation. In addition, analytical ultracentrifugation was used to measure directly chain-chain association constants. These results, in conjunction with recent antibody structural data, provide a structure-function framework for understanding how protein engineering efforts affect antibody stability.

Tu-Pos188
ELECTROSTATIC INTERACTIONS IN ANTIBODY–ANTIGEN ASSOCIATION.
((Stuart P. Slagle, Richard E. Kozack, & Shankar Subramaniam)) Beckman Institute, Center for Biophysics and Computational Biology, National Center for Supercomputing Applications, University of Illinois, Urbana, IL 61801

An anti–hen egg lysozyme monoclonal antibody fragment (HyHEL–5) has been structurally characterized to high resolution. The method of association is the formation of three salt–bridges between lysozyme and its antibody. Lysozyme species variants which lack the critical salt–linking residues or mutant antibody fragments without the salt–linking acidic residues form less stable complexes with respect to the wild–type complex. The electrostatics of association is modulated to a degree where the arginine's replacement in lysozyme by lysine results in a thousand–fold reduction in association. The Poisson–Boltzmann method has been used to solve for electrostatic potentials on a three dimensional grid for wild type and mutant complexes. The mutant structures were energy minimized prior to calculation of the electrostatic potentials. In the Poisson–Boltzmann equation, the proteins are described with atomic point charges. Relative electrostatic free energy differences of association were obtained. The role of solvation was also probed in these simulations. Electrostatic origins of the association were delineated at the residue level in the HyHEL–5–HEL system. NIH PHS T32 GM08726; NIH RO1–GM46535; ONR N0014–91–J–4096.

Tu-Pos189
GRASP: GRAPHICAL REPRESENTATION AND ANALYSIS OF SURFACE PROPERTIES
((Anthony Nicholls, Ranganathan Bharadwaj and Barry Honig)) Department of Biochemisty and Molecular Biophysics, 630, W. 168th St, Columbia University, New York, New York, 10032.

GRASP is a molecular modelling program for the Silicon Graphics Iris. It utilizes fast algorithms to calculate and display molecular and accessible surfaces of large molecules. Drawing modes for surfaces include solid, mesh and points. Surfaces can be color coded by property, which can be intrinsic, e.g. curvature, or projected from the properties of underlying atoms, or can be found from a 3D map, e.g. electrostatic potentials from a DelPhi calculation. Areas and enclosed volumes can be calculated. Local connectivity can find internal cavities. Electrostatic quantities from DelPhi, or an internal Poisson-Boltzmann solver, can also be displayed by color coded atom representations, isopotential contours, field lines and vectors, and a color coded projection plane. The program allows simple arithmetic on data fields for surfaces, atoms and 3D maps, e.g. average and sum. A versatile control language allows for subsets to be defined for both surface and atoms, upon which all GRASP functions can be performed, including independent spatial manipulation. Surface subsets can also be selected by hand. Data on atoms or surfaces can be written to screen or file. The user can also query atom or surface information by mouse. The program includes representations of bonds, protein backbones, DNA bases, sugars and backbones, site-site interactions, consensus volumes and molecular dipoles. Examples of GRASP images will be presented along with a complete listing of functions.

Tu-Pos190
PURO-INDOLINE: A NEW BASIC AND CYSTEINE-RICH PROTEIN WITH A UNIQUE TRYPTOPHAN-RICH DOMAIN ISOLATED FROM WHEAT ENDOSPERM.
((Jean-Erik Blochet and Didier Marion)) Laboratoire de Biochimie et Technologie des Protéines, INRA Nantes FRANCE ((André Désormeaux and Michel Pézolet)) CERSIM, Département de chimie, Université Laval, Québec, CANADA (Spon. by M. Auger)

Triton X114 phase partitioning has been used in order to extract wheat flour proteins able to interact with polar lipids. The main low molecular weight fraction is composed of a protein of molecular weight around 15 kD, as determined by polyacrylamide gel electrophoresis. About 15% of the residues of this protein are cationic, 10% are cysteine residues and no histidine is present. The sequence determination has been achieved and revealed an original polypeptide chain of 115 residues for a molecular weight of 13 kD and a unique tryptophan-rich domain. It exhibits some common features with wheat amylase-protease inhibitors. Preliminary studies, using tryptophan fluorescence, DPH fluorescence polarization and infrared spectroscopy show that the protein has a high affinity for anionic lipids. Infrared spectroscopy also reveals a high content in α-helix (about 41%). Puroindoline displays an interesting sequence between residues 38 and 45 which includes 5 tryptophan residues and 3 basic amino acids. Secondary structure prediction by the hydrophobic cluster analysis reveals that this sequence is characteristic of an amphiphatic α-helical structure that could be the preferential part of the protein involved in the interactions with lipids.

Tu-Pos191
BINDING OF A PHOTOAFFINITY LABELED RETINOL TO RETINOL BINDING PROTEIN
((J.M.Chapman, E.S. Hazard, R.K.Crouch and K.L.Schey)) Dept. of Ophthalmology and Pharmacology, Medical University of South Carolina, Charleston, SC 29425.

A photoaffinity ligand has been synthesized for labeling the binding site of human serum retinol-binding protein. The synthetic scheme begins with methyl retinoate which was brominated at the 4-position with NBS, the bromine was displaced with ammonia to produce methyl 4-aminoretinoate, the amino substituted retinoid was reduced with DIBAL to 4-aminoretinol, the amine functionality was derivatized with 2-diazo-3,3,3-trifluoropropionylchloride to yield 4diazotrifluoropropionamidoretinol (Structure 1). The ligand 1 binds to human serum retinol-binding protein as evidenced by the increase in fluorescence emission at 470nm with excitation at 350nm. Protein was titrated to the saturation point as determined by ligand fluorescence and UV-visible spectroscopy. The ligand bound to the protein was then subjected to photolysis for 2 minutes at 254nm to activate the diazo group. Matrix assisted laser desorption time of flight mass spectrometry was utilized to evaluate the presence of covalently bound ligand. After photolysis in the presence of 1, the molecular weight of the binding protein was increased suggesting crosslinking. Supported by NIH grants F32 EY06362 and R01 EY04939.

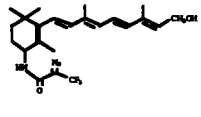

Tu-Pos192

RECONSTITUTION AND SPIN LABELING OF THE *E. coli* FERRIC ENTEROBACTIN RECEPTOR FepA. ((J. Liu†, J. M. Rutz‡, P. E. Klebba‡, and J.B. Feix†)) †Biophysics Research Institute and ‡Department of Microbiology, Medical College of Wisconsin, Milwaukee, WI 53226. (Sponsored by J. J. Yin).

FepA is an 81 kilodalton protein in the outer membrane of *E. coli* that is responsible for high-affinity uptake of the iron siderophore, ferric enterobactin. A model based on sequence analysis and immunological studies suggests that the protein contains a large number of transmembrane β-sheets and an extracellular ligand-binding domain. To further explore structure and topology, we have spin-labeled FepA with a maleimide spin label (MAL-6), and reconstituted the purified, spin-labeled protein into liposomes. FepA contains two cysteine residues, cys486 and cys493. Labeling with MAL-6 was only achieved following reduction by DTT and partial unfolding in urea, indicating that the cysteines are disulfide-linked. Following reconstitution into phosphatidylcholine liposomes, both native and MAL-6 labeled FepA bound ferric enterobactin and showed a pattern of recognition by monoclonal antibodies similar to that observed with intact *E. coli*. Lithium dodecyl sulfate-PAGE under non-denaturing conditions also indicated that the spin-labeled protein had retained its native, compact structure. These data indicate that the MAL-6-labeled receptor assumed a native conformation when reconstituted *in vitro*. The conventional EPR spectrum of MAL-6 labeled FepA indicated that the large majority (>95%) of spin labels were strongly motionally restricted. Using multiquantum and CW-saturation EPR, we found the accessibility of FepA-bound spin labels to both oxygen and to a paramagnetic metal complex, chromium oxalate to be highly limited. These results suggest that the native cysteine residues of FepA occupy a tightly-packed region of the protein structure that is not exposed to either the surrounding membrane lipids or the aqueous phase.

Tu-Pos193

THE MAIN CHAIN DYNAMICS OF A PEPTIDE BOUND TO CALMODULIN ((C. Chen†, J. Short†, Y. Feng†, A.R. Means§, A.J. Wand†)) †Department of Biochemistry, University of Illinois at Urbana-Champaign, Urbana, IL 61801, §Department of Pharmacology, Duke University, Durham, NC 27710

The main chain dynamics of a peptide corresponding to the smooth muscle MLCK calmodulin binding domain bound to calmodulin have have been studied by 15N relaxation and hydrogen exchange techniques. The global motion of the 1:1 complex is isotropic and is characterized by a correlation time of 10 ns/rad. The generalized order parameters of the nine labeled backbone amide N-H vectors of the peptide all fall closely about a value of 0.85. The effective correlation times all tend to zero indicating that backbone motion of the bound peptide is highly restricted and dominated by extremely fast motions. All amide NH have hydrogen exchange slowing factors significantly greater than one. These results are consistent with a structural model that involves tight packing interactions throughout the length of the peptide and suggest concerted motions lead to collapse of the hydrogen bonding network within the peptide.

Tu-Pos194

CHARACTERIZATION OF C-TERMINAL THONG MUTANTS OF *E-COLI* GLUTAMINE SYNTHETASE

((Robert H. Stoffel III and Joseph J. Villafranca)) Department of Chemistry, Pennsylvania State University, University Park PA 16802. (Spon. by J.C. Freeman)

Glutamine synthetase (GS) serves as the central element in the regulation of nitrogen metabolism by catalyzing the ATP-dependent condensation of NH_3 with glutamate to form glutamine. GS from *Escherichia coli* is a dodecameric metalloenzyme with M_r 622,000, which consists of twelve identical subunits arranged in two rings that stack face to face. Thermal denaturation studies have shown that the enzyme is very heat stable and undergoes partial unfolding without subsequent dissociation of the dodecamer (Shrake et al. Biochem. 28: 6281-6294), indicating that the inter-subunit contacts provide extensive stabilization. The inter-ring contact stabilization is due to two interactions: 1) a small four-stranded β-sheet formed by the β-loop of the subunit above and the β-loop of the subunit below and, 2) the carboxyl terminus of each subunit, which forms a helical thong that inserts into a hydrophobic pocket of the reciprocal subunit (Yamashita et al. J. Biol. Chem. 264: 17681-17688).

Four site-directed mutants have been created that truncate the helical thong by 8, 6, 3, or 1 amino acid(s) and are E461Stop, E463Stop, Y466Stop, and V468Stop. Each of the mutants fold and associate into dodecamers as seen from non-denaturing gel electrophoresis and electron microscopy. The largest truncation mutant, E461Stop, does exist as a dodecamer but seems to be more stable as a hexamer. Alkaline pH (>8) and acid pH (<6) cause the E461Stop and E463Stop mutants to separate into hexamers.

Research supported by NIH grant GM23529.

Tu-Pos195

RAT KIDNEY ANNEXIN V STRUCTURE & PROPERTIES

((N.O. Concha‡, M. Swairjo‡, J.F. Head‡, M.A. Kaetzel*, J.R. Dedman* and B.A. Seaton‡)) ‡Department of Physiology, Boston University School of Medicine, Boston, MA 02118, * Department of Physiology and Biophysics, University of Cincinnati College of Medicine, Cincinnati, OH 45267.

Annexin V belongs to a family of cytosolic calcium-binding proteins believed to be involved in stimulus-response coupling through calcium-dependent membrane interactions. Although the precise cellular function of annexin V is not clear, inhibition of various membrane-associated proteins and exhibition of voltage-gated calcium channel activity *in vitro* have been reported. We are studying annexin V structure in two forms: the soluble form (by X-ray crystallography), and the membrane-bound form (by biochemical and spectroscopic methods). The X-ray crystal structure of rat kidney annexin V has been solved to high resolution by multiple isomorphous replacement. The R3 crystals, with unit cell dimensions of a=b=156.9Å, c=37.03Å, were grown under high calcium conditions. In separate studies, the quaternary structure of annexin V, either free in solution or bound to PL membranes, was investigated by chemical cross-linking. Oligomerization was observed only in protein solutions containing both calcium and anionic phospholipid vesicles. The cross-linked species observed were trimers, hexamers, and higher aggregates. Nuclear magnetic resonance experiments were also performed to elucidate the effect of annexin binding on phospholipid membranes. Results are discussed in terms of putative membrane function.

Tu-Pos196

BINDING OF INFLUENZA NEURAMINIDASE MUTANTS TO ANTIBODIES IS WELL-CORRELATED WITH FREE-ENERGY CALCULATIONS AND CRYSTAL STRUCTURES. ((W. R. Tulip)) U. of Oregon, Eugene OR 97403, ((V. R. Harley)) I.C.R.F. Labs, London WC2A 3PX U.K., ((R. G. Webster)) St Jude Children's Res. Hosp., Memphis TN 38101, ((J. Novotny)) Bristol-Myers Squibb, Princeton NJ 08543-4000

X-ray crystallographic structures of influenza virus N9 neuraminidase (NA) in complex with Fab fragments of antibodies NC41 and NC10 were refined to 2.5 and 3.0 A resolution, respectively, (Tulip et al., J. Mol. Biol. 227 (1992) 122 and unpublished results). Using a previously described method (Novotny et al. Biochemistry 28 (1989) 4735), the change in free energy upon binding was calculated for each amino acid residue at the antibody-antigen interfaces. Despite the empirical nature and inherent simplifications of the method, there is a striking correlation between the predicted ΔG residue contributions and experimental binding data for N9 mutants. In general, NA residues with large calculated ΔG contributions (ΔG < -1 kcal/mol) lie at sites of mutation which cause a marked reduction in antibody binding relative to wild-type N9 NA. Conversely, NA residues for which the calculated ΔG > -1 kcal/mol are sites at which mutation does not have a marked effect on binding. The above general pattern is valid in 19 out of 27 cases for the NC41 complex and 7 out of 7 cases for the NC10 complex. The breakdowns in the pattern mostly occur at residues where different substitutions cause different effects on binding. The results strongly support the hypothesis of an energetic ("functional") epitope in antigen-antibody binding (Novotny et al., 1989; Jin et al. J. Mol. Biol. 226 (1992) 851).

Tu-Pos197

NMR INVESTIGATION OF E. COLI INTEGRATION HOST FACTOR.

((Michelle Fausel Ferland, Linda D. Kosturko* and Irina M. Russu)) Department of Molecular Biology and Biochemistry, Wesleyan University, Middletown, CT, 06459-0175. * Department of Zoology, Connecticut College, New London, CT, 06320-4196.

Sequence-specific recognition of DNA by proteins is an important component of many biological functions. Integration Host Factor (IHF) is a sequence-specific DNA binding protein from *E. coli* which is involved in many intracellular processes, including packaging and site-specific integration of λ phage DNA. The protein is a heterodimer, and the amino acid sequence of each chain shows high homology to that of the histone-like protein HU. The crystallographic structure of IHF is not yet available. We have used nuclear magnetic resonance spectroscopy (NMR) to investigate the conformation and dynamics of IHF in solution state. Specific resonance assignments were made using two-dimensional NOESY, COSY and DQF-COSY as well as one-dimensional NOE experiments. The dynamics of specific amino acids were investigated through measurements of the relaxation and NOESY build-up rates for the corresponding resonances. The exchange rates of individual amide hydrogens were monitored in real-time D_2O exchange measurements. Preliminary data will also be presented for IHF in complex with a 15 base-pair DNA oligonucleotide containing the IHF consensus sequence. (Supported by a Project Grant from Wesleyan University and the High-Technology Program of the State of Connecticut).

Tu-Pos198

MASS SPECTROMETRIC IDENTIFICATION OF OXIDATIVE MODIFICATIONS TO HUMAN SERUM ALBUMIN EXPOSED TO HYDROGEN PEROXIDE. ((K.L. Schey, J.W. Finch, D.R. Knapp, and R.K. Crouch*)) Dept. of Pharmacology and Ophthalmology*, Medical Univ. of SC, Charleston, SC, 29425.

Albumin has been proposed to serve as an antioxidant in biological systems subject to attack of oxygen radicals from species such as hydrogen peroxide (1). The purpose of our study was to identify sites of oxidation and determine the extent of oxidation of human serum albumin (HSA) exposed to H_2O_2. Mass spectrometric analysis of tryptic peptides from oxidized HSA was used to locate each modified residue and estimate the extent of oxidation. Sites of oxidation identified include Cys 34, Met123, Met298, Met446, and Met548. The extent of oxidation of methionine residues varied with location in the protein sequence and only limited oxidation of Cys34 occurred suggesting a relationship between oxidation and protein three-dimensional structure. This study provides evidence that HSA can indeed act as a sacrificial antioxidant. Furthermore, the utility of mass spectrometry for identifying amino acid modifications in large proteins is demonstrated. (1) B. Halliwell. 1988. *Biochem. Pharmacology* 37:569.

Tu-Pos199

PARADOXICAL STRUCTURE AND FUNCTION IN A MUTANT INSULIN ASSOCIATED WITH DIABETES MELLITUS IN MAN. Q. Hua, S. Shoelson, K. Inouye, and M. Weiss. Harvard Medical School, Boston, MA 02115.

The solution structure of a diabetes-associated mutant human insulin (insulin Los Angeles; PheB24→Ser) is determined by ^{13}C-edited NMR spectroscopy and distance-geometry/simulated annealing calculations. Among vertebrate insulins PheB24 is invariant, and in crystal structures the aromatic ring packs against in the hydrophobic core. B24 substitutions are of particular interest in relation to the mechanism of receptor binding. In one analogue (GlyB24-insulin) partial unfolding of the B-chain is observed with paradoxical retention of near-native bioactivity (Q. Hua., S. Shoelson., M. Kochoyan., & M. Weiss. (1991) *Nature* 354 : 238-241). The present study of SerB24-insulin extends this observation: relative to GlyB24-insulin, near-native structure is restored despite significant loss of function. Our results provide the first structural study of a diabetes-associated mutant insulin and support the hypothesis that insulin undergoes a change in conformation on receptor binding.

Tu-Pos200

ROLE OF β^2[NA2]HIS IN THE BOHR EFFECT. ((C. Fronticelli*, J. Kowalczyk* and W.S. Brinigar†.)) University of Maryland Med. Sch. Baltimore, MD 21201* and Chem. Dept., Temple U. Philadelphia PA 19122†. (Spon. by Clara Fronticelli). A human hemoglobin variant has been constructed in which the β^1[NA1]Val was replaced by Met and β^2[NA2]His was deleted. From Bohr effect measurements of HbA_0 and mutant hemoglobin in 15mM Hepes buffer it was calculated that the protons released at pH 7.3, in the T to R transition were ΔH^+= 1.13/tetramer in HbA_0 and ΔH^+= 2.08/ tetramer in the mutant hemoglobin. It, therefore, appears that, under these conditions the β^2[NA2]His of HbA_0 is a reverse Bohr effect group. However, Bohr effect measurements under the same conditions except with the addition of 100mM NaCl, resulted in a ΔH^+= 2.53/tetramer for HbA_0 and ΔH^+ = 2.08/tetramer for the mutant hemoglobin. This result indicates that in the presence of 100mM Cl^- ions β^2[NA2]His becomes an alkaline Bohr group which contributes 20% to the alkaline Bohr effect. These results are consistent with the proposition that the molecular mechanism of the Bohr effect is dependent on solvent composition (Bucci and Fronticelli Biochemistry 24: 371-376, 1985). Analyses of the oxygen binding curves obtained in 15mM Hepes and 100mM Cl^- indicated that 70% of the βNA2His protons are released upon binding of the first O_2 molecule.

Tu-Pos201

D-MELITTIN BINDING TO CALMODULIN. ((P.J. Fisher, S.S. Sedarous, and F.G. Prendergast)) Department of Biochemistry and Molecular Biology, Mayo Foundation, Rochester, MN 55905.

Melittin is one of several amphiphilic, α-helical peptides which bind to calmodulin. Peptides isolated from target enzymes for calmodulin, e.g., from smooth muscle myosin light chain kinase, which bind to CAM adopt the amphiphilic helical motif and may have specific binding determinants. To date, however, the issue of chirality apparently has not been addressed. The D & L-enantiomers of melittin (which has a single tryptophan) have been employed to examine such a chiral specificity of binding. These enantiomers are spectroscopically identical except in their far ultra-violet circular dichroic spectra: D-melittin yields positive mirror images of all the solution CD spectra of L-melittin. The two melittins have essentially identical fluorescence maxima, quantum yields, anisotropies and lifetimes in the three different solution conformations previously established: monomeric "random coils" in water, monomeric α-helices in 90% methanol, and tetramers in 0.8M phosphate solutions. They have equivalent NMR profiles and they co-elute on HPLC. Melittin binding to calmodulin was monitored through tryptophan fluorescence intensity and anisotropy changes attending interaction. Bjerrum plots show that calmodulin has a higher affinity for D-melittin than for L-melittin. In addition, the mirror image CD spectra observed with D- and L-MLT interaction allow us to differentiate calmodulin shifts from peptide CD shifts upon formation of the complex. (Supported in part by the Mayo Foundation and GM-34847.)

Tu-Pos202

KINETIC AND HYDRODYNAMIC STUDIES OF ACTIVATION OF RECOMBINANT PLASMINOGEN ACTIVATORS. ((Richard A. Smith, Jack Henkin and Thomas F. Holzman, [Spon: J. Cohen])) DRUG DESIGN AND DELIVERY AND THROMBOLYTICS RESEARCH, ABBOTT LABORATORIES, ABBOTT PARK, IL 60064.

An understanding of the activation of fibrinolytic enzymes is central to evaluating their roles in eliciting responses in normal and pathologic events. For example, following thrombolytic therapy, re-occlusion rates vary for tissue plasminogen activator (tPA), streptokinase (SK) and urinary plasminogen activator (uPA), suggesting one or more of the plasminogen activators can have prolonged effect. The physical associations occurring between plasminogen, tissue plasminogen activator, and urinary plasminogen activator in the presence and absence of fibrin peptides were studied in the ultracentrifuge. The kinetic behavior of these complexes were examined using chromogenic substrates. In parallel experiments peptide products, derived from natural substrates, were observed by SDS-PAGE, isolated by RP-HPLC, and identified by N-terminal sequence analysis. The interactions between plasminogen and the plasminogen activators is analyzed in relation to the respective physiological roles of these enzymes.

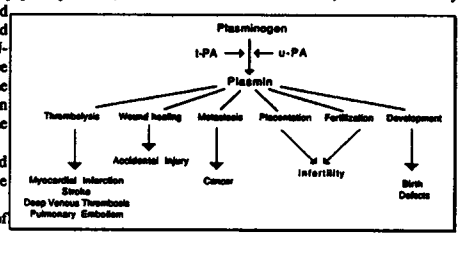

Tu-Pos203

COOPERATIVE CALCIUM BINDING BY CALMODULIN ((Susan Pedigo and Madeline A. Shea*)) Dept. of Biochemistry , U. of Iowa College of Medicine, Iowa City, IA 52242-1109

Calmodulin (CaM), the primary eukaryotic intracellular calcium receptor, binds up to 4 calcium ions cooperatively and activates target proteins. To identify the intermediate states populated as Ca^{2+} binds to CaM, we are monitoring individual Ca^{2+}-binding sites and other positions by quantifying changes in sensitivity to limited proteolysis by Endo GluC at partial degrees of calcium saturation. The fragments generated at each [Ca^{2+}] were separated and quantified using rpHPLC; amino acid analysis was used to identify their termini. Reactivity profiles determined from the relative abundance of each peptide product indicate the variable accessibility of a given peptide bond as a function of [Ca^{2+}]. Probing CaM with Endo GluC indicated that only 5 of the 16 possible cleavage sites were observed; this may indicate structural rigidity and differences between solution conformations and crystal structure of fully saturated CaM. In most cases, Ca^{2+} binding protected CaM from cleavage. Responses of sites in the C-terminal domain were cooperative and showed complete protection from cleavage at [Ca^{2+}] above 10^{-6}M, consistent with macroscopic binding data. Biphasic reactivity profiles were resolved for the susceptibility of residues in the N-terminal domain, indicating interdomain cooperativity. Studies to validate the proteolytic probe method allowing estimation of thermodynamically meaningful parameters are described. (NSF DMB 9057157, AHA 910148980 and U. I. Biocatalysis Traineeship)

Tu-Pos204

PROTEIN CONFORMATIONAL DYNAMICS: COMPARATIVE STUDIES OF *ESCHERICHIA COLI* ADENYLATE KINASE MUTANTS USING FLUORESCENCE AND CIRCULAR DICHROISM SPECTROSCOPY. ((T. Fulmer[1,2], T. Bilderback[1], M. Glaser[1] and W. Mantulin[1,2].)) University of Illinois at Urbana-Champaign, [1]Dept. of Biochemistry; & [2]Laboratory for Fluorescence Dynamics, Dept. of Physics, Urbana, IL 61801.

The enzyme adenylate kinase (AK) from *Escherichia coli* catalyzes the interconversion (synthesis and regeneration) of adenosine nucleotides and ligand binding sites exist for ATP and AMP. In general, the binding of substrates induces a large conformational change in AK. Through site directed mutagenesis we have expressed three tryptophan mutants (Y24→W; F86→W; Y133→W) of wild type AK, which is devoid of tryptophan. The enzymes are purified by liquid chromatography. The introduction of W residues allows us to exploit the high sensitivity and temporal response of fluorescence spectroscopy in studying conformational stability and dynamics, arising either from denaturation or substrate binding reactions. Changes in fluorescence of the wild type and W mutants are compared with corresponding changes in circular dichroism spectra, which provide a measure of secondary structure. These multiple spectroscopic studies are examined in the context of complementary studies of AK's enzyme kinetics. The ultimate goal of these studies is an enhanced understanding of the structure-function relationship in AK. This work was performed at the Laboratory for Fluorescence Dynamics (LFD) at the University of Illinois at Urbana-Champaign (UIUC). The LFD is supported jointly by the National Institutes of Health (RR03155) and by UIUC.

Tu-Pos205

RAMAN STUDIES OF MUTANT *ras*-p21

D. Xiao, G. Weng, D. Manor and R. Callender. Physics Dept. City College of CUNY, New York, NY10031

Ras-p21 protein is one member of the G-protein super-family. Point mutations of p21 are found in about 30% of human tumors and thus constitute the most prevalent oncogene in human carcinogenesis. The p21 mutation p21V12G, has an intrinsic GTPase activity much lower than that of wild type p21, and its binding to GAP does not result in accelerated hydrolysis of the bound GTP. The protein is therefore always in active or "on" conformation.

We utilized classical Raman difference spectroscopy to probe the protein-nucleotide interactions as well as protein conformational changes in the mutated protein p21V12G. The spectra will be presented and their relevance to the protein conformational changes and mechanism of protein action will be discussed.

Tu-Pos206

PREDICTED 3-D STRUCTURE OF α-CRYSTALLIN SUBUNITS USING MOLECULAR DYNAMICS: A WORKING MODEL. ((P. Farnsworth, T. Kumosinski, T. Schleich, and B. Groth-Vasselli)) Physiology Dept., NJMS, Newark, NJ 07103; EERC, USDA, Philadelphia, PA 19118; Dept. of Chemistry, UCSC, Santa Cruz, CA 95064.

α–Crystallin was originally identified as the major structural protein in vertebrate lenses. Interest in its function was heightened by the discovery that its two subunits, αA and αB, have been identified in a broad spectrum of cell types in normal and pathological conditions. In addition, αB appears to be a 'heat shock protein'. To date, the protein has not been crystallized and it aggregates to such a great extent that 2-D NMR techniques are not feasible. Therefore, molecular modeling techniques along with 2° structure sequence based prediction algorithms as well as experimental global 2° structure were utilized to construct energy minimized 3-D working models of the subunits. The local minimization problem for these energy minimized structures was solved by using molecular dynamics with a Kollman force field and constraint bond distances for backbone atoms until equilibrium structures were achieved. The resulting dynamic structures were in agreement with biochemical, physical chemical and solution structural data in the literature. These 'working' 3-D structures will be used for predictive purposes in designing experiments to confirm and/or modify these models. Speculation is made concerning the stoichiometry and orientation of these subunits within a micellar type oligomer which occurs in solution.

Tu-Pos207

MODULATION OF THE FUNCTIONAL BEHAVIOR OF α-CRYSTALLIN IN THE LENS. ((M. Reddy, D. Palmisano, K. Chima, M. Jilani, and P. Farnsworth)) Physiology Dept, UMDNJ-NJMS, Newark, NJ 07103. (Spon. by F.P.J. Diecke)

Reversible binding of small molecules (ligands) is of fundamental importance in the modulation of various biological macromolecular phenomena. Our first objective was to study the modulation of α-crystallin, the major lens structural protein, by its interaction with small metabolites. The rationale for selecting the metabolite ATP was based on previous NMR data which provided evidence for significant amounts of bound ATP in the lens. The relevance of this study extends beyond the confines of the lens since the subunits of α-crystallin, αA and αB, have been identified in a broad spectrum cell types. Also, αB functions as a small heat shock protein. In the present study ^{31}P NMR spectra showed significant changes in chemical shifts for the β and γ P atoms of ATP in the presence of α-crystallin. In addition, the spin-lattice T_1 relaxation times for α, β and γ P atoms were significantly decreased. These data indicate that ATP is bound to α-crystallin. The second objective was to demonstrate the affect of ATP/α-crystallin binding on the association of α-crystallin and MIP 26, the major lens membrane intrinsic protein. ^{31}P NMR and SDS-PAGE data show that ATP enhances α-crystallin/MIP 26 interaction. These results and a diminishing gradient of ATP from the cortex to the nucleus of the lens may decrease membrane bound α-crystallin and play a role in the change in supramolecular organization from cortex to nucleus.

Tu-Pos208

Ca^{2+}-INDUCED DOMAIN INTERACTIONS OF CALMODULIN ((Amy S. Verhoeven and Madeline A. Shea*)) Dept. of Biochemistry, U. of Iowa College of Medicine, Iowa City, IA 52242-1109

Intermediate states populated during cooperative Ca^{2+} binding to calmodulin (CaM) were probed by investigating changes in CaM backbone susceptibility to very limited proteolysis. This approach monitors localized ligand-linked conformational changes in CaM to indicate responses of specific residues. Thrombin was used to probe CaM at two arginines: R37, near Ca^{2+}-binding site 1 and R106, near site 3. Primary cleavage products for each position gave identical reactivity profiles. Secondary cleavage was not observed; thus, susceptibility at those positions reflects the Ca^{2+}-induced properties of whole CaM. The biphasic alternating susceptibility of R37 showed that its conformation responded to binding in N- and C-domains: cooperative binding at sites 3 and 4 induced proteolysis at R37 and subsequent binding at sites 1 and 2 protected it. The separation of effects also indicated that intermediate conformations are significantly populated during equilibrium ligation of CaM. An *identical* pattern of non-monotonic reactivity of residues near site 1 towards cleavage by thrombin, bromelain and Endo GluC demonstrated that the observed biphasic change reflected properties of CaM, not of the proteolytic probe. In the C-terminal domain, susceptibility of R106 to thrombin showed a monotonic decrease in susceptibility over the same range of low [Ca^{2+}] seen to induce susceptibility at R37 and was fit best by a cooperative binding model. The free energies of the cooperative binding events were estimated. (NSF DMB 9057157, AHA 910148980)

Tu-Pos209

A SELF-CONSISTENT METHOD FOR THE ANALYSIS OF PROTEIN SECONDARY STRUCTURE FROM CIRCULAR DICHROISM.

((N. Sreerama and R.W. Woody)) Department of Biochemistry, Colorado State University, Fort Collins, CO 80523.

We have developed a self-consistent method for estimating the secondary structure of proteins from CD spectra. In this method the spectrum of the protein analyzed is included in the matrix of CD spectra and an initial guess is made as a first approximation for the unknown secondary structure. The resulting matrix equation relating the CD spectra to the secondary structure is solved by the singular-value decomposition algorithm. The solution obtained replaces the initial guess, and the process is repeated until self-consistency is reached. We have incorporated the features of the variable selection and the locally linearized methods in our method. For most proteins considered, the self-consistent solutions obtained with different initial guesses were similar. However, the structure of the protein having the CD spectrum most similar to that of the protein analyzed is the best choice for the initial guess. The results obtained are as good as or better than the previous analyses. We have applied this method to examine the inconsistencies in the CD data, to compare the predictions with different ranges and resolutions of the CD data, and to compare different assignments of secondary structures from x-ray structure analysis in the context of secondary structure predictions. We find the Kabsch & Sander crystal structure analysis to be most suitable for our prediction method. (Supported by GM 22994.)

Tu-Pos210

CONFORMATION OF THE α-TUBULIN C-TERMINAL REGION: MOLECULAR MECHANICAL SIMULATIONS INDICATING INTERACTION AMONG SITES OF TYROSINATION AND GLUTAMYLATION.

Paul W. Chun, R. Donald Allison & Daniel L. Purich. Department of Biochemistry & Molecular Biology, University of Florida College of Medicine, Gainesville, FL 32610-0245

Tubulin is a αβ-heterodimer comprised of two related, nonidentical subunits with clusters of glutamyl residues at or near their carboxyl-termini. Subtilisin treatment releases several residues from the α-tubulin C-terminus and results in virtually irreversible polymerization, suggesting that critical concentration behavior may depend on C-terminal conformation. α-Tubulin becomes detyrosinated in assembled microtubules, whereas unpolymerized α-tubulin undergoes unique ATP-dependent retyrosination. Moreover, oligo-glutamylation is a recently discovered structural element located near the α-tubulin C-terminus. We are conducting molecular mechanical simulations with the peptides below,

(1) = VEGEGEEEGEE (2) = VEGEGEEEGEEY (3) = VEGEGEEEGEEF
(4) = VEGEGEEEGEE (5) = VEGEGEEEGEEY (6) = VEGEGEEEGEEF
E,E-E E,E-E E,E-E

where Y, F, and E,E-E are tyr, phe, and oligo-glu isopeptide side-chain. Energy minimization of (1) and (4) indicates that the 5th and 6th glu residues from the C-terminus have side-chains disposed equatorially relative to the open helix long axis. With (2) and (3), the γ-glu side-chains at the 4th, 6th, and 7th positions lie axially, parallel to the open helix. These findings suggest potential interactions between sites of tyrosination and glutamylation that may alter the susceptibility of tubulin to enzymatic oligo-glutamylation.

Tu-Pos211

NMR SOLUTION STRUCTURE OF THE NK-2 HOMEODOMAIN

((D. H. H. Tsao, L.-H. Wang, M. Nirenberg, J.A. Ferretti)) NHLBI, N.I.H., Bethesda, MD 20892

The *Drosophila* NK-2 homeobox gene is one of the earliest genes to be expressed in nuclei of the cellular blastoderm that becomes comitted to develop as neuroblasts, which give rise to neurons of the ventral nerve cord and subesophageal ganglion (1, 2). The homeodomain is a 60 amino acid segment of NK-2 which binds to specific sequences in DNA and thereby regulates the expression of the gene. Multidimensional NMR is employed to determine the solution conformation of the uniformly ^{15}N labelled NK-2 homeodomain. The stability and conformation of NK-2 will be discussed and compared to other homeodomains known to have the helix-turn-helix motif.

1. Y. Kim & M. Nirenberg, PNAS, 86, 7716 (1989).
2. K. Nakayaga, N. Nakayaga, Y. Kim, K. Webber, R. Ladd & M. Nirenberg, in preparation.

Tu-Pos212

RECOMBINANT HUMAN IMMUNODEFICIENCY VIRUS TYPE-1 (HIV-1) REVERSE TRANSCRIPTASE PRODUCES A MIXED POPULATION OF FOLDED PROTEINS.

((JE Wilson, LL Wright, GR Painter, JL Martin, PA Furman)) Burroughs Wellcome Co., Division of Virology, 3030 Cornwallis Rd., Research Triangle Park, NC 27709

HIV-1 encodes a p66/p51 heterodimeric RT (reverse transcriptase). This enzyme is the target of the three currently approved therapies for AIDS (AZT, DDI, and DDC). A major effort in the anti-HIV field is in structure/function studies using recombinant HIV-1 RT. Our group is currently studying the mechanism of HIV-1 drug resistance using site-directed mutagenesis. WT (wild type) HXB2D HIV-1 RT and mutant T215Y were subcloned from M13mp18HXBRT into an expression vector, pKK233 and transfected into E. coli strain TG1. The induced protein was purified using anion-exchange, cation-exchange, and immunoaffinity chromatography. Depending on the purification regimen used, three distinct populations of mutant RT, T215Y(a), T215Y(b) and T215Y(c), were isolated that differed in charge profile, dimer association, and the concentration of urea required to induce denaturation. While the kinetic constants for dTTP and AZTTP were similar to WT protein for both T215Y(b) and T215Y(c), T215Y(a) exhibited a three-fold elevated K_m for dTTP and a thirty-fold elevated K_I for AZTTP with respect to WT protein purified in the same manner. Equilibrium unfolding transitions of the three populations described above were determined by monitoring the change in enzymatic activity induced by urea. The urea denaturation profiles revealed that the conformational stability increased in the order of T215Y(b) < T215Y(c) < T215Y(a). The conformational stability of each mutant protein is not different from WT proteins purified in the same manner. Therefore, the mutation does not induce a conformational change, rather different purification procedures appear to select for different conformations. This observation is important when addressing mutant proteins and the point mutation's effect on the function of HIV-1 RT.

Tu-Pos213

CONTINUUM ELECTROSTATIC AND NONPOLAR SOLVATION ENERGIES IN PROTEIN LOOP CONFORMATIONAL SEARCH EVALUATIONS.

((K.C. Smith and B. Honig)) Dept. of Biochemistry and Molecular Biophysics, Columbia University, New York, NY 10032.

We used the random conformational search technique GENLOOP, followed by 2 ps of molecular dynamics using Xplor, followed by energy minimization, to produce a set of possible conformations for protein loops being modeled. We investigated the importance of adding accurate electrostatic and nonpolar solvation energies to the *in-vacuo* potential as a final screen in selecting good conformations. The electrostatic solvation energy was calculated using the program DelPhi, which solves the Poisson-Boltzmann equation. The nonpolar solvation energy was calculated as the molecular accessible surface area multiplied by the alkane vacuum to water transfer energy per unit area. The technique was applied to three loops in the known crystal structure of *E. Coli* RNase H. Addition of the solvation terms was found to improve the energy of conformations close to the crystal structure over the *in-vacuo* potential terms alone.

Tu-Pos214

EFFECT OF A HYDROGEN-BOND CONNECTING β-STRANDS ON *E. COLI* HPR STABILITY.

((P. K. Hammen*,J. M. Scholtz^,E. B. Waygood# and R. E. Klevit*)) *Univ. of Washington, Seattle, WA 98195; ^Stanford Univ., Stanford, CA 94305; #Univ. of Saskatchewan, Saskatoon, Sask. S7N 0W0 Canada (Spon. by R. Klevit)

We have reported unusual NMR behavior of two sidechain hydroxyl protons in the phospho-carrier protein, HPr, from *E. coli* (Hammen, *et al.* 1991). One such proton is the hydroxyl proton of Ser31, which is at the end of an interior strand of the four-stranded anti-parallel β-sheet in HPr. NOESY spectra indicate that this hydroxyl proton is close to backbone atoms of residues Asp69 and Glu70, which are in the adjacent β-strand. These data suggest a hydrogen-bond connecting adjacent strands at the end of the sheet.

A mutant of HPr in which Ser31 has been replaced with alanine (S31A) was designed to investigate the contribution of this hydroxyl group on HPr conformation and stability. Measurements of CD spectra as a function of urea concentration show that S31A is 0.5 kcal/mole less stable than the wild-type protein. Analysis of NOESY spectra indicate that S31A and wild-type HPr have the same global fold, and very similar secondary structure.

Furthur NMR measurements will provide more detailed conformational information and identify hydrogen-bonding patterns. The results presented will characterize the structural differences between wild-type HPr and S31A. What will emerge is a clearer view of the importance of the connection between β-strands to the stability of HPr.

Reference: Hammen, P. K., Waygood, E. B. & Klevit, R. E. (1991) Biochemistry 30. 11842-11850.

Tu-Pos215

CRYSTALLOGRAPHIC STRUCTURE OF AN FAB WHICH NEUTRALIZES RHINOVIRUS 14.

((H. Liu and T.J. Smith)) Department of Biological Sciences, Purdue University, West Lafayette, IN 47907.

An Fab from a monoclonal antibody (Mab17-IA) which neutralizes rhinovirus 14 was crystallized in 40% ammonium sulphate at pH 6.7. The crystals had the space group symmetry $P2_12_12_1$, and the unit cell dimensions were a=37.7 Å, b=97.3 Å, c=129.5 Å. X-ray diffraction data were significantly collected to 2.7 Å. Clear molecular replacement solutions were found for the Fab by using HyHEL-10 Fab as a searching probe. The solutions were further proved by a good uranyl derivative, which was found by the isomorphous replacement method. The electron density map was well resolved by simulated annealing refinement. The final crystallogrphic R factor was 19.0% for 8-2.7 Å data, and the Fab model had 0.013 Å deviations of bond lengths and 2.8° deviations of bond angles from ideality. The interactions between hypervariable loops of Fab17-IA and the epitope on rhinovirus 14 were modeled according to several available complex structures of macromolecular antigens with Fab fragments.

Tu-Pos216

DETECTION OF CONFORMATIONAL CHANGES IN THE COLICIN E1 CHANNEL PEPTIDE UPON ACTIVATION TO THE INSERTION-COMPETENT STATE USING FLUORESCENCE RESONANCE ENERGY TRANSFER.

((B.A. Steer and A.R. Merrill)), Guelph-Waterloo Center for Graduate Work in Chemistry Dept. of Chem. & Biochem., Univ. of Guelph, Guelph, ON, Canada N1G 2W1.

The single cysteine residue (Cys-505) in the colicin E1 COOH-terminal channel peptide was labeled with the thiol-specific fluorescence reagent, IAEDANS (5-[[[iodoacetyl)amino]ethyl]amino]-naphthalene-1-sulfonic acid). The labeling stoichiometry was nearly 1:1 (IAEDANS:peptide, mol:mol). Nine single tryptophan-containing mutants of the channel peptide were prepared and the distance between each of the tryptophan residues and the IAEDANS chromophore was determined using fluorescence resonance energy transfer. The distances between the various donor-acceptor pairs ranged from 23.1 Å to 29.4 Å in the native peptide in solution (pH 6.0). Activation of the channel peptide to the translocation-competent state by the addition of octyl β-D-glucoside (10,000:1, detergent:peptide, mol:mol) resulted in increases in the donor-acceptor distances. These increases ranged from 1.5 Å to 11.1 Å. In addition, fluorescence anisotropy measurements indicated a change in structure upon channel peptide activation. These results are consistent with the colicin E1 channel peptide being a compact solution structure and upon activation to the translocation-competent state a small but significant unfolding occurs [supported by the Medical Research Council of Canada, ARM].

Tu-Pos217

THERMODYNAMIC STUDIES OF THE INFLUENZA VIRUS HEMAGGLUTININ

((M. Krumbiegel[1], R. Blumenthal[1], A. Ginsburg[2], and D.P. Remeta[2])) [1]NCI and [2]NHLBI, National Institutes of Health, Bethesda, MD 20892 (Spon. by A. Shrake)

Entry of the influenza virus into target cells is mediated by the recognition of sialic acid containing cell surface receptors by hemagglutinin (HA), a major surface glycoprotein in the viral membrane. Subsequent fusion of the viral envelope with the endosomal membranes results in release of viral genome into the cell. This fusion process is triggered by a pH-dependent conformational change of HA in the acidic milieu of the endosomes. HA is a membrane integrating trimeric protein (220,000 M_r) comprising an ectodomain of identical subunits, each of which contains two polypeptides (HA_1 and HA_2) linked by a disulfide bond. The conformational stability of HA from the influenza strain X31 has been investigated by differential scanning calorimetry (DSC) in phosphate buffered saline (pH 7.3) to characterize thermodynamically the structural changes accompanying the unfolding process. The protocol employed to isolate HA involves solubilizing the virus in octyl glucoside, removing the insoluble nucleocapsid by centrifugation, and further purification by affinity chromatography on a ricin A column. DSC profiles of HA obtained at scan rates of 60 and 90 °C/hr reveal a single endotherm at a transition temperature of 66.5 °C with an enthalpy change of ΔH_{cal} = 980 kcal/mol. Deconvolution of the HA endotherm indicates that the protein unfolds in a cooperative manner which may be described by three two-state transitions. Evidence for three thermodynamic domains is consistent with the calculated cooperative ratio of $\Delta H_{cal}/\Delta H_{vH}$ = 3. Experiments are currently in progress to determine thermal stabilities and energetics of unfolding different conformational states of HA and thereby characterize cooperative interactions involved in the binding and fusion processes.

Tu-Pos218

USE OF ULTRACENTRIFUGATION AND FLUORESCENCE ANISOTROPY DECAY TO EVALUATE ASYMMETRY AND DYNAMICS OF THE HUMAN FACTOR VIIa:SOLUBLE TISSUE FACTOR COMPLEX

((E. Waxman, W.R. Laws, T.M. Laue, Y. Nemerson, and J.B.A. Ross)) Depts. of Biochemistry and Medicine, Mount Sinai School of Medicine of CUNY, New York, NY 10029, and Dept. of Biochemistry, University of New Hampshire, Durham, NH 03824.

Ultracentrifugation and fluorescence anisotropy decay measurements were used to evaluate the asymmetry and conformational dynamics of human blood clotting enzyme VIIa and the complex it forms with a soluble truncation mutant of its essential cofactor, human tissue factor (sTF). Sedimentation velocity experiments show that both VIIa and the sTF:VIIa complex are highly asymmetric. In each case, the friction ratio f/f_{sphere}, which describes the hydrodynamic behavior of VIIa and sTF:VIIa, is consistent with a family of general ellipsoids ranging from prolate to oblate. Fluorescence anisotropy decay experiments limit the family of possible shapes for both VIIA and sTF:VIIa by eliminating the oblate ellipsoids of revolution. In addition, the anisotropy data clearly show that upon forming the complex, VIIa loses segmental motion of a domain which includes its active site. The concepts used in combining the ultra-centrifugation and fluorescence anisotropy decay results will be presented. Supported by NIH grants HL-29019 and GM-39750 and by NSF grant DIR-9002027.

Tu-Pos219

FOURIER DECONVOLUTION FTIR OF GLOBULAR PROTEINS IN WATER: COMPARISON WITH X-RAY CRYSTALLOGRAPHIC STRUCTURE.

((T.F. Kumosinski and H.M. Farrell, Jr.)) USDA, ERRC, Philadelphia, PA 19118

Previous studies comparing the global secondary structure of globular proteins calculated from their X-ray crystal structure, with those determined from Fourier deconvolution FTIR spectroscopy were performed in D_2O. However, D_2O causes increased hydrophobic interactions which can lead to spurious 2° structural changes in some proteins, as well the as the essential elimination of the amide II peptide band. We have now performed FTIR experimepts on fifteen globular proteins with varying types and amounts of 2° structures know from X-ray crystallography. Calculation of the component 2° structural elements of the vibrational bands, i.e., 25 to 30 Gaussian bands, was accomplished by fitting both the amide I and II bands using nonlinear regression analysis of: the Fourier deconvoluted spectra, the second derivative spectra, and the original spectrum with fixed frequencies determined from both the deconvoluted spectra and 2nd derivative analysis. The criterion of acceptance of analysis was that the fractional areas calculated from all three methods were in agreement. Results clearly show that when compared with X-ray crystallographic data, the 2° structures of all proteins determined in water were in better agreement than the previous reported values obtained in D_2O.

Tu-Pos220

SMALL ANGLE NEUTRON SCATTERING STUDIES OF ALLOPHYCOCYANIN AND ITS SUBUNITS.

((Anand M. Saxena)) Biology Department, Brookhaven National Laboratory, Upton, NY 11973. (Spon. by R. Setlow)

Allophycocyanin, a photosynthetic antenna pigment protein, was isolated and purified from the cyanobacteria *Synechocystis 6701*. HPLC was used to determine the conditions for keeping the protein in a stable trimeric form, and also in a monomeric form using chaotropic salts, sodium perchlorate and sodium thiocyanate. The protein was also dissociated into α and β subunits by using ion-exchange chromatography in 8M urea solutions. Molecular weight and radius of gyration was determined for each of these forms with small angle neutron scattering. Higher angle scattering data from monodisperse allophycocyanin in trimeric and monomeric forms, collected in deuterated buffers to increase the contrast, were compared with theoretical scattering curves for different models to determine the best-fit shapes of these two aggregates. A model building approach was then pursued to fit three monomers in a trimer. The subunits were mixed together after removal of urea and, after suitable treatment, the trimeric form was regenerated as shown by HPLC, and also an analysis of the small angle scattering data.

Tu-Pos221

DSC AND DMA ANALYSES OF MODEL PROTEINS IN FROZEN SOLUTION INDICATE THAT COLD DENATURATION OF PROTEINS IS SIGNIFICANT IN FROZEN *POPULUS* TISSUE

((A.G.Hirsh*, L.I. Tsonev*, and T.J.Bentt))*Jerome Holland Laboratory of The American Red Cross, Rockville, MD 20855; †Comsat Labs, Clarksburg, MD 20871

Differential scanning calorimetry (DSC) demonstrated that very slowly cooled *Populus* (cottonwood) wood displays transient endothermic behavior upon warming between -60°C and -20°C. In dynamic mechanical analysis (DMA), slowly cooled *Populus* tissue displays a transient high loss modulus (E") and low storage modulus (E') in the range -60°C to -20°C. These results are exaggerated in cold injured hardy *Populus* or frozen tender *Populus* and are consistent with the hypothesis that (1) some of the proteins in these tissues cold-denature at low temperatures ; and (2) this process is inhibited by sugars. To establish the veracity of this model we have studied cold denaturation in concentrated solutions of several model proteins and sugars. Our results show similar transient endotherms upon warming either very slowly frozen proteins or proteins quench-cooled from high, denaturing temperatures. The behavior of E' and E" are also similar to that of the frozen *Populus*. Attempts to quantitate the enthalpy of the refolding proteins have been complicated by the unexpected discovery that C_p of denatured protein-water complexes appears to be lower than native protein-water complexes, in contrast to high temperature data.

Supported in part by NIH Grant BRSG 2-507RR05737

Tu-Pos222

RETENTION OF PROTONS IN PROTEIN SULFHYDRYL CHELATES WITH Zn^{2+} AND Cd^{2+}.

((X.Yu, and C.Fenselau)) Department of Chemistry and Biochemistry, University of Maryland Baltimore County, Baltimore, MD 21228. (Spon. by C.Fenselau)

Chelation of metal ions by sulfhydryl and histidine groups in proteins is recognized to stabilize the three dimensional conformation, remove (toxic) metals from solution, and to influence proper function in cellular processes. NMR and X-ray measurements have provided important structural information about metal-binding proteins. However, they can not always tell if sulfhydryl protons have been displaced or not by the metal ions. We have used electrospray mass spectrometry to examine the retention or displacement of sulfhydryl protons in several systems. Rabbit liver metallothionein 2a has been studied, in which twenty cysteine groups chelate seven divalent metal ions in two clusters. All twenty protons were displaced in the complex with seven Cd^{2+}. However, only eleven protons were displaced when seven Zn^{2+} were chelated. In the case of the p7 nuclear capsid protein from HIV-1 retrovirus*, in which two CCHC arrays bind two divalent metals, we found that all eight protons are retained when either two Cd^{2+} or two Zn^{2+} are coordinated. Retention or displacement of protons is thought to reflect the binding affinities of each system. The powerful capability of this technique is being extended to other metal ions and other proteins.

* Kindly provided by R.Sowder II and L.Henderson, PRI/DynCorp, NCI-Frederick Cancer Research and Development Center, Frederick, MD 21701.

Tu-Pos223

A SET OF DISTINGUISHABLE AMINO ACID CONFORMATIONS IN PROTEIN

((R. T. Miller, A. K. Dunker and R. J. Douthart)) Depart. of Biochem. & Biophys., Washington State U., Pullman, Pullman, WA 99164-4630 and the Life Sciences Center, Pacific Northwest Laboratory, Richland, WA 99352

The backbone dihedral angles in 99 proteins of known structure have been investigated using a simple cluster-seeking algorithm. The 19,121 amino acid residues in this data set partition into 125 distinct cluster centers. While only 18 of the 125 centers capture 1% or more of the data set each, the first cis-proline conformation ranks 49th in the population, suggesting that at least this many centers may be significant. The least populated centers probably represent errors in the data set, although the possibility of extremely rare conformations cannot be ruled out. The commonly recognized conformational classes are each represented by at least one of these centers; the β (extended) region sub-divides into several distinct classes. Several rare but significant centers are specific for one or a small number of amino acids (especially pro and gly). We demonstrate four applications of these centers: their use to represent and analyze individual proteins, their (tripeptide) sequence dependency, the distribution of neighboring centers in the data set, and a simple predictive algorithm based on these findings.

PROTEIN FOLDING

Tu-Pos224

STRUCTURAL ENERGETICS OF III^{GLC}, A β-SHEET SIGNAL TRANSDUCING PROTEIN.

((Kenneth P. Murphy†, Norman D. Meadow§, Saul Roseman§, and Ernesto Freire†)) †Biocalorimetry Center, §McCollum-Pratt Institute and Department of Biology, The Johns Hopkins University, Baltimore, MD 21218

III^{Glc} is a major signal transducing protein of the phosphoenolpyruvate phosphotransferase system in *E. coli*. The x-ray crystal and NMR structures of III^{Glc} (18.1 kD) show that it consists of about 52% β-sheet and only 6% helix. The folding/unfolding energetics of III^{Glc} have been determined by high-sensitivity differential scanning calorimetry (DSC). The wild type protein and two mutants, in which the two active site histidines were independently replaced with glutamine, were studied. Scans were found to be greater than 80% reversible. Both mutants are moderately less stable than the wild type, with H75Q being the least stable. The structural energetics of these proteins can be calculated from the crystal structures using our previously published approach. In contrast to previously studied, largely helical proteins, the calculated energetics assuming complete unfolding at high temperature differ significantly from the experimental parameters. In particular, the heat capacity change upon unfolding is smaller than expected from the structure, while the enthalpy change is larger. These effects suggest that residual structure may exist in this thermally denatured β-sheet protein.

Tu-Pos225

THERMAL AND GUANIDINE.HCl INDUCED DENATURATION OF PLASTOCYANIN.

((E.L. Gross, B. Pan, and J.E. Draheim)) Dept. of Biochemistry and Biophysics Program, The Ohio State University, Columbus, OH, 43210 and Chemistry Dept., Adrian College, Adrian, MI.

Thermal and guanidine.HCl (Gd.HCl) denaturation studies were carried out on the "blue" copper protein plastocyanin (PC). It was found that thermal denaturation produced two denatured forms, one of which was formed by an irreversible oxidation process and the other by a reversible oxidation process. Both denatured forms showed circular dichroic (CD) spectra which were not characteristic of a random coil. Gd.HCl-induced denaturation also produced similar far-UV CD spectra. Heating the samples after Gd.HCl treatment or Gd.HCl treatment after heating caused no further denaturation.

For spinach PC, the rate of denaturation of PC was very slow at Gd.HCl concentrations below 3M. Increasing the Gd.HCl concentration from 4 to 7 M increased the rate constant for loss of the copper center (A_{597}) from 0.4 to 36 min^{-1}. The rate of denaturation was independent of the PC concentration from 20 to 70 μM. The rate constant for denaturation of parsley PC using 3 M Gd.HCl was 2.53 min^{-1} which is 52 times that for spinach under the same conditions. Many of the 31 amino acid changes between spinach and parsley PC occur near the Cu center or the acidic patches thought to be involved in cytochrome f binding.

Tu-Pos226

ADIABATIC COMPRESSIBILITY OF A MOLTEN GLOBULE.
((Bengt Nölting, and Stephen G. Sligar)) Department of Biochemistry, University of Illinois, Urbana, IL 61801

We report the first measurement of the adiabatic compressibility for the molten globule state of a protein. Apo-cytochrome b_{562} has been shown by NMR structure determination, side-chain relaxation measurements, and calorimetry to be a "molten globule" with compact three dimensional structure and a fluid-like core. High precision density (ρ) and velocity of sound (u) measurements for apo- and native holo-b_{562} allow determination of the adiabatic compressibility β by $1 / \beta = \rho u^2$ [1]. For measurement of sound velocities in macromolecular samples, a small volume acoustic resonator was developed. Incorporating a thermistor bridge allows temperature drifts during measurement to be monitored within ± 0.001 K and corrected for in the measurement with resultant high precisition in density and sound velocity.

Supported in part by NIH GM31756.

[1] A. P. Sarvazyan, Annu. Rev. Biophys. Biophys. Chem. (1991) 20, 321-342

Tu-Pos227

CHARACTERIZATION OF THE AMINO FOLDING UNIT OF THE ALPHA SUBUNIT OF TRYPTOPHAN SYNTHASE.
((J. A. Zitzewitz and C.R. Matthews)) Department of Chemistry, The Pennsylvania State University, University Park, PA 16802.

The α subunit of tryptophan synthase, isolated from *Escherichia coli,* is a 268 residue, eight-stranded α/β barrel protein. The denaturant-induced unfolding of the α subunit is thought to involve a stable intermediate in which the amino folding unit (strands 1-6, helices 0-5) remains folded and the carboxy folding unit (strands 7-8, helices 6-8) becomes disordered [Beasty and Matthews (1985) *Biochemistry 25*, 2965; Miles, Yutani, and Ogasahara (1982) *Biochemistry 21*, 2586].

In this study, a peptide fragment corresponding to the proposed amino folding unit was isolated by limited tryptic digestion of the α subunit at Arg 188. The urea-induced equilibrium unfolding of this fragment was monitored by Tyr absorbance (AB) and far UV circular dichroism (CD). Coincident AB and CD curves suggest a two-state unfolding of the fragment and concerted disruption of secondary and tertiary structure. Estimates of stability imply that the stable intermediate observed in the unfolding of the full-length α subunit contains more structure than that observed in the isolated fragment. Additional thermodynamic and kinetic experiments are currently in progress to further characterize the folding of this fragment.
(This work was supported by NIH Postdoctoral Fellowship Award GM14954 to J.A.Z. and NIH grant GM23303 to C.R.M.)

Tu-Pos228

NMR CHARACTERIZATION OF MONELLIN IN ALCOHOL: OBSERVATION OF β-SHEET TO α-HELIX CONVERSION
((W. Clay Bracken, Pei Fan, and Jean Baum)) Department of Chemistry, Rutgers University, Piscataway, NJ 08855

To understand how and when different forces come into play to direct protein folding, the study of folding intermediates and denatured states has fundamental importance. Denatured states of proteins can be obtained by a number of different methods, including the use of short-chain-alcohols, such as methanol, ethanol, propanol and trifluoroethanol. Upon addition of either 50% ethanol or 50% trifluoroethanol (TFE), the native structure of monellin is disrupted resulting in an alcohol denatured state with properties different from the random coil state. Two dimensional ^{1}H NMR spectroscopy and hydrogen exchange methods have been used to characterize this state. In the alcohol denatured state, the backbone circular dichroism (CD) spectra displays a higher helical content relative to the native state and the intensity of the aromatic CD signal is completely lost. Utilizing hydrogen exchange trapping techniques, the slowly exchanging residues are identified at pH 2.0 in 50% ethanol and 50% TFE and are found to be clustered on one region of the protein. Preliminary 2D NMR assignments show that monellin undergoes structural reorganization, specifically, one strand of the native state β-sheet is converted into an α-helix in the alcohol denatured state.

Tu-Pos229

REFOLDING OF BRAIN-DERIVED NEUROTROPHIC FACTOR OCCURS VIA A MONOMERIC "MOLTEN GLOBULE" INTERMEDIATE WITH A STRUCTURE QUITE UNLIKE THE NATIVE STATE.
((J. Philo, R. Rosenfeld, T. Arakawa, L. Narhi, J. Wen)) Amgen Inc., Amgen Center, Thousand Oaks, CA 91320

We have studied the refolding kinetics and pathway for recombinant human BDNF. When BDNF unfolded in 6 M GdnHCl is diluted 20-fold into PBS, a partially folded intermediate is rapidly formed (<1 min). CD and fluorescence show this intermediate has extensive secondary structure, but no well defined tertiary structure. GPC with light scattering detection shows it is also compact and monomeric. It therefore meets all the criteria for a "molten globule". This molten globule disappears with a $t_{1/2}$ of ~30 min, concurrently with the appearance of native dimers, without accumulation of any monomeric species with the native tertiary structure. Remarkably, the monomer-dimer association of the molten globule is $>10^{10}$ weaker than the native structure, and it has a low tendency to form large aggregates. Given the very large hydrophobic surface present at the native dimer interface, these results suggest that these hydrophobic groups are not exposed in the molten globule. The molten globule is therefore quite dissimilar to the native structure. A significant conformational change in the molten globule is needed to form the dimer interface, which is the rate limiting step in reaching the native dimeric structure.

Tu-Pos230

MOLTEN GLOBULE IN SUPEROXIDE DISMUTASE.
((E. Gratton, N. Silva, N. Rosato*, A. Finazzi-Agro* & G. Mei*)) University of Illinois at Champaign-Urbana, Laboratory for Fluorescence Dynamics, Department of Physics, Urbana, IL 61801; & *Dipartimento di Medicina Sperimentale e Scienze Biochimiche, Universita' di Roma "Tor Vergata," Rome, Italy.

The enzyme, human superoxide dismutase is a homodimer containing a single solvent-exposed tryptophan residue per subunit. This protein denatures as the concentration of guanidine hydrochloride is increased to about 6M. The midpoint of the transition is at about 3.5M guanidine hydrochloride for the holo protein. The denaturation process is accompanied by a dissociation of the dimeric native protein into monomers. The monomer-dimer equilibrium can be independently followed by changing the total protein concentration of the solution. We have studied the fluorescence and circular dichroism (CD) properties of the monomer and we have shown that in the monomer state the protein has the typical characteristics of a molten globule. In the molten globule state, the CD signal in the 220 nm region is identical to the CD signature of the native protein. By contrast, in the aromatic region around 270 nm the CD signal in the monomer state is lost. The fluorescence properties show that in the molten globule state the fluorescence decay is very heterogeneous, indicating the existence of a disorganized tertiary structure. Also, the decay of the emission anisotropy is relatively fast, as compared with the native protein, indicating a fluid-like environment for the surrounding of the tryptophan residue.
Supported by NIH RR03155 and the Italian CNR.

Tu-Pos231

FOLDING FE(II)-CO CYTOCHROME *C* BY PHOTOLYSIS.
((S.D. Luck, A. Bhuyan, and H. Roder)) Dept. of Biochem. Biophys., U. Penn., and Fox Chase Cancer Center, Philadelphia, PA 19111.

Previous NMR measurements of magnetization transfer show that the Met 80 methyl resonance of unfolded Fe(II) cytochrome *c* (cyt *c*) occurs at 2.06 ppm, typical of a random coil. This indicates that in the unfolded state Met 80 is dissociated from the heme thus allowing ligation of extrinsic molecules such as CO, unlike native reduced cyt *c* to which such binding does not occur. NMR measurements also show that the guanidine (GuHCl) induced unfolding transition of Fe(II) cyt *c* which is cooperative with a mid-point of 4.8 M GuHCl at pH 7, is lowered in 1 atm of CO to 3.5 M GuHCl, due to preferential CO binding to the unfolded form. In this work we show that at GuHCl concentrations between these two mid-points, photodissociation of the cyt-CO complex triggers the folding reaction. During and after illumination with a 75 W xenon arc lamp, we have observed folding and unfolding kinetics of cyt *c* by monitoring absorbance at 550 nm. The kinetics can be modeled with a three state chemical kinetics scheme comprised of folded, unfolded, and CO complexed unfolded conformations. We have also measured CO rebinding kinetics after photodissociation with a 10 ns laser flash at 532 nm. Two kinetic processes, a fast process with $t \approx 15$ μs probably due to binding of a non-native histidine ligand, and a later CO rebinding process with $t \approx 5$ ms were observed. Under strongly native conditions, NMR studies of the cyt-CO complex show that cyt *c* has native-like structure and CO photodissociation produces a fast protein relaxation with $t < 1$ μs.
(Supported by NIH grants GM 35926 to HR, and RR 01348 to RLBL, U. Penn.)

Tu-Pos232
STABILITY AND FOLDING OF A TRYPTOPHAN-CONTAINING MUTANT OF UBIQUITIN. ((S. Khorasanizadeh*, I. D. Peters, H. Roder)) Dept. of Chem. University of Pennsylvania*, Fox Chase Cancer Center, Philadelphia, PA 19111.

Ubiquitin is a good model protein for folding studies, but it lacks a suitable chromophore for optically-monitored folding experiments. In order to introduce a fluorescence probe we have replaced Phe 45 with a Trp (F45W). 2D ^{1}H NMR spectra under the same conditions used in the determination of the WT solution structure show that the chemical shift changes in F45W are largely limited to the site of mutation and surrounding residues indicating that the mutant is structurally very similar to the WT. Equilibrium unfolding by GuHCl at pH 5.0 observed by 1D NMR and CD shows two-state behavior for WT and F45W. Thermodynamic analysis indicates that the mutation results in 0.4 kcal/mol decrease in apparent free energy of unfolding. Equilibrium unfolding of F45W observed by fluorescence shows similar behavior to that observed by NMR and CD. Refolding and unfolding kinetics are conveniently measured for F45W using fluorescence-detected stopped-flow. The fluorescence refolding kinetics of F45W has features similar to that of WT ubiquitin observed in pulse labeling studies (Briggs, M. & Roder, H. (1992) *Proc. Natl. Acad. Sci. 89*, 2017-2021). The folding kinetics exhibits a major phase with a strongly denaturant-dependent time constant approaching 0.5 ms at low concentration of GuHCl. Because of the remarkable similarity of F45W to the WT we are using it as a reference to investigate the effect of further mutations on the stability and folding of ubiquitin. Since pulse labeling studies with WT suggested that helix-sheet association is an early folding event, the effect of two mutations (V26A and V26I) at the helix-sheet interface are being studied.

Tu-Pos233
BOVINE PANCREATIC TRYPSIN INHIBITOR HYDROPHOBIC CORE MUTANTS: A ^{1}H NMR STUDY OF INTERNAL FLUCTUATIONS. ((F. Tao, J.A. Fuchs, and C.K. Woodward)) Department of Biochemistry, University of Minnesota, St. Paul, MN 55108

Variants in the core region of bovine pancreatic trypsin inhibitor have been constructed by site-directed mutagenesis. Studies of X-ray crystallography, hydrogen isotope exchange and differential scanning calorimetry show that the large destabilizations in the global stabilities for these mutants can be accounted for by the differences in the transfer free energy of the altered amino acid sidechains and the exposure of the new concave hydrophobic surface (Kim, K.S. et. al., manuscript submitted). Using ^{1}H NMR, we have shown that the change in the observed exchange rate constants for the slowest exchanging protons is dominated by an unfolding mechanism and gives $\Delta\Delta G°$(WT-mut) (Tao, F., Fuchs, J.A., & Woodward C.K. *Techniques in Protein Chemistry IV*, in press). Here, we are investigating the perturbation effects on the protons which exchange mostly from the folded conformation, and also on the ring flip rates of some aromatic sidechains. We find that k_{obs} for most of the fast exchanging protons do not change in the mutants, compared to WT, within the error of the experiment. There is also no change in the values of the exchange activation energy obtained from the Arrhenius plots for these amide protons. This implies that conformational fluctuation governing the exchange rates are highly localized, non-cooperative events and not related to the cooperative folding properties of globular proteins. Correlation for the hydrogen exchange reactions and the aromatic ring flip rates are currently being investigated.

Tu-Pos234
CONTRIBUTION OF THE N-TERMINAL TO C-TERMINAL SALT BRIDGE TO STABILITY OF BOVINE PANCREATIC TRYPSIN INHIBITOR ((M. Salvati, J. Fuchs, and C. Woodward)) Biochemistry Dept., Univ. of Minnesota, St. Paul, MN 55108

We are investigating the effects of salt and denaturant on low pH denaturation of BPTI variants. Because BPTI is so stable, its denaturation at accessible temperatures only occurs in the presence of added denaturants. To eliminate the need for chemical denaturants, we made destabilizing amino acid replacements. The two mutants studied first are Y23A, and F45A. Both have replacements in the hydrophobic core, and both are highly destabilized, with Tm of approximately 55°C and 49°C, respectively, at pH 2, compared to WT Tm of ~85°C at pH 2. Unfolding curves for these mutants at varying acidic pH are being determined by CD. Initial results for Y23A in the absence of urea and salt show the expected decreasing stability as the pH is lowered through the carboxyl titration. Addition of high salt causes a decrease in stability of approximately 2 kcal/mol at pH above the pKa of a carboxyl group. In contrast at pH 2, no salt effect on stability is observed. This pH dependence of the salt effect can be explained by a highly stabilizing ionic interaction. Considerable NMR evidence supports an ionic interaction between the N-terminal amino group and the C-terminal carboxylate (Brown et al. 1978, Eur. J. Mol. Biochem. 88; Tüchsen and Woodward 1985, J. Mol. Biol. 185; Tüchsen and Woodward 1987, J. Mol. Biol. 193). The magnitude of the contribution of this salt bridge to total stability is being determined.

Tu-Pos235
REFOLDING STUDIES ON A STREPTOCOCCAL PROTEIN G DOMAIN. ((J. Kuszewski and A. M. Gronenborn)) NIDDK, NIH, Bethesda, MD 20892 (Spon. by T. Strzelecka)

The G_{B1} domain of Streptococcal protein G is ideally suited for studies of protein folding: it is 56 residues long, contains no disulfide bridges, and has a calorimetric T_m of ~90° C. The unfolding and refolding of G_{B1} was investigated. Tryptophan absorbance titration indicates that G_{B1} is completely unfolded at pH 12.0 and refolded at pH 9.5. Urea gradient gels indicate that G_{B1} starts to unfold around 6.3 M urea, but cannot be completely unfolded. Unfolding by guanidinium chloride was followed by NMR and it was found that at pH 6.3 complete unfolding is observed at 4.5 M guanidinium chloride. For all these conditions (pD, urea, guanidinium chloride), complete reversibility was observed. The kinetics of refolding were studied using quenched-flow ^{2}H/^{1}H exchange. In these kinetic studies, protein refolding was induced in two different ways—either by pH jump, or by change in guanidinium chloride concentration—and the degree of ^{2}H/^{1}H exchange was determined by NMR at various times after refolding began. Full characterization of the exchange curves produced by each refolding mechanism is in progress.

Tu-Pos236
sCD4 STABILITY MEASURED BY CALORIMETRY AND GUANIDINE HYDROCHLORIDE DENATURATION. ((S.W. Tendian and C.G. Brouillette)) Southern Research Institute, Birmingham, AL 35205.

CD4, a cell-surface glycoprotein expressed on T-lymphocytes, is a receptor for class II major histocompatibility complex (MHC) molecules and, in humans is also the receptor for the HIV envelope glycoprotein gp120. The conformational stability of soluble CD4 (sCD4), the extracellular portion of CD4, was measured using differential scanning calorimetry and ultraviolet difference spectroscopy to monitor thermally- and denaturant-induced unfolding, respectively. The thermodynamic parameters, including free energy of unfolding, obtained by the two techniques were compared. sCD4 consists of four contiguous domains (D1-D4). D1D2 has been crystallized and the domains are immunoglobulin-like in structure (1,2). The stabilities of isolated D1D2 and D3D4 were also measured. D1D2 is the more stable of the two subdomains and the interdomain interaction between D1D2 and D3D4 stabilizes D3D4.

This work is supported by NIH-AI32687.

1) Ryu, S.-E., et. al. (1990) *Nature 348*, 419-425
2) Wang, J., et. al. (1990) *Nature 348*, 411-418

Tu-Pos237
TIME-RESOLVED FLUORESCENCE POLARIZATION STUDIES OF NOVEL *DE NOVO* DESIGNED ALPHA HELICAL BUNDLES. ((S.A. Williams[1], T. Handel[2], D. Rayleigh[2] and W. DeGrado[2]))
[1]Regional Laser and Biotechnology Laboratory, University of Pennsylvania, Philadelphia, PA. 19104 and [2]DuPont Merck Research Co., Wilmington, DE. 19880 (Spon. by Ben Cowen).

A novel class of *de novo* designed proteins have been synthesized to better understand the role of intermediate states in protein folding. These proteins, a set of four alpha helical bundles interconnected by various loop structural schemes, shows properties intermediate between a native protein and a molten globule. We have investigated the structural motions of these protein systems using the time-correlated single photon counting technique on the pico- to nanosecond timescale. Anisotropy decay analysis, with alpha systems selectively modified with tryptophan and/or incorporated with fluorescence dye probes, has revealed that these systems resemble a late folding intermediate with well defined secondary structure yet significant side chain randomization. A series of metal-binding proteins with anticipated structural characteristics similar to carbonic anhydrase has also been synthesized. We have demonstrated conversion from a molten globule to a more stable native-like state though the introduction of metal ion. The structural response to metal binding with several modified protein systems will be presented. (Supported by NIH RR 01348 and DuPont Merck Research Co.)

Tu-Pos238

DISSECTION OF DISSOCIATION AND UNFOLDING OF THE CATALYTIC SUBUNIT (c_2) OF E. COLI ASPARTATE TRANSCARBAMYLASE

((Hiroki Morizono and Norma Allewell)) Department of Biochemistry, University of Minnesota, St Paul MN 55108.

The urea-induced dissociation and unfolding of the catalytic trimer of E. coli aspartate transcarbamylase (c_3) have been studied with transverse urea gradient gel electrophoresis at pH 8.3, 25°C in 0.025M Tris-0.1925M Gly buffer and by high performance liquid chromatography (HPLC) at pH 7.0, 25°C in 0.04M phosphate buffer [Creighton, T. E. *Meth. Enz.* 131 156-172 (1986), Corbett, R. J. T. & Roche, R. S. *Biochem.* 23 1888-1894 (1984)].

A major shift in mobility at urea concentrations of approximately 4M is observed by urea gradient gel electrophoresis, corresponding to unfolding of c chains. Similar results were obtained by Bromberg using low pressure analytical gel chromatography [Bromberg *et al. J. Biochem. Biophys. Meth.* 20 143-56 (1990)]. PALA, a bisubstrate analog which binds to the active sites of c_3, located between c chains, significantly stabilizes the trimer to unfolding and dissociation. In the presence of 5μM PALA, no dissociation is observed at urea concentrations below 6M.

Changes in the distribution of various unfolding and dissociating species are being analyzed by size exclusion HPLC. Previous studies have shown that the catalytic trimer dissociates into compact monomers in 40mM pyrophosphate [Yang, Y.R. & Schachman, H.K. *Anal. Biochem.* 163 188-95 (1987)]. By studying the urea-induced unfolding of these monomers, unfolding can be separated from dissociation.

Our long term goal is to use these methods to analyze the effects of a series of catalytic chain mutants on the energetics of dissociation and unfolding.

Tu-Pos239

THERMODYNAMIC β-SHEET PROPENSITIES MEASURED USING A ZINC FINGER HOST PEPTIDE.

((C.A. Kim and J.M. Berg*)) Department of Chemistry and Department of Biophysics and Biophysical Chemistry, The Johns Hopkins University School of Medicine, Baltimore, Maryland 21205. (Spon. by Eaton Lattman)

Thermodynamic β-sheet propensities of each of the 20 commonly occurring amino acids have been measured. A previously studied zinc finger peptide[1] was used as the host system in which amino acids were substituted into a guest site, a solvent exposed position within an anti-parallel β-sheet. Since these peptides are unfolded in the absence of bound metal but fold in their presence, it is assumed that the thermodynamics of metal binding fully reflects peptide folding energy. A competitive Co^{2+} binding assay was used to determine these energies with high precision. The relative free energies obtained were found to correlate well with previously derived potential values based on statistical analysis of protein structures. To our knowledge, this is the first reported β-sheet thermodynamic scale for all the commonly occurring amino acids in aqueous solution.

Tu-Pos240

DIFFERENTIAL SCANNING CALORIMETRIC STUDIES OF THE TRYPTOPHAN SYNTHASE MULTIENZYME $\alpha_2\beta_2$ COMPLEX

((D.P. Remeta[1], E.W. Miles[2], and A. Ginsburg[1])) [1]NHLBI and [2]NIDDK, National Institutes of Health, Bethesda, MD 20892

Tryptophan synthase from *S. typhimurium* (146,000 M_r) is a bifunctional enzyme that catalyzes the final two reactions in L-tryptophan biosynthesis and is comprised of four polypeptide subunits arranged in an extended αββα geometry [Hyde et. al. (1988) *J. Biol. Chem.* 263, 17857]. The conformational stabilities of the $\alpha_2\beta_2$ complex, the α chains, and the β dimer have been investigated by differential scanning calorimetry (DSC) in a buffer containing 10 mM K-PO_4, 0.1 mM DTT, and 1.0 mM EDTA (pH 8.0). DSC profiles of the $\alpha_2\beta_2$ complex in the presence of 0.2 mM pyridoxal 5'-phosphate (PLP) exhibit two well resolved endotherms at transition temperatures of t_1 = 51.5 °C and t_2 = 80.5 °C. Analysis of the isolated subunits reveals that the low- and high-temperature transitions correspond to thermal unfolding of the α chains and β_2 subunit, respectively. Integration of the endotherms for the $\alpha_2\beta_2$ complex yields ΔH_{cal} = 140 kcal(mol α chains)$^{-1}$ and ΔH_{cal} = 390 kcal(mol β_2)$^{-1}$. Deconvolution of the DSC profiles indicates that the unfolding of α chains is a two-state process (i.e., CR = $\Delta H_{cal}/\Delta H_{vH}$ = 1.0), whereas unfolding of the β_2 subunit involves two to three thermodynamic domains (CR = 2.5). Although the unfolding enthalpies determined for the apo- and holo-β dimer are similar [ΔH_{cal} = 300 kcal(mol β_2)$^{-1}$], there are substantial differences in the t_m and C.R. in the absence and presence of the cofactor PLP. Specifically, transition temperatures of 57.5 °C and 79.5 °C, and cooperative ratios of 4.0 and 2.0 are measured for the apo- and holo-β dimer, respectively. Our thermodynamic measurements therefore provide additional insight into the stabilizing effect of PLP on the overall conformation of the multienzyme complex.

Tu-Pos241

TEMPERATURE AND GUANIDINE INDUCED UNFOLDING OF DODECAMERIC GLUTAMINE SYNTHETASE FROM *E. COLI*.

((M. Zolkiewski and A. Ginsburg)) NHLBI, NIH, Bethesda, MD 20892.

Glutamine synthetase (GS) undergoes a reversible, thermally induced unfolding without dissociation of the dodecamer (M_r ~ 622,000). The transition involves an exposure of subunit Trp and Tyr residues and produces a single endotherm (t_m = 51.6 °C) in differential scanning calorimetry (DSC) in the presence of 1 mM Mn^{2+} and 100 mM KCl at pH 7. Deconvolution of DSC data shows only two two-state transitions which demonstrates highly cooperative unfolding processes. The small enthalpy change (0.34 cal/g) indicates that the thermal transition leads to a partially unfolded state of GS with disruption of 2-3 % of protein structures. GS is dissociated into subunits in 4.0 M guanidine•HCl (Gdn•HCl) as demonstrated by a 12-fold decrease in 90° light scattering at 37 °C. A maximum exposure of Trp and Tyr occur in 2.5 M Gdn•HCl. However, ≥5 M Gdn•HCl is required for total unfolding of subunits as shown by calorimetric experiments in which heats were measured for the transfer of GS from a buffer with 0.1 mM $MnCl_2$ into 2 to 7 M Gdn•HCl. The enthalpy of subunit dissociation at 37°C was estimated to be ~15 cal/g and the enthalpy of the subsequent unfolding to be ~13 cal/g. These studies demonstrate the importance of intersubunit interactions in an oligomeric protein in maintaining its native structure and their contribution to the thermostability of dodecameric GS.

Tu-Pos242

THERMODYNAMIC CHARACTERIZATION OF THE STRUCTURAL STABILITY OF THE bZIP TRANSCRIPTION FACTOR GCN4.

((Kelly S. Thompson*, Charles R. Vinson‡, Jon D. Shuman‡‡ and Ernesto Freire*))
*Dept. of Biology and the Biocalorimetry Center, The Johns Hopkins University, Baltimore, MD 21218, ‡Laboratory of Biochemistry, NCI and NIH, Bethesda, MD 20892, and ‡‡Dept. of Medicine, University of Alabama, Birmingham, AL 35294

The thermal stability of the transcriptional factor GCN4 has been studied by high sensitivity differential scanning calorimetry and circular dichroism. The thermal unfolding of GCN4 is a reversible process and can be well represented by a reaction of the form N_2 <--> 2U, indicating that unfolding of the leucine zipper is a two-state process in which the helices are only stable when they are in the coiled coil conformation. As expected, the transition temperature is concentration dependent. At pH 7.0 and a protein concentration of $4x10^{-4}$ M the transition temperature is close to 70°C while at 10^{-5} M it is close to 50°C. The enthalpy change for the transition is 31 kcal/mol of monomer at 60°C. Structural thermodynamic calculations using the parametrization developed by Murphy et al (J. Mol. Biol. (1992) 227 293-306) and the crystallographic structure reported by O'Shea et al (Science (1991) 254 539-544) predict a ΔH(60) of 27 kcal/mol and a ΔC_p of 0.35 kcal /K*mol in close agreement with the experimental values. (Supported by a grant from the National Institutes of Health RR04328).

Tu-Pos243

STRUCTURAL STABILITY OF SHORT SUBSEQUENCES OF THE TROPOMYOSIN CHAIN.

((M.E. Holtzer & A. Holtzer)) Dept. of Chem., Washington University, St. Louis, MO 63130.

The native tropomyosin molecule is a parallel, registered, 2-chain, α-helical coiled coil made from 284-residue chains. Long, excised subsequences (>95 residues) form the same structure with comparable thermal stability. Here, we investigate local stability using shorter subsequences (20-50 residues) that are chemically synthesized or excised from various regions along the protein chain. CD thermal unfolding studies of such shorter peptides indicate very low helix content, almost no coiled-coil formation, and high thermal lability of such secondary structure as does form. This behavior is in stark contrast to extant data on short, "designed" synthetic peptides, many of which have high α-helix content and form highly stable coiled coils. The latter observation calls into question the older idea that short subsequences of a protein have little structure. The present study supports the older view, at least in its application to tropomyosin. It is somewhat ironic that intrinsic local α-helical propensity of this protein is sufficiently weak as to require not only dimerization, but macromolecular amplification in order to attain its native almost totally helical conformation. [Supported by NIH and MDA.]

Tu-Pos244

INFRARED EVIDENCE FOR RETENTION OF SECONDARY STRUCTURES IN CYTOCHROME *C* UPON ACIDIFICATION. Aichun Dong, Ping Huang, and Winslow S. Caughey. Department of Biochemistry, Colorado State University, Fort Collins, CO 80523.

Protein amide I infrared spectroscopy has been used to monitor quantitatively and qualitatively the pH-induced unfolding process in horse heart cytochrome *c*. In contrast to the generally held view that the secondary structure of acid-denatured cytochrome *c* is essentially all random coil, we find either oxidized or reduced cytochrome *c* in a minimum ionic strength solution at pH 2.0 contains all secondary structure components in relative amounts similar to those at neutral pH except for loss of redox-dependent conformational changes in β-sheet and β-turn structures. Further decreases in pH cause the random structure content to increase to a maximum value of ~22% at pH 1.5 and then return to ~10% at pH 1.0, an amount similar to ~9% random structure at neutral pH. Upon return to pH 6.0, the amide I spectrum of oxidized cytochrome *c* is the same as the original oxidized pH 6.0 spectrum. However, dithionite reduction of oxidized cytochrome *c* that had been exposed to pH 2.0 or lower resulted in an amide I spectrum similar to the reduced spectrum obtained at pH 2.0 with a band at 1715 cm^{-1}, presumably due to protonated carboxyl side chains, and distinctly different from the original reduced spectrum at pH 6.0, which has no 1715 cm^{-1} band. High ionic strengths strongly protect against acid-induced unfolding in cytochrome *c*. These findings provide further evidence of different conformations for the oxidized and reduced forms of cytochrome *c*. (Supported in part by a gift from Strohtech, Inc. and by Colorado Agricultural Experiment Station Project 643)

Tu-Pos245

REFINEMENT OF THE KINETIC FOLDING MECHANISM FOR DIHYDROFOLATE REDUCTASE FROM *ESCHERICHIA COLI*. ((B. E. Jones, P. A. Jennings and C. R. Matthews)) Department of Chemistry, The Pennsylvania State University, University Park, Pa 16802.

A kinetic study of the folding of dihydrofolate reductase from *E. coli* has led to a refinement of the kinetic mechanism for folding [Jennings *et al.* (1992), *Biochemistry*, submitted]. Based upon a combination of stopped-flow circular dichroism, absorbance and fluorescence spectroscopies, folding appears to occur in three stages: (1) The formation of an intermediate containing an appreciable amount of secondary structure and nonpolar surfaces within the dead time of mixing (<5 ms). This species has marginal stability. (2) The formation of a set of four intermediates which all have a native-like contact between two tryptophans in a hydrophobic core. These intermediates have approximately half the stability of the native conformation. (3) The rate-limiting formation of a set of four native conformers via parallel channels from the preceding intermediates. Double jump experiments (native → unfolded → native) show that these channels are unlikely to be due to cis/trans proline isomerization in the unfolded protein. (This work was supported by NSF grant DMB-9004707.)

Tu-Pos246

THE ROLE OF PROLINE ISOMERIZATION IN THE SLOW FOLDING REACTION OF *trp* APOREPRESSOR. ((C. J. Mann, T. R. Garber, and C. R. Matthews)) Department of Chemistry, The Pennsylvania State University, University Park, PA 16802.

Escherichia coli trp aporepressor (TR) is an all α-helical, intertwined, dimeric protein whose folding has been shown [Gittelman & Matthews, (1990) *Biochemistry 29*, 7011-7020] to involve at least three slow kinetic phases. The lack of a urea dependence for the slowest of these phases and an activation energy of 25.6 kcal/mol led to the suggestion that this reaction is due to proline isomerization.

This hypothesis was tested in the present study by measuring the sensitivity to prolyl isomerase and by mutagenesis. Human cyclophilin accelerates the slow folding reaction, consistent with the its attribution to proline isomerization. To identify the specific proline residue involved, each of the three, structurally well-defined proline residues in TR were replaced singly by site-directed mutagenesis and the effects on the stability and folding of the resulting mutant proteins were assessed. Equilibrium CD experiments demonstrated that the P45G and P93G mutant proteins were slightly *destabilized* while the P37A mutant was *stabilized* compared to wild type. However, kinetic experiments conducted on all three single proline mutants showed no difference in the number of phases detected and only small changes in the relaxation times and relative amplitudes compared to wild type TR. Taken together, these data suggest that the slow folding reaction in TR catalyzed by cyclophilin does not involve proline residues, but may involve some other type of peptide bond isomerization. (This work was supported by an NIH Postdoctoral Fellowship Award GM13571 to C.J.M., and NIH Grant GM23303 to C.R.M.)

Tu-Pos247

ANALYSIS OF THERMALLY INDUCED PROTEIN FOLDING/UNFOLDING TRANSITIONS USING FREE SOLUTION CAPILLARY ELECTROPHORESIS. ((Vincent J. Hilser†, Gregory D. Worosila††, and Ernesto Freire†)) †Department of Biology and Biocalorimetry Center, The Johns Hopkins University Baltimore, MD 21218 ††Physical and Analytical Chemistry Department, CIBA-GEIGY Corporation Suffern, NY 10901

It is shown that free solution capillary electrophoresis (FSCE) can be used to monitor the temperature dependent folding/unfolding transitions of proteins. Furthermore, analysis of the data obtained by FSCE can be used to estimate the apparent thermodynamic parameters (enthalpy change (ΔH_{vH}), entropy change (ΔS), and transition temperature (T_m)) associated with the folding/unfolding transition. In addition to mobility changes associated with the transition, FSCE analysis is unique in its ability to provide access to the population distribution of mobility states. This is demonstrated by the temperature dependent change in the electrophoretic peak width and by the appearance of multiple peaks for very slow or irreversible processes. Moreover, by comparing the mobility of the denatured state to that of unstructured peptides, it is possible to characterize the relative degree of structure present in the unfolded state of a protein. This methodology has been applied to the analysis of the thermally induced unfolding of lysozyme at low pH. It is shown that the mobility of thermally denatured lysozyme can be described by the same function that describes unstructured, fully solvated peptides. On the contrary, the mobility of native lysozyme is significantly higher than the value predicted by that same function.The accuracy of the thermodynamic parameters obtained by this methodology compare within error with values obtained by direct calorimetric measurements using differential scanning calorimetry. (Supported by grants from the National Institutes of Health GM37911, NS24520 and RR04328).

Tu-Pos248

DEFINING AND IDENTIFYING PROTEIN TERTIARY STRUCTURE ((E. K. Insko*, L. Bolinger#, and J. S. Leigh#)) University of Pennsylvania: *Department. of Biochemistry & Biophysics, #Department of Radiology.

A hypothesis is made that protein domains are self-stabilized folding units. In particular, domains must be self-stabilized by their non-bonding interactions. This definition allows identification of domains, folding nucleation sites, and potential folding intermediates.

As a test case; Calmodulin, a protein with two visually distinct domains, is chosen. From the minimized structure, the Van der Waals and Coulomb contacts of residues in every possible length strand with other residues in the same strand are extracted. The strand self-contact energies are normalized both to strand length and to the strand contact energies of the extended chain with intact helices to insure elimination of secondary structure effects from our search.

The results identify many continuous domain structures and demonstrate how they may serve as nucleation sites for folding. The two large domains of Calmodulin are identified as being at residues 10-61 and 80-140 with normalized non-bonded self-energies of -4.44 and -4.32 kcal/mole/residue respectively. The entire protein has a normalized non-bonded self-energy of -3.97 kcal/mole/residue. A subdomain clearly exists in Calmodulin at residues 19-32 with a normalized nonbonded self-energy of -3.89 kcal/mole/residue.

Additional continuous strand domains and folding nucleation sites have been identified in proteins with domains that are not necessarily visually distinct such as HIV Protease, Lysozyme, Ribonuclease, and Pancreatic Trypsin Inhibitor.

Tu-Pos249

THERMODYNAMIC STRATEGIES FOR STABILIZING PARTLY FOLDED STATES OF PROTEINS.

((D.T. Haynie and E. Freire)) Departments of Biophysics and Biology and the Biocalorimetry Center, The Johns Hopkins University, Baltimore, MD 21218.

A comprehensive understanding of protein folding depends on knowledge of the energetics of structures populated along the folding pathway. But the high cooperativity of structural transitions typically limits the maximum population of intermediates to ~10%. Therefore, it would be desirable to have access to conceptual and computational tools useful for predicting, for example, which proteins can form stable intermediate states and the conditions under which the population of intermediates is maximal. Particularly helpful would be methods which depend only on the experimentally accessible properties of the native and denatured states. Using statistical mechanics, we demonstrate why intermediate states are so sparsely populated under typical conditions (absence of denaturant and neutral pH) and indicate the specific conditions required for their increased stabilization. Also, we provide a means of calculating the ligand activity associated with the maximum population of an intermediate state, showing that this activity is independent of the energetics of the intermediate. The statistical thermodynamic approach presented here constitutes a rational guide to the study of partly folded conformations. Supported by the National Institutes of Health (RR04328, GM37911, and NS24520).

Tu-Pos250
THERMODYNAMICS OF THE MOLTEN GLOBULE STATE.
((D. T. Haynie and E. Freire)) Departments of Biophysics and Biology and the Biocalorimetry Center, The Johns Hopkins University, Baltimore, MD 21218.

The partly ordered molten globule state may represent a universal protein folding intermediate. Structural models of molten globule states of α-lactalbumin,[1] cytochrome *c*, apo-myoglobin,[2] and a kinetic intermediate of lysozyme,[3] have been used to compute values of two of the three energetic parameters needed to define the Gibbs free energy of stabilization, ΔC_p and ΔH.[1] Values of ΔS were estimated otherwise.[1] We find that a framework based on a) thermodynamics and statistical mechanics and b) values for fundamental protein interactions[1,4] can account for the observed behavior of partly folded states of different proteins; that the molten globule state is structurally and energetically distinct from the denatured state; and that the absence of a heat absorption peak displayed by some molten globules during thermal denaturation is a consequence of the energetic balance rather than an inherent and general property of the molten globule state. Supported by the National Institutes of Health (RR04328, GM37911, and NS24520).

1. Haynie, D.T., Freire, E. Submitted.
2. Hughson, F.M., Wright, P.E., Baldwin, R.L. Science 249:1544-1548, 1990.
3. Mark, A.E., van Gunsteren, W.F. Biochemistry 31:7745-7748, 1992.
4. Murphy, K.P., Freire, E. Adv. Prot. Chem. In press.

Tu-Pos251
TRANSFER FREE ENERGY OF AMINO ACIDS FROM WATER TO OSMOLYTE SOLUTIONS ((Yufeng Liu & D.W.Bolen)) Dept. of HBC & G, Univ. of Texas Med. Branch, Galveston, TX 77550

Natural occurring osmolytes like sarcosine and sucrose can provide extraordinary protection of a protein toward thermal denaturation. In order to investigate the origin of the enhanced stabilization by these osmolytes, measurements were made of the solubilities of amino acids in water and in sucrose and sarcosine solutions. These data were used in determining transfer free energy changes of the peptide backbone unit and amino acid side chains from water to sucrose or sarcosine solutions of defined concentration.

The side chain and backbone transfer free energy changes were used to estimate the difference in unfolding free energy change ($N \rightleftarrows U$) of ribonuclease A in water in comparison to unfolding in sucrose and sarcosine. The unfolding free energy change was calculated by summing the free energy contribution of each amino acid side chain and backbone unit multiplied by the degree of exposure to solvent. The exposure was determined using a solvent accessible surface area algorithm. The transfer free energy of the peptide backbone unit from water to these osmolyte solutions makes a considerable positive free energy contribution to the calculated unfolding free energy change. This large positive contribution is only partially offset by the negative free energy contribution due to exposure of side chains on unfolding. The presence of sucrose or sarcosine appears to favor the N state over the U state as a result of the unfavorable exposure of the peptide backbone unit to these osmolytes.

Tu-Pos252
INVESTIGATIONS OF SOLVATION FREE ENERGY USING MOLECULAR DYNAMICS SIMULATIONS.((Stewart R. Durell)) Lab of Mathematical Biology, NCI, NIH, Bethesda, MD 20892.

Computer studies are underway to calculate the thermodynamic free energy change of the binding reactions of small hydrophilic and hydrophobic solutes in water. This work is based on the formalism developed by A. Ben-Naim ("Solvation Thermodynamics," Plenum Press, New York, 1987) to describe the thermodynamics of solvation. The main goal is to determine the relative energetic contributions of hydrophilic and hydrophobic groups to the folding of biomacromolecules. Special attention is paid to understanding the role of hydrogen bonding. A number of different methods, implemented in the CHARMM computer program, are used to calculate the free energy changes (incl. thermodynamic integration and integration of the mean force). A number of water models (incl. TIP3P and ST2) are used for comparison.

Tu-Pos253
MONTE CARLO SEARCH OF CRAMBIN STRUCTURE ((N. Kurochkina and B. Lee)) NCI, NIH, Bethesda, MD 20892.

A multi-step Monte Carlo procedure was developed to search for the native conformation of protein molecules with known arrangement of disulfide bonds. The energy function used consisted of a weighted sum of the contact energy of Miyazawa and Jernigan (1985, *Macromolecules*, **18**, 534), the hydrogen bond energy, and the disulfide bond energy. The search was performed on a dihedral angle set of 8 states per each residue (Lim *et al.* 1992, *FEBS*, **302**, 57). The procedure was applied to crambin molecule, a 46-residue protein, the x-ray structure of which is known at 1.5 A (Teeter M. M., 1984, *Proc. Natl. Acad. Sci. USA*, **290**, 107). The multistep procedure finds structures that deviate from the x-ray structure by 2.99-3.5 A (c-rms on C_α atoms) among the local minimum energy structures.

Tu-Pos254
PHYSICAL BASIS OF THE STABILITY OF FOLDED PROTEIN CONFORMATION. ((G.I. Makhatadze and P.L. Privalov)) Department of Biology, The Johns Hopkins University, Baltimore, MD 21218. (Spon. by W.E. Love)

In determining thermodynamic properties of proteins, particularly their stability, hydration effects certainly play a principal role. Hydration of polar groups determines the overall contribution of hydrogen bonding to stabilization of the native protein structure, and hydration of non-polar groups determines the so-called hydrophobic interactions. Up to the present time we were only speculating on the relative magnitudes of all these effects because of a lack reliable thermodynamic information on the hydration of protein groups, and because of great uncertainty in the absolute values of interactions between these groups in the tightly packed native protein structure. The effect of hydration of the polar and non-polar groups upon protein unfolding in terms of the enthalpy, entropy and Gibbs energy, can be calculated using structural information on protein groups exposed to water in the native and unfolded states and calorimetric information on transfer into water over a broad temperature range (0-130°C) of compounds modeling these groups. Comparing these hydration effects to the calorimetrically determined total enthalpy and entropy of protein unfolding one can estimate the magnitude of intramolecular interactions in the native protein (van der Waals interactions and hydrogen bonding) and the conformational entropy of the unfolded polypeptide chain. It is shown that the main stabilization effect comes from internal van der Waals interactions, hydrogen bonding and hydration of aliphatic groups, and that the hydration of aromatic and polar groups has a negative contribution to the stability.

Tu-Pos255
EFFECTS OF METHANOL ON THE DISSOLUTION THERMODYNAMICS OF CYCLIC DIPEPTIDES ((Litian Fu, Kenneth P Murphy and Ernesto Freire)) Department of Biophysics, Department of Biology and Biocalorimetry Center, The Johns Hopkins University, Baltimore, MD 21218

Previously, we have observed that ΔC_p for protein unfolding decreases at increasing methanol concentrations (0-10% vol/vol). This effect manifests itself on a larger ΔH of unfolding at temperatures lower than 100°C. For a given protein at 100°C the unfolding enthalpies at 100°C are equal and independent of methanol concentration within the region studied (Fu, L. and Freire, E. (1992) *Proc. Natl. Acad. Sci., USA* 89, 9335-9338). In order to test the origin of this effect, we have begun a series of experiments aimed at measuring directly the heat, and the heat capacities of dissolution of several dipeptides in water containing increasing methanol concentration. The results obtained so far for cyclo (Gly-Gly) and cyclo (Leu-Gly) indicate that ΔC_p of dissolution in 5% methanol is larger for cyclo (Gly-Gly) than for the more hydrophobic cyclo (Leu-Gly). In water the relation is the opposite (Murphy, K. P. and Gill, S. J. (1990) *Thermochim. Acta* 172, 11-20). These results suggest that the heat capacity of dissolution of hydrophobic side chains is reduced in solvents containing a higher methanol concentration. (Supported by NIH grants RR04328 and NSF MCB-91186870)

Tu-Pos256

THE ENERGETICS OF BINDING OF PROTEINS AND LIGANDS TO DNA.

((Vinod K. Misra, Jonathan Hecht, and Barry Honig)) Department of Biochemistry and Molecular Biophysics, Columbia University, New York, NY 10032 (Spon. by A. Yang)

We have been studying the energetics of the interaction of ligands and proteins with nucleic acids. The free energy of binding of two macromolecules, $\Delta\Delta G_{bind}°$, consists of electrostatic, hydrophobic, and entropic free energy changes upon complex formation. The electrostatic free energy of binding of ligands to nucleic acids has been calculated with the finite-difference solution to the nonlinear Poisson-Boltzmann equation for detailed atomic level descriptions of the macromolecules in water represented as a dielectric continuum. The hydrophobic free energy of binding has been calculated from the curvature corrected total buried surface area upon complex formation where the magnitude of the hydrophobic effect is about 60 cal/mol/Å^2 based on the surface tension of a hydrocarbon-water interface. The electrostatic model provides an accurate and detailed description of both salt and pH dependent effects on the binding of several proteins and ligands to DNA. Together, the electrostatic and hydrophobic components of the binding free energy accurately describe the relative binding energies for the three minor groove binding drugs 4'-6-diamine-2-phenyl indole (DAPI), netropsin, and Hoechst 33258 to d[(CGCGAATTCGCG)$_2$]. In the systems studied, these analyses reveal that the hydrophobic interaction is the major driving force for ligand-DNA binding. In each case, the electrostatic free energy of binding opposes the formation of the charged ligand-DNA complex due to a large desolvation penalty.

Tu-Pos257

IDENTIFICATION OF THE METAL COORDINATING RESIDUES AND CHARACTERIZATION OF A PUTATIVE ZINC FINGER IN METHIONYL -tRNA SYNTHETASE.. ((Xu Bo, G.A. Krudy, and P. R. Rosevear)) Dept. of Biochemistry, Univ. of Texas Medical School at Houston, Houston, Texas 77225.

The methionyl -tRNA synthetase is a member of the Class I aminoacyl -tRNA synthetases and has been shown to be a zinc metalloprotein. The *E. coli* methionyl -tRNA synthetase contains a potential metal binding sequence Cys-X$_2$-Cys-X$_9$-Cys-X$_2$-Cys which is inserted in the nucleotide fold. A truncated form of the methionyl -tRNA synthetase (ΔMTS) which has been cloned and overproduced was used to prepare apo-, Zn^{2+}-, Co^{2+}- and $^{113}Cd^{2+}$- substituted proteins. Apoenzyme prepared by growing E. coli, carrying the plasmid which overproduces ΔMTS, in zinc free media was devoid of enzymatic activity in the aminoacylation, ATP-pyrophosphate exchange, and α-carbon proton exchange assays. Kinetic constants in both the aminoacylation and ATP-pyrophosphate exchange reactions for the Co^{2+}- and $^{113}Cd^{2+}$- substituted ΔMTS proteins were found to be identical with those of the native Zn^{2+} protein. The low energy absorption spectrum of Co^{2+}- substituted ΔMTS resembles the d-d transition bands characteristic of tetrahedrally coordinated Co^{2+}- substituted proteins. The absorption maxima of the spectral pattern was red shifted and closely resembles that reported for cobalt tetrathiolate derivatives. A strong S'Co^{2+} charge-transfer absorption at 350 nm was also clearly evident. The environment of the metal center was further probed by measuring the ^{113}Cd chemical shift of $^{113}Cd^{2+}$- substituted ΔMTS. A single resonance at 760 ppm was observed. This chemical shift is within the range expected for Cd^{2+} coordinated to four thiolate ligands. Thus, the enzyme-bound metal is likely coordinated to the four Cys residues located in the zinc finger-like motif inserted within the nucleotide fold.

Tu-Pos258

PHYSICO-CHEMICAL AND NUCLEIC ACID BINDING PROPERTIES OF HIV-1 AND SIV NUCLEOCAPSID PROTEINS AND PEPTIDES

((José R. Casas-Finet[1], Raymond C. Sowder II[2], Kazuyasu Sakaguchi[3], Ettore Appella[3], Louis E. Henderson[2], and John W. Erickson[1])) [1]Structural Biochemistry and [2]AIDS Vaccine Programs, NCI-FCRDC, Frederick, MD 21702; [3]Lab. of Cell Biology, NCI, NIH, Bethesda, MD 20892 (Spon. by John W. Erickson)

The nucleocapsid proteins (NCPs) p7 and p8, purified from suspensions of human immunodeficiency virus type 1 (HIV-1, MN isolate) and simian immunodeficiency virus (SIV, Mne isolate), resp., contain two copies of a CCHC-type zinc finger whose integrity is required for specific viral RNA packaging. Fluorescence and CD studies of apo- and Zn(II)-p7 (55 a.a.; 1Trp, 2 Phe) and -p8 (50 a.a.; 2 Trp), and of chemically synthesized peptides spanning residues 13-51 and 1-55 of p7 showed that the unstructured apo-peptides exhibit an increase in β-turn content upon addition of Zn(II). Concomitantly, Trp fluorescence quantum yields increased by 90-150% and remained constant above 1.9 ± 0.1 g atom/mole peptide. NCP Trp fluorescence was typical of a solvent-exposed, freely-rotating chromophore. Considerable flexibility between the two fingers was deduced from dynamic anisotropy measurements. Fluorimetric equilibrium binding isotherms of Zn(II)-p7 and -p8 with homooctanucleotides showed a linear dependence between log K and limiting Trp quenching, suggesting Trp stacking with nucleic acid bases. Oligo affinities ranked in the order G>U>C>A, with 70-95% Trp quenching at saturation; p8-Zn(II) showed similar Trp quenching but bound with a 12-fold higher affinity, in agreement with a higher contribution of Trp to binding free energy, relative to Phe. Interestingly, the occluded binding site size of p8-Zn(II) (n = 7.0 ± 1.0 nucleotides/NCP monomer) was double that observed for p7-Zn(II) (n = 3.7 ± 0.4). Forward (NCP added to oligo) and reverse (oligo added to NCP) titrations performed with p7-Zn(II) suggested that the two zinc fingers in NCPs may bind nucleic acids independently. This results in the occurrence of at least two distinct binding modes.

Tu-Pos259

OPTICALLY DETECTED MAGNETIC RESONANCE (ODMR) OF POINT-MUTATED E. COLI AND F PLASMID SINGLE-STRANDED DNA-BINDING (SSB) PROTEINS

((B.D. Schlyer, J.R. Casas-Finet, D.H.H. Tsao, and A.H. Maki)) Chem. Dept., UCD, Davis, CA 95616 (Spon. by C. Meares)

Earlier ODMR studies have shown that amongst the 4 Trp of *E. coli* SSB, only Trp 40 and 54 participate in stacking interactions with nucleic acid bases, whereas Trp 88 and 135 do not. SSB complexes with poly(dC), poly(rC), poly(dA), poly(rA), poly(rU), poly(2,S-rU) or poly(dT) showed Trp phosphorescence 0,0-band red-shift, lifetime reduction and decrease in the magnitude of the zero field splitting parameters, indicative of Trp stacking. Only SSB/poly(dT) complexes, however, displayed negative polarity ODMR signals originating from Trp 54. Heavy atom effects (HAE) on Trp, most notably the appearance of its normally dark |D|+|E| ODMR signal and a 2-3 orders of magnitude reduction in lifetime, have been observed previously in complexes of the *E. coli* and F plasmid-encoded SSBs with poly(5,Br-rU) and poly(5,Hg-rU). We have extended this work to the study of Trp HAE induced upon SSB labelling with the Cys-specific reagent, CH_3HgI. As wild type *E. coli* SSB does not contain Cys, we have used F SSB (carrying a single Cys at position 70) and the point-mutated *E. coli* SSB-Y70C and -K87C. Fluorescence equilibrium binding isotherms with poly(dT) indicated that the occluded site size (n = 65 ± 2 nucleotides/SSB tetramer), limiting fluorescence quenching, apparent affinity and salt-back midpoint were unchanged upon reaction of F SSB with CH_3HgI. ODMR spectra of CH_3Hg-labelled F SSB, *E. coli* SSB-Y70C or -K87C exhibited HAE on Trp in SSB/poly(dT) complexes but not in the free form, indicating a protein conformational change induced upon polynucleotide binding. Since negative ODMR signals from Trp 54 were still observed in such complexes, the HAE occurred on Trp 40 or 88 (F SSB lacks the homologous Trp 135). Complexes of F SSB with $p(dT)_n$ oligonucleotides (n = 4, 8, 12,16) showed a progressive increase in the magnitude of the Trp phosphorescence red-shift and lifetime reduction measured upon binding increasingly longer oligos. ODMR of F SSB-CH_3Hg/$p(dT)_n$ complexes suggested a $p(dT)_n$-induced protein conformational change for all oligo lengths. Interestingly, complexes of singly (-W40F, -W54F) and doubly (-W88F,W135F) point-mutated *E. coli* SSB with synthetic 16-mer oligos containing dT and 5,Br-dU at defined positions showed that binding occurred with slippage of at least 3 nucleotides about the SSB monomer. This sets limits for the *interacting* binding site of 8 ≤ m ≤ 13 nucleotides/SSB monomer.

Tu-Pos260

THERMODYNAMICS OF NUCLEOTIDE BINDING TO *E. COLI* PRIMARY REPLICATIVE HELICASE, DnaB PROTEIN.

((Wlodzimierz Bujalowski and Malgorzata Maria Klonowska))
Department of Human Biological Chemistry & Genetics, University of Texas Medical Branch in Galveston, Galveston, TX 77555-0653

The interactions of nucleotides with *E. coli* primary replicative helicase DnaB protein have been studied using fluorescent nucleotide analogs, 2'(3')-O-(2,4,6-trinitrophenyl) derivatives, TNP-ATP, TNP-ADP, TNP-AMP and 1,N^6-ethenoadenosine diphosphate (εADP). The binding of the analogs is accompanied by strong quenching of the protein fluorescence. Using a thermodynamically rigorous method, we determined that DnaB hexamer binds at saturation 6 molecules of TNP-ATP, TNP-ADP and εADP. The binding isotherm is biphasic, i.e. three molecules of nucleotide are bound in the first high affinity binding phase and the subsequent three molecules are bound in the second low affinity binding phase. At higher temperatures the separation of the two binding steps is even more pronounced. The change of the monitored fluorescence is sequential, i.e. the first binding nucleotide causes the largest quenching of the protein fluorescence with subsequent nucleotide binding inducing progressively less quenching. The simplest explanation is that there is a negative cooperativity among nucleotide binding sites on DnaB hexamer. This binding behavior reflects an intrinsic property of the DnaB helicase, since it is observed with nucleotide analogs which differ in the type and location of the modifying group. A statistical thermodynamic model is proposed, the hexagon model, which provides an excellent description of the binding process using only two interaction parameters, intrinsic binding constant K and cooperativity parameter σ. Biological implications of studied interactions will be discussed.

Tu-Pos261

INHIBITION PATTERNS OF REVERSE TRANSCRIPTASE BY NON-NUCLEOSIDE INHIBITORS.

((R.A. Spence[1], G. Jin[1], W.M. Kati[1], L.F. Jerva[2], K.S. Anderson[2], and K.A. Johnson[1],)) [1]Pennsylvania State University, University Park, PA , 16802, and [2] Pharmacology, Yale Medical School, New Haven, CT 06510. (Spon. Jim Howe).

The forward kinetic mechanism of the next correct nucleotide incorporation into DNA by the polymerase activity of HIV reverse transcriptase (RT) has recently been determined (Kati, et. al., 1993, *Biochemistry*, in press). Analysis of the dATP concentration dependence of burst rates provided a K_d value of 4 μM and a maximum rate of single nucleotide incorporation of 33 s^{-1}. The steady state rate showed that the dissociation of primer/template from RT occurred at a rate of 0.2 s^{-1}. We are currently investigating the reverse reaction (pyrophosphorolysis) to complete the pathway. Pre-steady state analysis of TIBO derivatives (Pauwels, et. al., 1990, Nature 343:470-474.) is being pursued to gain further information about the inhibition patterns of non-nucleotide inhibitors. Titrations of O-TIBO and Cl-TIBO showed a reduction in the burst amplitudes with K_i values of 1.5 and 1.0 μM, respectively. Nucleotide binding appearred to be tighter in the presence of the inhibitor. When the RT-DNA complex was preincubated with a saturating amount of O-TIBO, the single turnover rates for dATP revealed a K_d of 0.3 μM and a maximum rate of 0.3 s^{-1}. Future experiments are directed toward establishing the kinetic pathway of these and other non-nucleoside inhibitors (Supported by NIH grant GM 44613).

Tu-Pos262

THE FIDELITY OF T7 DNA POLYMERASE AND HIV-REVERSE TRANSCRIPTASE IS DETERMINED BY AN INDUCED FIT MECHANISM. (S.G. Edwards, K.A. Johnson, Steven Kerr and Karen S. Anderson) Dept. of Molecular & Cell Biology, 106 Althouse Laboratory, Pennsylvania State University, University Park, PA and Department of Pharmacology, Yale Medical School, New Haven, CT

In this report we show that both T7 DNA polymerase and HIV- reverse transcriptase(RT) check not only the correct Watson-Crick geometry of the incoming base but also the bases already incorporated in the duplex region of the primer-template. Primer-templates with mismatches at various positions(n-1, n-2 to n-7) from the 3'-end were used as substrates to examine the rate of correct nucleotide incorporation in single turnover experiments. The single turnover experiments provided estimates of the K_d for dTTP, the rate of the incorporation and DNA binding as a function of the distance of the mismatched base-pair from the 3'-OH terminus. This presteady state kinetic analysis reveals that mismatches at the n-1, -2 and -3 positions reduce the rate of continued correct polymerization without substantially weakening the binding of the correct nucleotide. Mismatches at the n-4, -5 or beyond have little effect on the rate of continued polymerization and nucleotide binding. These data serve to map out the binding pocket as it relates to the ability of the polymerase to undergo a conformational change responsible for Watson-Crick base-pair recognition. We have also examined the kinetics of incorporation of nucleotide analogs such as AZT triphosphate. We argue that the fidelity of DNA polymerization is established globally by an induced fit mechanism and is operative for at least two DNA polymerases (Supported by NIH grant GM 44613).

Tu-Pos263

INDUCER LINKED HETEROLOGOUS COOPERATIVE INTERACTIONS IN THE BINDING OF THE CRP AND CYTR PROTEINS TO THE *E. COLI* DEO OPERON. ((D.F. Senear, and L. Perini)) Dept. of Molecular Biology & Biochemistry, University of California, Irvine 92717.

Interactions of the CRP and CytR proteins are responsible for both positive and negative control of transcription from *E. coli* deoP2 as well as several other *E. coli* operons, providing for coordinate expression of proteins involved in nucleoside transport and catabolism from different operons. The footprint titration method has been used to study the site specific binding of the CRP and CytR proteins to their operators at deoP2. CRP binds to tandem sites 5' to the deoP2 start site for transcription. In the absence of CytR, CRP binds noncooperatively with about ten-fold greater intrinsic affinity for CRP-2 then for CRP-1. Intrinsic binding of CytR to its primary site between CRP-1 & CRP-2 is unaffected by its inducer, cytidine. Each protein displays heterologous cooperative interactions in the presence of saturating concentrations of the other protein, accounting for an increase in the loading free energy for CytR of about 3 kcal/mol. Studies with reduced valency mutant operators in which specific binding to either CRP-1 or CRP-2 has been eliminated show that CytR interacts cooperatively with CRP bound at both sites. Cooperativity in the wildtype operon does not reflect the sum of the pairwise terms and is largely eliminated by addition of cytidine. The concentration dependence for cytidine induction of cooperativity is consistent with a transition mediated by the binding of a single cytidine ligand. The results are consistent with the interpretation that CytR is an allosteric protein with intramolecular coupling between DNA binding, cytidine binding and CRP interacting domains. Supported by NIH grant GM41465.

Tu-Pos264

LIFETIMES OF CAP-DNA COMPLEXES IN POLYACRYLAMIDE GEL MATRICES ((M. G. Fried and G. Liu)) Department of Biological Chemistry, Pennsylvania State University College of Medicine, Hershey, PA 17033

The gel electrophoresis mobility shift assay is widely used for qualitative and quantitative characterization of protein complexes with nucleic acids. Often it is found that complexes that are short lived in free solution ($t_{1/2}$ on the order of minutes) persist for hours under the conditions of gel electrophoresis. We have investigated the influence of the polyacrylamide gel, of linear polyacrylamide, and of acrylamide monomer on the pseudofirst-order dissociation kinetics of complexes containing the *E. coli* cyclic AMP receptor protein (CAP) and lactose promoter DNA. Within gels, k_d values decreased with increasing [polyacrylamide]. A similar decrease in k_d was found with increasing [polyacrylamide] in solutions of linear polyacrylamide. Acrylamide monomer had no significant effect on k_d over the same range of concentrations. In free solution, k_d was proportional to $[DNA]^2$, while in gels of [polyacrylamide] ≥ 10%, k_d was nearly independent of [DNA] until fragment concentration exceeded 10μM. Even in the absence of competitor DNA, $k_d(gel) < k_d(solution)$. These results suggest that the lifetime of CAP-DNA complexes in free solution is limited by the frequency of collision with molecules of DNA or with protein-DNA complexes; some or all of the stabilization observed in gels may be due to a reduction in this frequency. Supported by NSF grant DMB-91-96154.

Tu-Pos265

SPECIFIC CONTACTS IN T3 AND T7 RNA POLYMERASE-PROMOTER INTERACTIONS: KINETIC ANALYSIS USING SMALL SYNTHETIC PROMOTERS. ((Charles Schick and Craig T. Martin‡))
Program in Molecular and Cellular Biology and ‡Dept. of Chemistry Univ. of Massachusetts, Amherst, MA 01003 (spons. by L. Thompson)

The T7, T3, and SP6 RNA polymerases recognize very similar, yet distinct, promoter sequences. The high homology among the promoter sequences suggests that differential promoter recognition must derive from relatively small changes in the protein. Steady state kinetic analyses of transcription from the T3 and T7 consensus promoters and from promoters modified in the region critical to differential recognition reveal details concerning which functional groups in the DNA contribute to this recognition. Modifications include base pair substitutions, single base substitutions, and simple functional group modifications at unique sites in the promoter. The results show that T3 RNA polymerase recognizes, primarily, the amino groups on the nontemplate cytidines in the major groove at positions -11 and -10, while the identity of the base on the template strand at these positions is not critical to binding. Preliminary data suggest the T7 enzyme recognizes the 6-carbonyl of the nontemplate guanine at position -11 of the T7 promoter, consistent with extrapolations from T3. While major groove modifications weaken binding at positions -10 and -11, modifications in the minor groove at these positions do not disrupt binding, further supporting a model for promoter recognition in which the enzyme binds to one face of closed duplex DNA in this region.

Tu-Pos266

ALTERNATING PYRIMIDINE-PURINE SEQUENCES INCREASE DNA FLEXIBILITY IN THE COMPLEX BETWEEN CRO PROTEIN AND THE LAMBDA O_R3 BINDING SITE

[Yuri L. Lyubchenko[1,2], Lyuda S. Shlyakhtenko[1], Ettore Appella[3] and Rodney E. Harrington[1]] [1]Department of Biochemistry, University of Nevada Reno, Reno, NV 89557,[2]Departments of Physics and Microbiology, Arizona State University, Tempe, AZ 85287,[3] Laboratory of Cell Biology, NCI, National Institutes of Health, Bethesda, MD 20892. Sponsored by Rodney E. Harrington

We have used a ligation/cyclization procedure followed by 2-dimensional gel electrophoresis assay of circular/linear species to study the cyclization properties of a carefully selected set of single base (point) mutations and mismatches in the Cro protein O_R3 (DNA) binding sequence in the presence and absence of bound protein. Mutations were designed to preserve the tight binding of wild-type O_R3 in accord with recently published thermodynamic criteria. Our results provide information on induced bending and flexibility in the operator DNA which appears to improve the fit between protein and DNA. The alternating pyrimidine-purine elements CA, CAC and CACA are found to be anisotropically flexible and apparently promote DNA bending in the specific binding region of the complex. They may also facilitate twisting in the central nonbinding region. Effects for CACA are exceptionally large and suggest that an alternative DNA structure may occur in this element.

Tu-Pos267

"FOOTPRINTING" OF PROTEIN-DNA INTERACTIONS USING POTASSIUM PEROXONITRITE. ((Peter A. King[1], Elizabeth Jamison[1], Daniel Strahs[1], Vernon E. Anderson[1] & Michael Brenowitz[1])) [1]Department of Chemistry, Brown University, Providence, RI 02912 & [2]Department of Biochemistry, Albert Einstein College of Medicine, Bronx, NY 10461.

Synthesis of the peroxonitrite anion (ONOOK) is carried out via neutralization of peroxonitrous acid formed transiently during the reaction of nitrous acid with hydrogen peroxide. A convenient preparation has been developed, based on the procedure of W. G. Keith and R. E. Powell (*J. Chem. Soc. (A), 90,* 1990), which results in an ONOOK concentration of 90-110 mM. Addition of the ONOOK containing solution to a sample solution buffered at pH 7.0 results in protonation of a significant fraction of the peroxonitrite anion as the pKa of peroxonitrous acid is 6.8. The peroxonitrous acid formed undergoes homolytic fission to form hydroxyl radical ('OH) and nitrogen dioxide (NO_2'). At pH 7.4, ONOOK has a half-life of 1.9 sec. Recombination of the 'OH and NO_2' in the solvent cage reduces the amount of free 'OH trapped in solution by two-thirds.

Quantitative ONOOK footprint titrations were conducted of the binding of *cI*-repressor (*cI*) to the three-site right operator, O_R in pH 7 buffer containing 25 mM KPO_4, 2 mM $MgCl_2$ and 75 mM KCl . Binding isotherms that are identical within experimental error were determined whether ONOOK, Fe-EDTA or DNase I was used as the probe of binding site occupancy. The equilibrated mixtures of protein and DNA were exposed to the probes for ~2 sec., 7 min. and 2 min. exposures, respectively, highlighting the independence of the resolved isotherms on the sampling time of the reagent. Comparable regions of the DNA are protected from ONOOK and Fe-EDTA mediated cleavage although the degree of protection from ONOOK is less pronounced and not symmetric relative to the two-fold symmetry axis of the binding sequence. Supported by NIH grants GM39929 (M.B.) and GM36562 (V.E.A.).

Tu-Pos268

SELF-ASSEMBLY OF λ cI REPRESSOR DIMERS IMPLICATES A ROLE FOR OCTAMERS IN COOPERATIVE BINDING AND REGULATION OF TRANSCRIPTION.

((D.F. Senear[1], T. M.Laue[2], J.B.A. Ross[3] & E. Waxman[3])) [1]Dept. of Molecular Biology & Biochemistry, U. of California, Irvine 92717; [2]Dept. of Biochemistry, U. of New Hampshire, Durham 03867; [3]Dept. of Biochemistry, Mount Sinai School of Medicine, NY 10029.

Cooperative binding of the λ cI repressor dimer to specific sites of the phage operators O_R & O_L controls the developmental state of the phage. Cooperativity is believed to be mediated by protein-protein interactions between dimers bound to adjacent operator sites, to form tetramers. Sedimentation equilibrium and fluorescence anisotropy were used to study the higher order assembly reactions of the wildtype, and of three variant or mutant repressor proteins, with either higher or lower stability dimers. The primary assembly mode is found to be dimer to octamer, with only negligible effects of the monomer-dimer equilibrium on this higher order assembly process. A small fraction of tetramer might also be present, in accord with the expectation that tetramer should be an intermediate in the assembly to octamers. A role for higher order assemblies of repressor dimers in cooperative binding requires thermodynamic linkage between operator binding and dimer assembly. Preliminary experiments with bound O_R1 DNA show that the octamer binds operator DNA and is not dissociated to tetramers. Sedimentation velocity experiments indicate an elongated shape for the octamer. This conformation could allow octamers to bind simultaneously to all three operator sites at O_R and at O_L. Therefore, octamers as well as tetramers must to be considered in developing models to explain cooperativity. Supported by NIH grants GM41465 (DFS) and GM39750 (JBAR) and NSF grant DIR9002027 (TML).

Tu-Pos269

SPECTRAL ENHANCEMENT OF PROTEINS: INCORPORATION OF 5-HYDROXYTRYPTOPHAN INTO PHAGE λ *cI* REPRESSOR

((B.B. Kombo, Y.T. Huang, E. Waxman, E. Rusinova, W.R. Laws, C.A. Hasselbacher, T.M. Laue, D.F. Senear, and J.B.A. Ross)) Dept. of Biochem., Mount Sinai Sch. Med. of CUNY, New York, NY 10029, Dept. of Biochem., Univ. of New Hampshire, Durham, NH 03824, and Dept. of Molec. Biology & Biochem., Univ. of California-Irvine, Irvine, CA 92717.

The major obstacle to the use of intrinsic protein fluorescence to probe intermolecular interactions is spectral overlap. Most proteins contain one or more tryptophans (Trp) and nucleic acid absorption covers the same spectral region. We have used a Trp *E. coli* auxotroph to replace the 3 Trp residues of bacteriophage λ cI repressor with 5-hydroxyTrp which has absorbance to the red of Trp and DNA. This spectrally enhanced protein (SEP), obtained by metabolic engineering, is functionally indistinguishable from wild type repressor as determined by protein dimerization and operator DNA binding constants. Thus it can be studied by its 'intrinsic' fluorescence even in the presence of other proteins that contain Trp. Furthermore, it has enabled an ultracentrifuge study of higher order repressor oligomerization in the presence of operator DNA that suggests octamers bind to the DNA. SEPs will obviously facilitate thermodynamic analysis of many protein-protein and protein-DNA interactions. Supported by NIH grants GM-39750, HL-29019, and GM-41465, and NSF grant DIR-9002027. BBK is a Fulbright scholar.

Tu-Pos270

HIGH SALT, pH AND TRYPTOPHAN DESTABILIZE HIGHER ORDER OLIGOMERS OF *trp* REPRESSOR

((Kathleen S. Martin and Catherine Royer)) Pharmacy UW-Madison, WI 53706

Fernando and Royer (Biochemistry 31, 3429, 1992) demonstrated that *trp* repressor (TR) formed oligomers of higher order than dimer in solution at concentrations above 0.1 uM and that these oligomers were specifically destabilized by the binding of tryptophan. The oligomer dissociation was monitored by the anisotropy of fluorescence of a covalently bound dansyl group. Using the same approach we have investigated the effect of increasing salt concentration and pH on these higher order oligomers at several tryptophan concentrations. Both increasing salt and increasing pH destabilize the higher order oligomers, indicating that the interactions between TR dimers are ionic in nature. We have determined that the dansyl moiety is bound to the amino terminus of TR. Changes in the lifetime and energy of the dansyl emission upon dissociation of the oligomers suggests that the amino terminus may be involved in these contacts. Given the dipolar nature of the TR dimer, with the DNA binding face of the protein carrying an overall negative charge and the backside of the repressor being positive, we propose that the higher order oligomers of TR which form in solution may be back-to-back stacked structures. This would be consistent with oligomers having low affinity for DNA and which would be specifically destabilized by the corepressor, tryptophan.

Tu-Pos271

A NOVEL FLUORESCENT DNA BINDING ASSAY IMPLICATES PROTEIN-PROTEIN INTERACTIONS IN REGULATING *trp* REPRESSOR

((Veronique LeTilly and Catherine Royer)) Pharmacy UW-Madison, WI 53706

The study of interactions between proteins and nucleic acids is central to the understanding of the control of genetic expression. Of particular interest is the role of interactions between homologuous and heterologuous polypeptides in the specific enhancement and repression of transcription. We have developed a highly sensitive solution-based assay for detection and quantitation of the binding of proteins to nucleic acids, based upon an increase in the anisotropy of fluorescence of a 5'-fluorescein (or eosine) labeled oligonucleotide upon binding of protein. The sensitivity of the assay is now 9 pM in oligonucleotide, allowing the determination of dissociation constants in this concentration range. Because anisotropy depends upon molecular weight, the assay informs not only on the affinity of the protein for the DNA, but also on complex number and relative size. The studies on the *trp* repressor (TR) demonstrate the existence of both dimeric and tetrameric specific complexes, in addition to higher order non-specific complexes, the relative population of which depends upon the concentration of the three elements. The exploration of a wide range of concentration conditions, made possible by the nature of the assay itself, reveals that reported contradictions in the specific complex of TR with its target site arise primarily from differences in the concentration, and suggests that TR regulation involves both high and low affinity oligomers.

Tu-Pos272

BINDING INTERACTIONS OF ANTI-SSDNA ANTIBODIES BV0401 WITH OLIGONUCLEOTIDES: A STEADY-STATE AND TIME-RESOLVED FLUORESCENCE STUDY.

((S.Y. Tetin, T.L. Hazlett*, C.A. Rumbley, E.W. Voss Jr.)) University of Illinois at Urbana-Champaign; Dept. Microbiology & *Dept. Physics, Laboratory of Fluorescence Dynamics, Urbana, IL 61801.

The binding affinities of numerous synthetic oligonucleotides to anti-ssDNA autoantibodies BV0401 (IgG2b,K), the corresponding Fab fragments and the single chain antibody, SCA0401/212, were determined, and the intrinsic fluorescence of each protein was characterized. Hapten binding to BV0401, Fab0401, and SCA0401 resulted in quenching of the proteins' tryptophan fluorescence and permitted the direct measurement of ligand binding under equilibrium conditions. Deoxythymidine (dT_n) oligonucleotides of differing lengths (n) were evaluated and dissociation constants for the binding of dT_3, dT_6, and dT_8 to IgG were 5.6×10^{-5}M, 1.5×10^{-7}M, 1.3×10^{-7}M, respectively. Binding constants for Fab0401 fragments were similar to BV0401 while SCA0401 displayed a 10-fold weaker association, k_d (dT_6) = 6.9×10^{-6} M and k_d (dT_8) = 1.6×10^{-6} M. Lifetime quenching data for SCA0401 and dT_6 was comparable to the steady-state data, indicating that the quenching process is primarily dynamic rather than static in nature and thus inferring a certain mobility of the SCA0401 binding site tryptophan residues in the presence of hapten. Dissociation constants for other polyoligonucleotides generally displayed weaker affinities. The results are discussed in terms of conformational differences between the BV0401 and SCA0401 oligonucleotide binding sites and on the questions of site length, hapten orientation and site specificity. Partially supported by NIH R03155 and UIUC.

Tu-Pos273

DYNAMICS OF DNA CONTAINING TATA BOX REGIONS: A TIME RESOLVED FLUORESCENCE STUDY.

((M. R. Otto[1], L. B. Bloom[2], R. Eritja[2], M. F. Goodman[2], J. M. Beechem[1])) [1]Vanderbilt University, Nashville, TN, [2]University of Southern California, Los Angeles, CA, and [3]Dept. of Molecular Genetics, CID-CSIC, Barcelona, Spain.

The TATA box sequence of DNA is of considerable importance in both prokaryotic and eukaryotic transcription because TATA sequences have been found in the promoter regions of many prokaryotic and eukaryotic genes. This study investigates internal dynamics of the TATA box using the fluorescent nucleotide base 2 aminopurine monophosphate (dAPMP) which forms Watson-Crick base pair opposite thymidine. dAPMP is an excellent stuctural probe in DNA because it can monitor internal base dynamics while causing minimal perturbation of DNA structure. The three oligonucleotide sequences studied are: 5'GGGGCTATAAAAGGGGG-3',where each underlined adenine has been singly replaced with dAPMP. Steady state and time resolved fluorescence spectroscopy will be used to investigate the dynamics of the three different sites. Experiments will be done to compare dAPMP environment in single stranded (ss), double stranded (ds) DNA, as a function of excitation/emission wavelength, temperature and salt. DNA binding experiments using Transcription Factor IID (binds at the TATA box) will be performed to obtain additional information concerning effects of bound protein on internal DNA dynamics. Early time resolved data show the total intensity and anisotropy decay to be very similar for ss and ds oligonucleotides. However, if dAPMP is excited in a region where thymine absorbs (293 nm), both ss and ds DNA total intensity and anisotropy decay change and there is a significant difference in the anisotropy decay between them. This difference may be due to energy transfer from DNA bases to dAPMP. J.M.B. is a L.P. Markey Scholar, M.O. MBTG.

Tu-Pos274

GLOBAL MOTIONS, DYNAMICS, AND DISTANCES IN SMALL FRAGMENTS OF DNA CONTAINING THE TATA BOX SEQUENCE: A TIME-RESOLVED FLUORESCENCE STUDY. ((M. Pilar Lillo and Joseph M. Beechem.)) Vanderbilt University, Dept. of Molecular Physiology and Biophysics, Nashville, TN 37232.

This study investigates the rotational hydrodynamics of the TATA box containing the fluorescently end-labeled oligonucleotide: 5'GCTATAAAAGGG-3'. Fluorescent labeling was performed by attaching a $(CH_2)_6$-NH_2 linker to the 5'-end and reacting this material with a variety of isothiocyanate fluorophores (e.g., tetramethylrhodamine-ITC, Malachite green-ITC, etc.). Both singly labeled and doubly labeled DNA is being examined. Time-resolved fluorescence anisotropy experiments are being performed at both 560nm and 293nm excitation wavelengths in order to exploit the large change in absorption/emission oscillator angle (almost a 90° shift). Simultaneous analysis of the multi-excitation experiments allow resolution of two dominant rotational modes for the rhodamine labeled 12mer at 20°C, 10mM tris pH=8, 0.1mM EDTA of 240psecs and 1.5ns. Time-resolved energy-transfer experiments are on-going in an attempt to obtain length distribution(s) and intrinsic DNA end-to-end dynamics. The changes in the dynamics of the DNA upon assembly of the basal level transcription machinery at the TATA box are examined. J.M.B. is a L.P. Markey Scholar, MPL supported from M.E.C. and C.S.I.C Spain.

Tu-Pos275

EXTRINSIC DNA LABELING, INTRINSIC TRYPTOPHAN FLUORESCENCE, AND SITE-DIRECTED MUTAGENESIS STUDIES OF TFIID/DNA INTERACTION. ((Gina M. Perez-Howard, P.A. Weil, and Joseph M. Beechem)) Vanderbilt University, Dept. of Molecular Physiology and Biophysics. Nashville, TN 37232.

Transcription factor IID is the first component of the basal level transcription machinery which complexes with the TATA box promoter region located just upstream of the transcription start site. Due to its pivotal role in the formation of this complex, TFIID-DNA interactions are of profound interest. Thus far, we have examined the protein conformational changes that TFIID undergoes upon binding DNA by utilizing intrinsic tryptophan fluorescence (both steady-state and time-resolved). It is clear from this work that both the carboxy-terminal DNA binding domain and the amino-terminal domain (location of the single tryptophan) become uncoupled from each other upon binding DNA. Additional tryptophan studies of six site-directed single tryptophan mutants are ongoing. Due to the improving techniques in extrinsically labeling DNA, studies presented here will also examine TFIID binding using fluorescence energy-transfer. 5'-labeled DNA with Rhodamine Isothiocyanate and Malachite Green were selected as the transfer pair in order to determine protein-induced DNA bending (DNA sequence from Major Late Promoter: GGGGCTATAAAAGGGGG, TATA box underlined). Sponsored in part by the L. P. Markey Foundation.

Tu-Pos276

TIME-RESOLVED FLUORESCENCE STUDIES OF GENE ACTIVATION: A MODEL STUDY USING GAL4-VP16 AND TRANSCRIPTION FACTOR IID. ((Scott M. Blackman, P. A. Weil, and Joseph M. Beechem)) Vanderbilt University, Dept. of Molecular Physiology and Biophysics. Nashville, TN 37232.

Time-resolved fluorescence measurements were performed on the end- and internally-labeled oligonucleotide: 5'-CGGAGTACTGTCCTCCGGATCC GCGCTATAAAAGCG-3', which contains both a GAL4 binding sequence and a TATA box (underlined). This construct allows us to target specific gene activators to the GAL4 site, close to the basal level transcription machinery which assembles around the TATA box region. Binding to this DNA by a chimeric fusion protein, consisting of the DNA binding domain of GAL4 coupled to the activation domain of VP16, is examined. VP16 has been shown to be one of the most powerful activators of class II genes in eucaryotic systems. In addition, spectroscopic studies are performed on the ternary complex of DNA with GAL4-VP16 and purified *S. cerevisiae* transcription factor IID (TFIID). TFIID is the first protein of the basal level transcription machinery to assemble at the TATA region just upstream from the transcription start site. Oligonucleotides 5'-labeled with Rhodamine (donor) and Malachite Green (acceptor) provide an energy-transfer pair to monitor both the kinetics of binding and of protein-induced DNA bending in this system. These fluorescent DNA's are also being utilized to examine changes in the hydrodynamic properties of protein-DNA complexes utilizing time-resolved anisotropy experiments exciting into both the $S_0 \rightarrow S_1$ (585nm) and $S_0 \rightarrow S_2$ (293nm) transitions of Rhodamine. The internal dynamics at selected locations within the DNA (+/- proteins) are being examined using 2-aminopurine fluorescence (substituting for adenine). JMB is a L. P. Markey scholar, SMB is an MSTP training fellow.

Tu-Pos277

SEQUENCE CONTEXT EFFECTS ON THE RECOGNITION AND INCISION OF ANTI(+)-BPDE-DNA ADDUCTS BY THE ESCHERICHIA COLI UVRABC EXCISION REPAIR SYSTEM. ((Y. Sun and S. J. Mazur)) The American University, Washington DC 20016

In *Escherichia coli*, bulky adducts in DNA are repaired by the UvrABC system. Recognition of adducts by the UvrABC enzyme is influenced by adduct structure and the DNA sequence in which the adduct is embedded. The principal adduct formed by the reaction of (7R,8S)-dihydroxy-(9S,10R)-epoxy-7,8,9,10-tetrahydro-benzo[a]pyrene (anti(+)BPDE) with DNA is a relatively stable adduct attached to the N-2 position of guanine (N2-dG adducts). However, the extent of labile adduct formation, which occurs primarily at the N7 position of guanine, has been controversial. Using 3H-anti(+)BPDE, adduct stability was determined under assay conditions and by hot piperidine treatment. Results show that less than five percent of the BPDE adducts are labile. Since 95% of the adducts formed by anti(+)BPDE are the relatively stable N2-dG adducts, the effect of the surrounding sequence on the recognition of damage by a DNA repair enzyme was studied. The UvrABC enzyme incises the 8th phosphodiester bond 5' and the 4th phospho-diester bond 3' to the adducted base, which is the same cleavage pattern observed for other bulky adducts. The efficiency of incision of DNA containing BPDE adducts was determined by high resolution gel electrophoresis followed by densitometric scanning of the autoradiograms. The UvrABC incision spectrum was compared to the binding spectrum of anti(+)BPDE. In general, the extent of incision by UvrABC is proportional to the extent of damage. At some sites, however, such as the NarI recognition sequence (GGCGCC), the efficiency of incision varies markedly, showing a large effect of the surrounding DNA sequence.

Tu-Pos278

STRUCTURAL KINETICS OF BASE EXCISION FROM DNA WITH BACTERIOPHAGE T4 POLYMERASE. ((M. R. Otto[1], L. B. Bloom[2], R. Eritja[3], M. F. Goodman[2], J. M. Beechem[1])) [1]Vanderbilt University, Nashville, TN, [2]University of Southern California, Los Angeles, CA, and [3]Dept. of Molecular Genetics, CID-CSIC, Barcelona, Spain.

The DNA polymerase from bacteriophage DNA is an enzyme containing both polymerase activity and a 3'-5' proofreading exonuclease. In this study, which focuses on substrate structural effects on T4 exonuclease kinetics, experiments are performed with four ds DNA primer-templates (17/30mers) varying only in the base pair preceding a fluorescent base, 2 aminopurine monophosphate (dAPMP), located at the 3' primer end. Stopped flow steady state fluorescence spectroscopy is used to study excision of dAPMP from the DNA primer by T4 exonuclease. Upon dAPMP release from DNA, a large increase in dAPMP fluorescence is observed, allowing detailed kinetic analysis of the exonuclease rate(data obtained every millisecond). Preliminary data show the exonuclease rates vary only slightly between the four primer-templates. Equivalent experiments will be done with mismatched bases immediately preceding dAPMP in the primer-template. Data obtained thus far shows dAPMP release from these templates to be more rapid than with correctly matched primer-templates. Another result shows the exonuclease activity of a T4 exo deficient mutant to be highly active against mismatched primer-templates but apparently inactive against correctly paired. J.M.B. is a L. P. Markey Scholar, M.O. NIH Mol. Biophys.

Tu-Pos279

THE EFFECT OF CIPROFLOXACIN, A QUINOLONE ANTIBACTERIAL, ON DNA REPAIR IN ARL-18 CELLS AND IN PRIMARY HEPATOCYTES. ((J.E. Rosen, G.M. Williams and G. Schluter)) American Health Foundation, Valhalla, New York 10595 and Bayer A.G., Pharma-forschungszentrum, Wuppertal, Fed. Rep. of Germany.

Unscheduled DNA synthesis (UDS) measured by autoradiography was induced in vitro in primary cultures of rat hepatocytes by the quinolones, norfloxacin, pefloxacin and ciprofloxacin (McQueen et al., Tox. and Appl. Pharm., 111 255-261 (1991)). UDS was not observed in vivo after rats were exposed to ciprofloxacin and there was no evidence of DNA adduct formation in cultured hepatocytes exposed to ciprofloxacin in vitro. Previously, UDS was observed only with adduct-forming chemicals as a consequence of DNA repair synthesis. These findings therefore suggested that since ciprofloxacin is not DNA reactive it induced UDS as a consequence of another effect such as inhibition of DNA topoisomerase II (a homolog to bacterial DNA Gyrase) which induces a cleavable complex of duplex DNA. We examined the effect of ciprofloxacin on DNA repair in ARL-18 cells, a proliferating cell line as well as the effect of ciprofloxacin on DNA repair in rat hepatocytes which are non-proliferating. In both cell types, the BrdU technique utilizing CsCl equilibrium sedimentation was used to study DNA repair in isolated parental DNA. We observed that ciprofloxacin did not induce repair synthesis in either line, but rather inhibited repair synthesis at 0.25 mM and 0.5 mM in both cell lines. We have also observed that ciprofloxacin at 0.5 mM inhibited DNA replication and RNA transcription in ARL-18 cells. These results suggest that the mechanism for the induction of UDS by ciprofloxacin in primary hepatocytes may be independent of repair synthesis. Efforts are under way to elucidate the mechanism for the UDS and the decreased DNA repair levels observed due to ciprofloxacin in rat hepatocyte cultures by studying its effect on purified topoisomerase II from these cells.

Tu-Pos280

Origins of the Osmoprotective Properties of Betaine in *E. coli*

Scott Cayley, Barbara A. Lewis, and M. Thomas Record, Jr.
Depts. of Biochemistry and Chemistry, University of Wisconsin, Madison, WI 53706

We have determined the volumes and osmolyte composition of osmotically stressed *Escherichia coli* grown in the presence and absence of the osmoprotectant betaine. Our goal is to thermodynamically understand how the accumulation of exogenous betaine increases the growth rate, μ, of osmotically stressed cells. The accumulation of betaine reduces the cytoplasmic amounts of K^+ (n_K), glutamate, and trehalose (the osmolytes accumulated in cells grown in the absence of betaine) and increases the volume of free cytoplasmic water (V_{cyto}). We previously observed that both μ and V_{cyto} decrease, whereas n_K increases, as the osmolarity of medium lacking betaine increases. We propose that V_{cyto}, μ, and n_K are physiologically linked variables, and that V_{cyto} and n_K are linked through their theoretically large and approximately compensating effects on the binding of gene-regulatory proteins to DNA in the cell. We analyze thermodynamically how betaine increases V_{cyto} and propose that V_{cyto} determines μ. (Supported by NSF and NIH).

1. Cayley *et al., J. Bacteriol.* 174:1586-1595 (1992).
2. Cayley *et al., J. Mol. Biol.* 222:281-300 (1991).

Tu-Pos281

STRUCTURE/FUNCTION STUDIES OF BACTERIOPHAGE T4 regA PROTEIN: PROBING DOMAINS OF NUCLEIC ACID BINDING.

((S.M.O'Malley, A.K.M. Sattar, and E.K. Spicer)) Yale University School of Medicine, New Haven, CT 06510.(Spon. by LArmitage)

The bacteriophage T4 regA protein is a translational repressor that is known to regulate the synthesis of 10-12 T4 proteins. Earlier studies have demonstrated photocrosslinking to dT_{16} occurs at Phe 106. To evaluate the role of Phe 106 in nucleic acid binding, tyrosine and cysteine substitutions were introduced at residue 106. Intrinsic protein fluorescence quenching assays have been used to measure the binding affinities of the mutant proteins for specific and nonspecific RNAs. These studies indicated little difference between the K_{app} for the Phe 106 substitutions and the wild type protein for either poly (U) or for specific target sequence RNA of gene 44-4. The effects of salt on the K_{app} of the mutant proteins for specific target RNAs are being investigated. We have also examined the relative accessibility of the three intrinsic tryptophanyl residues of regA protein in the absence and presence of gene 44-4 RNA to acrylamide and iodide quenching. The quenching data indicate a reduction in the average dynamic quenching constant (K_D) of the tryptophan residues in the RNA-protein complex for either quenching agent. Iodide quenching of the RNA-protein complex was essentially negligible. These results provide evidence for RNA interaction near the tryptophan residues, which are located entirely in the COOH-terminal half of regA protein.

STRUCTURAL AND MOLECULAR DYNAMICS

Tu-Pos282

NMR STRUCTURAL STUDIES OF COMPLEXES FORMED BY COMPLEMENTARY RNA STEM-LOOPS AND THE COL E1 ROM PROTEIN

((John P. Marino, Razmic S. Gregorian Jr., James H. Prestegard and Donald M. Crothers))
Department of Chemistry, Yale University, New Haven, CT 06511

Regulation of replication of the plasmid Col E1 involves the interaction of two plasmid-specific RNA transcripts, RNA I and RNA II, and a plasmid encoded protein, ROM. RNA II acts to prime DNA replication, but is repressed by RNA I which is fully complementary to its 5' end. The complementary regions of RNA I and RNA II form several stem-loop structures and the binding of the RNAs begins by interaction at the loop regions. The initial RNA-RNA complex (or so called "kissing" complex) is stabilized with respect to dissociation by the ROM protein. Gel studies have shown that individual complementary stem-loops derived from the plasmid RNAs will mimic this interaction and are also stabilized with respect to dissociation by ROM.[1]

The wild type complementary RNA stem-loop sequences have been chosen for initial NMR studies. Formation of the binary RNA-RNA and the ternary RNA-RNA-protein complexes has been demonstrated by using one-dimensional exchangeable NMR experiments. The ^1H assignment strategy driven by the assignment of exchangeable resonances using gradient enhanced 2D H_2O NOESY experiments will be presented. In addition, the use of isotopically labeled RNA molecules and ROM protein to study the "kiss" (12 kdal) and "kiss"-ROM (26 kdal) complexes will be presented.

[1] Eguchi, Y. and Tomizawa, J. (1991) J. Mol. Biol., 220, 831-842.

Tu-Pos283

FLUORESCENCE STUDIES OF THE BINDING OF BACTERIOPHAGE Ø29 TO NUCLEIC ACIDS.

((M.A.Urbaneja, S.Rivas, F.M.Goñi, J.L.Carrascosa and J.M.Valpuesta)) Departamento de Bioquímica, Universidad del País Vasco and Centro de Biología Molecular, Universidad Autónoma de Madrid, Spain (Spon. by E.Padros)

Bacteriophage Ø29 connector exhibits an intrinsic tryptophan fluorescence sensitive to DNA binding. The present results indicate that the intrinsic fluorescence is differentially modified by DNA binding, producing a hyperbolic saturation monitored by fluorescence quenching at 335 nm, the maximal emission wavelength. On the contrary, proteolyzed Ø29 connectors, that have lost their capability of DNA binding, do not show such saturation. RNA binding to Ø29 connectors needs a higher RNA: protein molar ratio to reach measurable quenching. Moreover, DNA induces a protein conformational change increasing the accessibility of tryptophan residues to acrylamide. This conformational change has been corroborated by the fact that, upon DNA interaction, Ø29 connectors are more easily denatured when subjected to guanidinium-HCl treatment. This DNA-dependent denaturing behaviour has not been observed with proteolyzed connectors. RNA addition to Ø29 connectors does not cause differencies in the protein denaturing pattern, therefore suggesting that RNA interacts with viral connectors in a different way than DNA does.

Tu-Pos284

BACKBONE AND SIDE CHAIN DYNAMICS OF STAPHYLOCOCCAL NUCLEASE IN SOLUTION AS STUDIED BY PROTON-DETECTED ^{13}C AND ^{15}N NMR SPECTROSCOPY.

((*Linda K. Nicholson, ‡Lewis E. Kay, †Frank Delaglio, †Ad Bax and *Dennis A. Torchia)) *BRB, NIDR, and †LCP, NIDDK, NIH, Bethesda, MD 20892, and ‡Depts of Med. Genetics, Biochem. and Chem., Med. Sci. Bld., U. Toronto, Toronto, Ontario, Canada M5S 1A8. (Spon. by D. Torchia)

Recently developed nuclear magnetic resonance (NMR) pulse sequences to measure relaxation parameters of AX and AX_3 spin systems have been applied to investigate the internal dynamics of the backbone and selected side chains of staphylococcal nuclease (SNase) in the presence and absence of ligands thymidine 3',5'-bisphosphate (pdTp) and Ca^{2+}. The two-dimensional spectra generated by the pulse sequences enable the accurate measurement of nuclear Overhauser effects (NOE) and longitudinal (T_1) and transverse (T_2) relaxation times of isotopically enriched sites in proteins. We report the measurement of the ^{13}C T_1, T_2 and NOE values for the SNase alanine, leucine and methionine methyl carbons, and for the alanine alpha carbons. The dynamics of hydrophobic side chains are of particular interest because they provide probes of internal motions in buried regions of the protein. In addition, ^{15}N T_1, T_2 and NOE values for the backbone amide sites for uniformly ^{15}N enriched SNase are reported. The relaxation parameters are analyzed using the formalism of Lipari and Szabo to yield generalized order parameters and correlation times which characterize the internal motions of the labeled sites. Comparison of the order parameters obtained from liganded and unliganded SNase provides insight on the dynamic response of the protein to ligand binding. The order parameters are also compared with temperature factors obtained from X-ray crystal studies, providing insight on the differences between crystalline and solution states of the protein. These comparisons reveal a localized stiffening of the protein upon ligand binding in regions near the ligand binding sites, and demonstrate that in solution, the internal motions of selected sidechains of SNase are significantly larger than suggested by the X-ray structures.

Tu-Pos285

ENERGETICS OF THE DISULFIDE BRIDGE: AN *AB INITIO* STUDY.

((W. Qian and S. Krimm)) Biophysics Research Division, University of Michigan, Ann Arbor, MI 48109

The disulfide bridge is an important component of the structure of proteins. We have calculated its characteristic Raman-active SS and CS stretching modes as a function of the conformation of the bridge (1). It is also important to know the energetics of such structures, not only for analyses of native proteins but for predictions of potential disulfide bridges in engineered proteins. We have assumed, as a first approximation, that the energy (E) is an independent sum of $E(\chi^2_1\chi^3\chi^2_2)$ ($\chi^2 = \tau(CCSS)$, $\chi^3 = \tau(CSSC)$), which can be obtained from diethyl disulfide, and $E(\chi^1)$ ($\chi^1 = \tau(NCCS)$). We have computed the optimized 3-21G* *ab initio* energies of $C_2H_5SSC_2H_5$ at 30° intervals in the $\chi^2_1 - \chi^2_2$ space and obtained an energy map as well as a χ^3(min) map. Energy changes as a function of $\Delta\chi^3$ have also been computed. These calculations show that, in addition to the expected energy dependence on χ^2_1 and χ^2_2, χ^3(min) depends significantly on χ^2_1 and χ^2_2. These results permit determination of the relative energies of disulfide bridges as a function of χ^2_1, χ^3, and χ^2_2.

Research supported by NSF grants MCB-9115906 and DMR-9110353.

1. W. Qian and S. Krimm, Biopolymers 32, 1025 (1992).

Tu-Poa286
PROTEIN CONTRIBUTIONS TO THE REDOX POTENTIAL OF HOMOLOGOUS RUBREDOXINS. ((P. Swartz, T. Ichiye)) Dept. of Biochemistry and Biophysics, Washington State University, Pullman, WA, 99164.

Contributions to the redox potential of rubredoxin, a bacterial iron-sulfur (FeS) protein, have been studied via energy minimization. This study involves comparison of homologous rubredoxins from *Clostridium pasteurianum* and *Desulfovibrio gigas*, which experimentally have been shown to differ by -63 mV in redox potential (i.e., the redox reaction of *C. pasteurianum* is 1.45 Kcal/mol higher than that of *D. gigas*). From the results here, it appears that the protein alone contributes 110 Kcal/mol due to the change in the charge of the FeS site (without relaxation) while - 11 Kcal/mol is contributed by structural relaxation. A majority of the difference between the protein charge contributions is due to charged sidechains but this is apparently cancelled by the solvent contribution according to Born approximation estimates. The remaining contribution from nearby protein dipolar groups is 5 Kcal/mol, which is more in line with the experimental data. The contributions of individual sidechain changes and of backbone structural changes to the difference in redox potentials of the two rubredoxins are also presented.

Tu-Poa287
INFLUENCE OF SUBSTRATE AND ALLOSTERIC LIGAND ON TRYPTOPHAN DYNAMICS IN E. COLI PFK. ((J.L. Johnson and G.D. Reinhart)). Univ. of Oklahoma, Dept. of Chem. and Biochem., Norman, OK 73019.

MgADP serves as a "K-type" allosteric effector of E. coli phosphofructokinase (PFK), a tetramer of identical subunits containing one tryptophan per subunit, by increasing its affinity for the substrate fructose 6-phosphate (F6P). The free energy of interaction between MgADP and F6P equals –1.3 kcal/mol @ 25°C. Temperature studies indicate that this net activation arises from opposing enthalpy (ΔH = –1.9kcal/mol) and entropy (TΔS = –0.6 kcal/mol) contributions. Frequency-domain anisotropy studies have characterized the response of the tryptophan to the ligation of MgADP and F6P, both individually and in combination. Although phase differences in the frequency spectrum of each enzyme form vary by less than 1° at any given frequency, these changes are clearly significant and titratable. Analysis of the dynamic anisotropy indicate little change in the global rotation of each enzyme form, but the cone angle of rotation available to the tryptophan is quite responsive to the state of PFK ligation. The flexibility of the tryptophan in PFK-F6P (cone angle=17.5°) is notably greater than that in the other enzyme forms (cone angles of 7.6°,12.6°, and 9.4° for PFK, F6P-PFK-ADP, and PFK-ADP, respectively). Since the action of the activator MgADP is defined by the equilibrium PFK-F6P + ADP-PFK ⇌ ADP-PFK-F6P + PFK, the greater flexibility associated with the species on the left is consistent with the negative coupling ΔS measured for this equilibrium. Supported by grant GM 33216 from NIH and HR0-025 from OCAST.

Tu-Poa288
THE MECHANISM OF BINDING OF COLICIN E1 TO MEMBRANES: EVIDENCE FROM TIME-RESOLVED STUDIES OF SPIN LABELED MUTANTS ((Yeon-kyun Shin, Cyrus Levinthal, Francoise Levinthal, and Wayne L. Hubbell)) Jules Stein Eye Institute and Department of Chemistry & Biochemistry, University of California, Los Angeles, CA 90024 and Department of Biological Sciences, Columbia University, New York, NY 10025. (Spon. by Z. Farahbakhsh)

The protein Colicin E1 is a water-soluble bacterial toxin that binds irreversibly to membranes to form voltage-dependent ion channels. To investigate the mechanism of membrane interaction, three cysteine substitution mutants and the wild type of the channel forming domain of Colicin E1 were prepared and spin labeled at the unique thiol (Site-Directed Spin Labeling). The positions of the mutations were chosen so that the attached spin label would selectively detect either physical adsorption to the membrane or insertion of the hydrophobic domain into the membrane interior. Time-resolved interaction of these labeled proteins with membranes was investigated with rapid-mixing electron paramagnetic resonance. The results demonstrate that the interaction of the channel forming fragment with membranes occurs in three distinct steps: (1) diffusion to the membrane surface; (2) rapid hydrophobic adsorption to the surface and (3) slow, rate-limiting insertion of the hydrophobic central helices into the membrane interior. The rate of adsorption to the neutral membrane surface greatly increases with decreasing pH; the half time at pH 4.3 is 160 sec, while at pH 3.0 it is 7 sec. A negative charge also greatly enhances the rate of adsorption; the rate at pH 3.5 for 17 mole % negative charge is 40 msec, about 250x faster than adsorption to neutral membrane at the same pH. Full analysis of effects of pH and membrane surface charge on the kinetics of each step will be presented. These experiments demonstrate the ability of site-directed spin labeling to provide specific structural information on time-dependent molecular events in proteins.

Tu-Poa289
SITE-DIRECTED SPIN LABELING STUDIES OF COLICIN E1: INTERACTIONS BETWEEN THE C AND N TERMINAL DOMAINS AND SOME TOPOLOGICAL FEATURES OF THE MEMBRANE BOUND STATE. ((Lukasz Salwinski, Cyrus Levinthal, Francoise Levinthal, and Wayne L. Hubbell)) Jules Stein Eye Institute and Department of Chemistry & Biochemistry, University of California, Los Angeles, CA 90024 and Department of Biological Sciences, Columbia University, New York, NY 10025.

A series of cysteine substitution mutants (487-492) in the hydrophobic helical hairpin of colicin E1 have been prepared, digested with trypsin and the C-terminal, channel forming fragment of each isolated. All were derivatized at the introduced cysteine with a methanethiosulfonate nitroxide spin label. The nitroxide side-chains at 487,488,490 and 492 show significant increase in motion upon trypsinolysis, suggesting that the surface of the C-terminal fragment defined by these residues is in direct interaction with the N-terminal domain removed in the proteolysis. Consistent with this interpretation is the fact that the accessibility of these side-chains to collision with chromium oxalate and O_2 increases upon trypsinolysis. In contrast, side chains 489 and 491 show limited changes in mobility and accessibility upon trypsinolysis.

After binding to negatively charged phospholipid vesicles, all of these residues appear to lie near the membrane/solution interface, as judged by accessibility to collision with polar (NiAA, CrOx) and non-polar (O_2) radicals. The spin labeled side-chain at 491 undergoes rapid reduction by impermeable reducing agents trapped inside the vesicles. This suggests that the interhelical loop in which the residue resides appears on the *trans* surface of the vesicles upon membrane insertion.

Tu-Poa290
MODELING SOLVATION EFFECTS ON PROTEIN DYNAMICS

((Peter J. Steinbach, Milan Hodoscek and Bernard R. Brooks)) DCRT, NIH, Bethesda, MD 20892

Molecular dynamics simulations of carboxy-myoglobin (MbCO) have been performed using several different protocols to study the effects of protein hydration. Dynamics was simulated at 300 K for MbCO explicitly hydrated in vacuum at 14 different levels, ranging from 0 to 3832 water molecules, and for a periodic box of solvated MbCO. Implicit methods using atomic solvation parameters (ASP) were also evaluated. Here no waters were included, but their effects were modeled by potential energy penalties for burying hydrophilic atoms and exposing hydrophobic atoms.

Structural and dynamical effects of hydration on MbCO were characterized in terms of the rms deviation from the X-ray structure, the protein's radius of gyration, atomic fluctuation, and dihedral transitions. The simulations indicate that MbCO is fully hydrated by about 350 water molecules. These hydration waters form clusters, covering only about 60 % of the protein surface. They stabilize the X-ray structure throughout the entire protein, enhance the fluctuation of surface groups while halving the rate of dihedral transitions, and promote the glass transition (to anharmonic fluctuation) near 220 K. Their positions were compared to those of the waters resolved in MbCO crystals by neutron and X-ray diffraction. The implicit ASP simulations more closely resembled the simulations of MbCO in vacuum than the simulations of explicitly hydrated MbCO.

Tu-Poa291
APPLICATIONS OF A NEW CARBOHYDRATE FORCE FIELD
((Timothy M. Glennon and Kenneth M. Merz Jr.)) 152 Davey Laboratory, Department of Chemistry, The Pennsylvania State University, University Park, PA 16802

We have designed a force field for the study of carbohydrate dynamics. We have applied this force field to studies of intra- and intermolecular interactions of isolated saccharide molecules in an aqueous solvent. Analysis of various geometric parameters, radial distribution functions, and the organization of the solvent structure surrounding the saccharide molecule reveal several interesting points of saccharide dynamics. We have also studied the interactions of saccharides in the presence of a continuum surface. The results of the surface/saccharide simulation shall be compared and contrasted with the aqueous environment simulations.

Tu-Pos292

CONFORMATIONAL PREFERENCES AND INTRAMOLECULAR MOTIONS OF THE PARATHYROID HORMONE FRAGMENT 20-34: INVESTIGATION IN AQUEOUS SOLUTION AND BIOMIMETIC MEDIA BY ^{1}H NMR AND HETERONUCLEAR RELAXATION EXPERIMENTS.

François ANDRÉ, John C.T. RENDELL, Gordon WILLICK, Witold NEUGEBAUER and Harold C. JARRELL. Institute for Biological Sciences, National Research Council of Canada, OTTAWA, K1A 0R6 Canada.

The deletion analogue 20-34 of human parathyroid hormone (hPTH) was examined by NMR and molecular dynamics simulations for the presence of secondary structure in aqueous solution, in a solvent mixture of water and trifluoroethanol (TFE), and in sodium dodecyl sulfate (SDS) micelles. In solution, this fragment is found to adopt predominantly a random-coil conformation according to the ^{1}H 2D-NMR analysis, though the molecular dynamics simulations suggest that the whole peptide shows a tendency to be structured. This observation is experimentally confirmed by the analysis of the backbone dynamics as viewed by the ^{13}C NMR relaxation parameters. Moreover, the same experimental conformational analysis performed in water/TFE, combining results from chemical shift analysis and NMR relaxation parameters, shows that the peptide experiences a marked alpha helical tendency.

In addition, CD studies concluded that there is a significant secondary structure induced in the fragment by the presence of micelles. We investigated this membrane interaction using the biomimetic interface provided by SDS micelles. Titration experiments reveal that the fragment 20-34 strongly binds to the SDS micelles, and, on the basis of the chemical shift index, that it is markedly structured in a alpha helical type configuration. The sequence-specific resonance assignment of the micelle-bound peptide is presented and compared with that in the absence of SDS and in the mixture water/trifluoroethanol.

TRANSPORT ACROSS BILAYERS

Tu-Pos293

P-LIPID LATERAL DIFFUSION,WATER TRANSPORT & THE ORDER PARAMETER:A MOLECULAR MODEL OF WATER TRANSPORT THROUGH BILAYERS.((T. H. Haines & L. Liebovitch)) Chem. Dept., CCNY, NY 10031 and Eye Res. Div.,Columbia U. P&S. NY 10038 (Spon by T.H.Haines)

Raising phospholipid bilayers above T_m to the liquid-crystal provokes: water diffusion; bilayer thinning; kink diffusion or g-t isomerization; (a plateau of the frequency of kinks per $-CH_2-$ segment from 2 to 9 has been described. H. Trauble has proposed a mechanism in which the water molecules cross the bilayer on kinks that diffuse along the chain. Kinks were conceived by Flory who postulated that they must begin at either end of the chain. We assume that kinks beginning at the head group end of the chain imply both a lateral movement of the headgroup and the entry of a water molecule into the vacancy. We propose that each lateral step of a headgroup is accompanied with the entrance of a water molecule into the low dielectric. We have found that a random walk calculation on the two dimensional surface permits us to predict from lateral diffusion measurements the rate of water transport.

Tu-Pos294

TRANSBILAYER MOVEMENT OF UNESTERIFIED FATTY ACIDS ((Frits Kamp and James A. Hamilton)) Biophysics Department, Boston University School of Medicine, 80 East Concord St., Boston MA 02118.

We report a new method for monitoring movement of fatty acids (FA) across protein-free phospholipid bilayers. Pyranin, a water soluble, pH-sensitive fluorescent molecule was trapped inside well-sealed phosphatidylcholine (PtdCho) vesicles (with and without cholesterol) in Hepes buffer (pH 7.4). Upon addition of oleic acid to the external buffer (also Hepes, pH 7.4) an immediate decrease in fluorescence was observed, reflecting a decrease in pH of the internal volume. This was the result of "flip" of un-ionized FA to the inner leaflet, followed by a release of protons from ~50% of these FA (apparent pK_a in the bilayer=7.6). The proton gradient thus generated dissipated slowly because of slow cyclic proton transfer by FA. Subsequent addition of albumin to vesicles instantly removed the pH gradient, indicating complete removal of FA, which requires rapid "flop" of FA from the inner to the outer monolayer. We conclude that un-ionized FA "flip-flops" rapidly ($t_{1/2} \lesssim 2$ sec) and ionized FA slowly ($t_{1/2}$=min). The same result was found for octanoic, palmitic, arachidonic, and (doxyl-) stearic acid, as well as for other lipophilic acids (retinoic acid and bile acids). Since un-ionized FA move across PtdCho bilayers spontaneously and rapidly, complex mechanisms (e.g., transport proteins) may not be required for translocation of FA in biological membranes. This method uses a fluorescent probe which is not covalently attached to, nor interacts with, the lipophilic acids or the membrane and provides the first assay for flip-flop of native fatty acids across model membranes.

Tu-Pos295

EFFECTS OF ETHANOL-INDUCED LIPID INTERDIGITATTION ON PROTON PERMEABILITY IN DPPC VESICLES

((Junwen Zeng and Parkson L.-G. Chong)) Dept. of Biochemistry, Meharry Medical College, Nashville, TN 37208

6-Carboxyfluorescein (6CF) fluorescence has been used to study the proton permeability in the large unilamellar vesicles (LUV; diameter = 1000 ± 200 Å) of dipalmitoylphosphatidylcholine (DPPC) at 20 °C in the ethanol concentration range of 0 - 1.8 M. The fluorescence intensity of 6CF in an aqueous medium is known to decrease with decreasing pH. The probe 6CF was trapped inside the vesicle. When a pH gradient was established by the acidification of the external buffer, the proton peameability through the membrane was determined by monitoring the decrease of 6CF fluorescence as a function of time. The data were fitted by a single-exponential decay law, and the half-time, $t_{1/2}$, of the intensity decay was calculated. The $t_{1/2}$ value decreases abruptly at ethanol concentrations between 1.0 - 1.2 M. This concentration range comes close to the critical ethanol concentration for the formation of fully interdigitated DPPC (LUV) as inferred by the data of Prodan fluorescence and by the DSC results. It is therefore concluded that proton permeability increases when DPPC vesicles are transformed from the non-interdigitated gel phase to the fully interdigitated gel phase. The apparent change in proton permeability will be discussed in terms of membrane thickness (supported by ARO and NSF-MRCE).

Tu-Pos296

IONIC PERMEATION OF LIPID BILAYERS.

((David W. Deamer)) Molecular Biosciences, UC Davis CA 95616

Ion permeation of lipid bilayers has been described in terms of the Born energy required to bring a charged particle from a high dielectric phase (water) to a low dielectric phase (the bilayer interior). However, the measured ionic permeability of lipid bilayers is orders of magnitude greater than expected from Born energy considerations. An alternative explanation is that ion permeation occurs through rare transient defects. This was tested by measuring ionic permeabilities of liposomes composed of phospholipids with varying acyl chain lengths. If only Born energy considerations are relevant, ionic flux would be reduced to a minimum at the point that stable bilayers formed and would not change significantly as longer chain lipids were used. Alternatively, if transient defects were a primary factor, short-chain lipids should have many more such defects, leading to a much higher ionic permeability than longer chain lipids. Liposomes (20 mM synthetic phosphatidylcholines, 12 to 18 carbon chain lengths) were prepared in citrate-buffered 0.2 M potassium sulfate (pH 6.0) and pH gradients of 3.0 units were produced by diluting 1 volume of liposomes with 9 volumes of pH 9.0 borate buffer. Proton flux was monitored by pH-sensitive dyes, and potassium flux was followed with a potassium electrode after gel filtration into isosmotic 0.3 M choline chloride. The permeability to both protons and potassium was a function of chain length, decreasing approximately ten-fold for each two carbon increment. It follows that thermal fluctuations in short-chain lipids produce large numbers of transient defects that cause such bilayers to be highly permeable to ions. As chain length increases, the fluctuations become rarer, but do not entirely disappear. Their presence accounts for the unexpectedly high permeability of typical lipid bilayers to ions. Supported by NASA NAGW-1119.

Tu-Pos297

CA^{2+} TRANSPORT BY IONOPHORES A23187, 4-BrA23187, AND IONOMYCIN IN A DEFINED SYSTEM: ELECTRONEUTRAL OR ELECTROGENIC? ((W.L. Erdahl, C.J. Chapman, R.W. Taylor, and D.R. Pfeiffer)) Dept. of Medical Biochemistry, Ohio State Univ., Columbus OH 43210 and the Dept. of Chemistry and Biochemistry, Univ. of Oklahoma, Norman OK 73019

Ca^{2+} ionophores are used as experimental tools under the assumption that they transport primarily Ca^{2+} via a strict electroneutral mechanism. However, solution chemistry data (e.g. A.B.B. 281, 44-57 (1990); J.B.C. 266, 8336-8342 (1991)) and data obtained in whole cells (J.B.C. 264, 19630-19636 (1989)) suggest that electrogenic transport, cation-anion cotransport and transport of +1, +2, and +3 charged cations may occur under some conditions. Such unrecognized activities could profoundly effect the interpretation of ionophore actions on biological systems. We have tested a model for neutral Ca^{2+} transport by these ionophores in a well-defined phospholipid vesicle model system. Measurements of transport rate vs ionophore and Ca^{2+} concentration, Ca^{2+}:H^+ ratios, membrane potential and the effects of uncouplers and of permeant acids and bases on the system show that the transport mode is predominately charge neutral. The transport rate and extents of transport are determined primarily by ΔpH. This system can now be used to search for unrecognized transport activities of Ca^{2+} ionophores. (Supported by NIH Grant HL49181).

Tu-Pos298

KINETICS OF THE INTERACTION OF AEROLYSIN WITH LIPID MONOLAYERS AND BILAYERS. R. MacDonald[1], F. Pattus, G. van der Goot, K. Leonard and J.T. Buckley[2]. Northwestern University[1], Evanston, IL; EMBL, Heidelberg, Germany; University of Victoria[2], Victoria, B.C.

The penetration of aerolysin, a channel-forming toxin from Aeromonas hydrophila, into phospholipid monolayers at the air-water interface and into bilayer vesicles has been examined by monitoring monolayer surface pressure and release of a fluorescent marker from large unilamellar vesicles, respectively. Proteolytic activation of proaerolysin generates a species which penetrates monolayers at rates proportional to proaerolysin concentration. Its surfactivity is quite modest; penetration ceases at surface pressures of 12-15 dynes/cm. Oligomers of toxin at the monolayer surface are observable by electron microscopy. Release of marker, initiated by addition of protease to liposome suspensions containing proaerolysin, is strongly dependent upon proaerolysin concentration and duration of proteolysis, but not upon vesicle concentration. Between the time of protease addition and the onset of leakage, there is a pronounced lag in release, the duration of which is inversely related to the proaerolysin concentration. The linear portion of the concentration-leak rate relationship is proportional to proaerolysin concentration at concentrations above about 75 ug/ml but dependent upon the 3-4 power of concentration at lower concentrations. The lysin is spontaneously inactivated in a concentration-dependent manner. These data appear consistent with previously postulated sequences involving oligmerization in solution to generate oligomers which either insert into the bilayer to induce leakage or aggregate to form an inactive species. Bilayer vesicle lysis is very inefficient; under our conditions, the majority of proteins do not breach the bilayer.

Tu-Pos299

CHANNELS PRODUCED BY CLOSTRIDIUM SEPTICUM ALPHA TOXIN IN LIPID BILAYERS. ((Y.Sokolov*, B.L.Kagan*, W.Yuan*, R.K.Tweten&, J.Ballard&) *UCLA, Los Angeles, CA 90024, &University of Oklahoma, Oklahoma City, OK 73190

C. septicum is responsible for a number of human diseases, the most serious of which is the frequently fatal nontraumatic gas gangrene. It ix known that a single extracellular toxin (alpha toxin is both hemolytic and cytotoxic. Addition of alpha toxin or its processed form to the solution bathing a planar lipid membrane to a concentration of 2-20 nM resulted in discrete increases of membrane conductance. The channels remained open in the range of voltages from -100 to +100 mV and demonstrated a tendency for closing in the range of 100-150 mV both at positive and negative voltages. C. septicum channels have a weak preference for anions over cations (reversal potential in 10-fold concentration gradient of KCl was about 20 mV) and are permeable for such ions as Tris, TEA, glucosamine, gluconate, NAD (d=9 A°) and phytate The channel's conductance is characterised by an open state (appr 160 pS), closed state (appr. 15 pS) in 100 mM KCl, and a number of intermediate substates. The closed state demonstrated a cation selectivity (reversal potential in the same conditions as described above was 15-18 mV opposite polarity) and the values of reversal potential for substates were correspondingly in the range from -18 to +20 mV. These data lead to the suggestion that cytotoxity of C. septicum toxin may result from either efflux of essential ions and other cellular constituents or influx of toxic ions.

Tu-Pos300

ELECTROCHEMICAL CHARACTERIZATION OF BLM AND LIPOSOMES CONTAINING GRAMICIDIN A BY EIS ((L.M. Gassa, S. Alonso-Romanowski and J.R. Vilche)) INIFTA, UNLP Suc. 4, C.C. 16-1900 La Plata, ARGENTINA (Spon. by A. Killian)

Electrochemical Impedance Spectroscopy (EIS) and contrast phase microscopy have been employed to study the interaction of the polypeptide GA with bilipidic model systems (liposomes and BLM) in electrolyte solutions. The lipidic suspension behaviour changes in the presence of GA. The system was studied with BLM and/or liposomes - solution where GA was added to the solution or was already incorporated.

The most striking feature is the increase in the magnitude of the impedance difference when changing the lipid for the lipid/GA system. The complete set of data revealed that both real and imaginary impedance components are strong function of the GA incorporation. In order to understand the dynamics of the transport processes of the system GA/membrane an adecuate transfer function was used according to the physical model proposed and analized by non-linear fit routines and parametric identification procedures The microscopy data can be correlated, as a first approach, with the conclusions derived from the electrochemical results.

Tu-Pos301

THE Hg^{2+} SENSITIVE RESIDUE AT CYS-189 IN THE CHIP28 WATER CHANNEL ((G.M. Preston, J.S Jung, W.B. Guggino, and P. Agre)) Johns Hopkins University School of Medicine, Baltimore, MD 21205.

Specialized channels provide the plasma membranes of red cells and renal proximal tubules with high permeability to water. CHIP28 protein was identified as the first molecular water channel by measurement of osmotic swelling of *Xenopus* oocytes injected with CHIP28 cRNA (Preston *et al.* (1992) *Science* 256, 385-387). Since water channels are pharmacologically inhibited by submillimolar concentrations of Hg^{2+}, site-directed mutagenesis was undertaken to demonstrate which of the four cysteines (87, 102, 152, or 189) is the sensitive residue in CHIP28. Each cysteine was individually replaced by serine, and oocytes expressing each of the four mutants exhibited osmotic water permeability (P_f) equivalent to wild-type CHIP28. After incubation in $HgCl_2$, all were significantly inhibited, except C189S which was not inhibited even at 3 mM $HgCl_2$. CHIP28 exists as a multisubunit complex in the native membrane, but although oocytes injected with mixed CHIP28 and C189S cRNAs exhibited P_f corresponding to the sum of their individual activities, exposure to Hg^{2+} only reduced the P_f to the level of the C189S mutant. Of the six substitutions at residue-189, only the serine and alanine mutants exhibited increased P_f and had glycosylation patterns resembling wild-type CHIP28 on immunoblots. These studies demonstrated: i) CHIP28 water channel activity is retained despite substitution of individual cysteines with serine; ii) cysteine-189 is the Hg^{2+} sensitive residue; iii) the subunits of the CHIP28 complex are individually active water pores; iv) residue 189 is critical to proper processing of the CHIP28 protein.

Tu-Pos302

STALK STRUCTURES AS INTERMEDIATES IN MEMBRANE FUSION & BILAYER/NON-BILAYER PHASE TRANSITIONS ((D. P. Siegel))
Procter & Gamble Co., P.O.Box 398707, Cincinnati, OH 45239-8707

Studies of membrane fusion and $L_\alpha/Q_{II}/H_{II}$ transition mechanisms are hampered by lack of information about the intermediates involved. I used results of research on L_α/Q_{II} & L_α/H_{II} phase transitions to develop methods for comparing the relative free energies of lipid intermediates of different geometries. Two models for fusion intermediates have been proposed: stalk-based structures [1] and inverted micellar intermediate (IMI)-derived structures [2]. I show that stalks are generally lower in energy than IMIs, and hence probably form more readily. The lipid composition dependence of the energies of stalks and subsequent structures are consistent with observed fusion & lipid mixing behavior from a wide range of systems. Stalks are also better models for bilayer/non-bilayer transition intermediates than IMIs: stalks are lower in energy; can generate all the observed structures (ILAs, Q_{II} & H_{II} lattices); and can transform into line defects [2] much faster than IMIs, yielding L_α/H_{II} transition rates more consistent with observations [3]. Preliminary TRC-TEM results also favor a stalk-based transition mechanism [4]. The modeling method can also be used to generate and refine models of protein-induced fusion [5].
[1] Markin et al., Gen. Physiol. Biophys. 5:361 (1984); [2] Siegel, Biophys.J. 49:1155 (1986); [3] Tate et al. Biochem.31: 1081 (1992); [4] Siegel, this meeting; [5] Siegel, chapter in *"Viral Fusion Mechanisms"* (J. Bentz,ed.), CRC Press, (1993).

Tu-Pos303

Inhibition of Membrane Fusion by t-boc-FlFlF. P. L. Yeagle†, A. R. Dentino†, J. Young† & T. Flanagan§, Departments of †Biochemistry and of §Microbiology, University at Buffalo School of Medicine, Buffalo, NY 14214

The hydrophobic peptide, t-boc-FlFlF, a chemotactic peptide antagonist for neutrophils, inhibited viral fusion in a manner analogous to the inhibition of the antiviral peptide, ZfFG[1], but with greater potency. t-boc-FlFlF inhibited Sendai virus fusion with Hep2 cells and Sendai virus fusion with erythrocyte ghosts in a dose-dependent manner, as measured by the R_{18} lipid mixing fluorescence assay. This peptide also inhibited the fusion of large unilamellar vesicles of N-methyl dioleoylphosphatidylethanolamine. Further-more this peptide inhibited the formation of SUV by sonication of egg phosphatidylcholine, as did ZfFG. These experiments indicate that t-boc-FlFlF inhibits viral fusion and lend further support to the hypothesis that viral fusion involves intermediates with highly curved surfaces, such as stalks. This work was supported by grants from NIH (AI26800; DE05608).
[1] J. Biol. Chem. 265, 12178-12183 (1990); Virology, 182, 690-702 (1991); Biochemistry, 31, 3177-3183 (1992)

Tu-Pos304

PRE-FUSION INTERMEDIATES OF BOTH pH AND Ca^{2+} - TRIGGERED BIOLOGICAL MEMBRANE FUSION CAN BE REVERSIBLY ARRESTED WITH LYSOLIPIDS.
((S.S. Vogel, E.A. Leikina, L.V. Chernomordik)) LTPB, NICHD, NIH, Bethesda MD 20892.

We have previously shown that lysolipids and related amphiphilic compounds added exogenously between fusing membranes are potent and reversible inhibitors of biological fusion in a number of distinct physiological processes including Ca^{2+} and GTP-γ-S triggered exocytosis, and pH - triggered viral fusion. Now we show that lysolipids arrest a stage of fusion between triggering and actual merging of the membranes for both virus-mediated fusion and calcium-triggered exocytosis. pH - triggered fusion of cells infected with baculovirus was assayed by i) counting of cells in syncytia, and ii) observing the redistribution of the fluorescent membrane marker rhodamine-phosphatidylethanolamine between fusing cells. Ca^{2+}- triggered exocytotic fusion of sea urchin egg cortices was monitored by direct DIC observation of granule content release. In both experimental systems the fusion trigger (H^+ or Ca^{2+}) was applied in the presence of inhibiting concentrations of short-chain lysophosphatidylcholine. Next the cells and granules were washed with buffers containing lysolipid but without the trigger. No fusion or lysis was observed at this stage. Removal of the lysolipid 5-10 min later by washing with buffers lacking the fusion-trigger now resulted in the initiation of fusion. The extent of fusion was comparable with samples which were not treated with lysolipids. Possible mechanisms of fusion inhibition and the structure of the fusion intermediates arrested by the lysolipids will be discussed.

Tu-Pos305

CHANGES IN LIPID ASYMMETRY DURING FUSION
((Curtis Balch and Richard G. Sleight)) Dept. of Molecular Genetics, Biochemistry, and Microbiology, University of Cincinnati Medical Center, Cincinnati, OH 45267. (Spon. by W. David Behnke)

Changes in the transbilayer distribution of lipids across membranes during fusion were measured using fluorescently-labeled liposomes. Small unilamellar vesicles (SUVs) and large unilamellar vesicles (LUVs) were prepared using various phospholipids. Liposomes were labeled on the inner leaflet, outer leaflet, or both leaflets with 1-palmitoyl-2-(N-4-nitro-benzo-2-oxa-1,3-diazole)-aminocaproyl phospholipid (NBD-lipid). Before and after fusing the vesicles with either calcium, poly (ethylene glycol) (PEG), or spermine, the amount of NBD-lipid in the outer leaflet was measured using a recentlydeveloped assay (McIntyre and Sleight, 1991, Biochemistry 30: 11819-27). Evidence for the reliability of this assay was provided by similar measurements using NMR and labeling of vesicles with trinitro-benzene sulfonic acid. The change in lipid distribution across the membrane during fusion was found to be dependent on liposome size, lipid composition, and the fusogen used. Calcium-induced fusion of SUVs resulted in complete randomization of lipid between leaflets, while PEG-induced fusion of LUVs resulted in minimal lipid redistribution. Spermine caused a partial lipid randomization in both SUVs and LUVs. Partial lipid redistribution also occurred during LUV fusion by calcium and SUV fusion by PEG.

Tu-Pos306

PHOTOINDUCED FUSION OF LIPOSOMES.
((Doyle E. Bennett and David F. O'Brien*)) Department of Chemistry, The University of Arizona, Tucson, AZ 85721

Fusion of two-component unilamellar liposomes (160 nm diam.) composed of the polymerizable 1,2-bis-[10-(2',4'-hexadienoyloxy) decanoyl]phosphatidylcholine (SorbPC) and either DOPE or DOPC was examined via fluorescent lipid mixing assays. The rate and extent of lipid mixing of DOPE/SorbPC (3:1) liposomes at pH 7.5 increased with increasing UV irradiation time (% conversion of monomer), sample temperature, and liposome concentration. Photoreaction of SorbPC (90% conversion) in liposomes (750 μM total lipid) resulted in 7-17% lipid mixing at 25°C and 37-47% lipid mixing at 37°C. When the lipid concentration was decreased to 150 μM, the extent of lipid mixing was depressed to 11-17% (37°C). The incorporation of 1 mol% of the negatively charged DOPA into the DOPE/SorbPC liposomes inhibited lipid mixing as well. Photolysis of the control DOPC/SorbPC liposomes did not cause lipid mixing. These observations indicate that photopolymerization induced lipid phase separation and formation of enriched domains of PE in unilamellar liposomes allows the close approach of apposed regions of enriched PE lamellae and facilitates the lipid mixing between the liposomes in a manner consistent with liposome fusion.

Tu-Pos307

POLY(ETHYLENE GLYCOL)-INDUCED FUSION OF TWO PHASE-SEPARATED LARGE, UNILAMELLAR VESICLE SYSTEMS. ((Donald Massenburg, Jogin R. Wu, Jan Prevratil, & Barry R. Lentz)) Department of Biochemistry and Biophysics, School of Medicine, University of North Carolina, Chapel Hill, NC 27599-7260.

Previous reports have proposed that vesicle fusion might result from the presence of membrane gel-fluid phase separations. To test this hypothesis in the case of poly(ethylene glycol) (PEG)-induced fusion, large, unilamellar vesicles (LUV) were prepared by the extrusion method and incubated with various concentrations of PEG for 30 minutes at temperatures shown to correspond with the gel, fluid, or gel-fluid mixed phase states. DPHpPC fluorescence lifetime measurements, ANTS/DPX contents mixing and leakage measurements, and quasi-elastic light scattering (QELS) measurements showed that vesicles composed of pure DPPC did not fuse above or below the main phase transition, but QELS and fluorescence lifetime measurements suggested that fusion did occur during incubation at the main phase transition temperature. These same methods suggested that the onset of fusion occurred between 25 and 30 wt% PEG above the phase-separated temperatures in the DMPC/DPPC mixed lipid system, while fusion was initiated at approximately 15 wt% PEG during phase separation. No indication of fusion occurred at all below the phase separated temperatures. We conclude that PEG-mediated fusion of LUV is enhanced by the co-existence of gel and fluid phases in membranes. This supports the view that PEG serves mainly to aggregate vesicles and bring membranes into close contact, with fusion occurring only when the bilayer structure is disrupted. Supported by GM32707.

Tu-Pos308

POLY(ETHYLENE GLYCOL)-MEDIATED LIPID TRANSFER AND FUSION BETWEEN PHOSPHOLIPID LARGE UNILAMELLAR VESICLES IN THE DEHYDRATED STATE.

((Jogia R. Wu and Barry R. Lentz)) Department of Biochemistry & Biophysics, University of North Carolina, Chapel Hill, NC 27599-7260

A model for lipid mixing detected by the fluorescence lifetime of the DPH$_2$PC probe has been developed to distinguish between lipid transfer and fusion between large unilamellar vesicles occurring in the presence of poly(ethylene glycol) (PEG). The model took into consideration the heterogeneity of microenvironments experienced by the probe in a sample containing vesicle aggregates of different sizes. Assuming the aggregate size distribution was a delta function, the observed lifetime yielded the vesicle aggregate size under conditions of lipid transfer only or lipid transfer accompanying fusion. Large, unilamellar phospholipid vesicles were prepared by a rapid extrusion technique either in the presence or the absence of the DPHpPC probe. Lipid transfer between probe-containing and probe-free vesicles was then monitored by following changes in the observed DPHpPC fluorescence lifetime. Analysis of fluorescence lifetime data obtained with vesicles of varying composition revealed that only small aggregates formed. For vesicles that could be demonstrated by other means not to have fused, the data were consistent with lipid transfer occurring only between the outer leaflets of 2 - 4 vesicles, even at high PEG concentrations. For vesicles that could be demonstrated to fuse by contents mixing and size changes, the fluorescence lifetime data obtained at sub-fusing PEG concentrations were also consistent with lipid transfer between the outer leaflets of 2 - 4 vesicles. At fusogenic PEG concentrations, the fluorescence data were consistent with lipid transfer between both the inner and outer leaflets of 2-4 vesicles still gathered into small aggregates. These predictions agreed with quasi-elastic light scattering and other data showing that fusion products were large, unilamellar vesicles with diameters consistent with incorporation of a small number of vesicles (Massenburg & Lentz, submitted). At very high PEG concentrations, where extensive rupture was observed, the lifetime data were consistent with much more extensive lipid transfer within larger aggregates. Aside from providing a framework within which to interpret the DPHpPC fluorescence lifetime changes observed in the presence of PEG, the model and data presented here provide strong evidence that fusion occurs between small numbers of PEG-aggregated vesicles before the removal of PEG. Supported by NIH GM-32707.

Tu-Pos309

HOW DO HEXADECANE AND DIGLYCERIDE INCREASE DIVALENT CATION-INDUCED LIPID MIXING RATES IN PS LUV? ((A. Walter*, P. L. Yeagle+ and D. P. Siegel)) *Dept. Physiol. & Biophys., Wright State Univ., Dayton OH 45435; +Dept. Biochem. SUNY, Buffalo NY 14214; Procter & Gamble Co., POB 398707 Cincinnati)H 45239

We recently reported that 3 lipid mol % dioleoylglycerol (DOG) or 6 mol% hexadecane (HD) doubled the rates of Ca^{2+} or Ba^{2+}-induced lipid mixing between BBPS LUVs. This is not due to a change in LUV aggregation rate. HD & DOG are equally effective on a moles-of-added-chain (volume) basis. We used ^2H NMR to determine the orientation of d_{34}-HD and d_{62}-dipalmitoyl-glycerol (DPG) in PS bilayers. DSC shows that DOG, HD & DPG have little effect on T_m of BBPS. Ca^{2+} or Ba^{2+} addition doesn't induce phase separation of HD or DOG, but DPG forms some DPG-rich PS phase. ^2H-NMR shows that HD aligns roughly parallel with PS chains, but resides near the bilayer midplane, whereas DPG (and presumably DOG) is oriented as is PS. When Ca^{2+} is added, HD appears to move to a less-ordered locale, while DPG is frozen into the Ca^{2+}-PS matrix (though a small fraction may be in a very disordered region). Surprisingly, Ba^{2+} has little effect on HD or DPG ^2H NMR spectra: Ba^{2+} binding to PS induces less chain ordering than Ca^{2+}. Despite different dispositions before and after Ca^{2+} or Ba^{2+} addition, and differences in the presence of Ba^{2+} vs. Ca^{2+}, both HD and DOG doubled Ca^{2+}-induced mixing rates, and DOG doubled the rates in both Ca^{2+} & Ba^{2+} systems. HD and DOG may stabilize a transient lipid mixing intermediate by packing hydrophobic voids within the structure.

Tu-Pos310

FUSION OF LIPOSOMES INDUCED BY [des 1-12] LIPOCORTIN I

((O. Eidelman, H.B. Pollard, M. de la Fuente and G. Lee)) Laboratory of Cell Biology and Genetics, NIDDK, NIH, Bethesda, MD.

Membrane mixing and aggregation of PS large unilamellar vesicles were found to be induced by a naturally occurring form of bovine annexin I missing the first 12 a.a. on the N-terminal ([des 1-12] lipocortin I). Membrane mixing was studied by NBD-PE/Rho-PE dequenching using extruded PS LUV. Fusion of was induced by bovine [des 1-12] lipocortin I but not by the intact annexin, while porcine lipocortin I induced fusion in its intact form. Vesicle aggregation and fusion were found to be dependent on the concentration of divalent cations in a sigmoid fashion: Ca^{++} had a half maximal effect ($K_{1/2}$) at 270±20 μM and Hill coefficient (K_H) of 3.8 ± 0.3, and for Ba^{++} $K_{1/2}$ was 170±50 μM and K_H was 3±1. Mg^{++} induced fusion at a higher concentration range (2.5 mM) and the activation seemed to be linear with $[Mg^{++}]$. Fusion rates were enhanced by isotonic replacement of salt with sucrose, with half maximal effect at ~15%sucrose. Fusion decreased with pH and the apparent pK was about pH 6 in sucrose solutions. We conclude that (a) lipocortin I can mediate fusion induced by sub-millimolar concentrations of Ba^{++} or Ca^{++}; (b) the fusion process is apparently cooperative, either in the binding of divalent cations to activate a single polypeptide or in the action of 2-4 polypeptide molecules to induce a fusion event; and (c) in bovine lipocortin I this function depends on the truncation of the first 12 amino acid residues.

Tu-Pos311

USE OF SYNTHETIC PEPTIDES TO LOCALIZE AND CHARACTERIZE LIPID BILAYER FUSION ACTIVITY OF PULMONARY SURFACTANT PROTEIN B

((K. J. Longmuir, S. Haynes, and A. J. Waring)) Dept. Physiol. & Biophys., U. Calif., Irvine CA 92717 and Dept. Pediatr., King-Drew Med. Ctr. and UCLA, Los Angeles, CA 90059

The 79 amino acid human surfactant protein B (SP-B) promotes lipid bilayer fusion. The lipid-mixing activity can be studied in divalent-cation-free buffer containing 1) fluid liposomes [dioleoylPC with a rhodamine-PE, BODIPY-PC resonance energy transfer pair], and 2) liposomes below their phase transition temperature [100% dipalmitoylphosphatidylglycerol (PG), or 70:30 dipalmitoylPC:dipalmitoylPG]. A comparison of synthetic peptides corresponding to SP-B amino acids 1-25 (n-terminal region), 30-78, and 49-78 (c-terminal region) revealed that the n-terminal region catalyzed lipid mixing at the fastest rate and to the greatest extent. The 1-25 n-terminal region was further characterized by examining several 25 amino acid synthetic analogues. Activity was not significantly affected by 1) replacing the cysteines (cys-8, cys-11) with alanine, 2) replacing four hydrophobic amino acids (leu-10, leu-14, ile-18, ile-22) of the amphipathic helix with phenylalanine, 3) replacing the arginines (arg-12, arg-17) with lysine, and 4) replacing all four positively-charged residues (arg-12, lys-16, arg-17, lys-24) with serine. Neither positively-charged amino acids nor divalent cations are necessary for activity. Instead, the amphipathicity of the n-terminal region may be the feature responsible for promoting lipid bilayer fusion.

Tu-Pos312

INTERACTIONS BETWEEN DMPC AND THE FUSION-INHIBITING PEPTIDE, Z-Phe-Phe-Gly, DETERMINED BY FT-IR.

((Mark A. Davies[1], Brian M. Peek[2], and Bruce P. Gaber[2])) [1]Dept. of Biochemistry and Molecular Biology, Georgetown Univ. School of Medicine, Washington, DC 20007; [2]Center for Bio/Molecular Science and Engineering, Code 6900, Naval Research Laboratory, Washington, DC 20375.

We have used FT-IR to investigate the interaction of the fusion-inhibiting peptide, Z-Phe-Phe-GLy (Z = benzyloxycarbonyl) with lipid membranes. The CH_2 wagging modes occurring in the acyl chain infrared spectra between 1370 cm^{-1} and 1300 cm^{-1} are sensitive conformational probes. They have been used to monitor the trans-gauche isomerization process in the acyl chains of dimyristoyl phosphocholine (DMPC) in the presence of Z-Phe-Phe-Gly. Populations of kink, multiple gauche, and end-gauche conformers were determined, thus placing the DMPC-peptide interactions in a quantitative structural context. These results will be compared with similar experiments using dimyristoyl phosphoethanolamine (DMPE). Supported by the Office of Naval Research.

Tu-Pos313

ACTIVITY OF THE FUSION PEPTIDE OF INFLUENZA VIRUS AS MEASURED BY A NEW MICROPIPETTE ASSAY FOR MEMBRANE FUSION

((S.A. Soltesz and D.A. Hammer)) School of Chemical Engineering, Cornell University, Ithaca, NY 14853

Membrane fusion is a wide-spread biological phenomenon involved in viral infection, exocytosis, and fertilization of egg by sperm. In our laboratory, we have assembled a micropipette aspiration assay for membrane fusion in which two large (20-30 μm diameter) unilamellar vesicles are manipulated into close contact. Large unilamellar vesicles are synthesized by dehydrating lipid films onto Teflon substrates and then carefully rehydrating the lipids with aqueous solutions. The vesicles are formed with both lipid-soluble (NBD-PE/Rh-PE) and water-soluble (ANTS/DPX) donor/acceptor fluorescent pairs so that mixing of membrane lipids and internal aqeuous contents can be monitored simultaneously. Single fusion events can be seen with the light microscope and are recorded using both an intensified video camera and a photomultiplier tube.

Biological membrane fusion events are known to be protein-mediated, and our research focuses on the ability of peptides to induce the fusion of egg phosphatidylcholine vesicles. We have performed control experiments with polylysine and melittin, and have shown that these proteins cause membrane lysis very rapidly, on a time-scale close to the time for mixing of the peptide in the fusion chamber. We will measure the ability of two peptides representing the N-terminus of the hemagglutinin protein of influenza virus, the so-called "fusion peptide", to induce the fusion of large unilamellar vesicles. These peptides have been reported to promote membrane fusion in suspensions of smaller vesicles, and we will compare the results from our assay to those published previously.

Tu-Pos314

FUSION PORES CONNECTING CELLS TO PLANAR MEMBRANES: FLICKERING TO FINAL EXPANSION. ((G.B. Melikyan, W.D. Niles, M.E. Peeples, F.S. Cohen)) Rush Medical College, Depts. of Physiology and Immunology/Microbiology, Chicago, IL 60612. (Spon. by F. Quandt)

Fusion between cells expressing influenza virus hemagglutinin (HA) and voltage-clamped planar lipid bilayers is being characterized by electrical admittance and fluorescent dye measurements. Currents in-phase and 90° out-of-phase with applied sinusoidal voltages determine the conductances of fusion pores. These currents are due to fusion as verified by including 1 mM ethidium bromide in the solution of the cell-free side of the bilayer -- upon each current increase characterizing fusion, an individual cell nucleus becomes fluorescent due to the ethidium entering the cytosol through the fusion pore. Fusion is pH dependent and facilitated by gangliosides. The initial fusion pore is reversible, characterized by flickering between open (about 1 nS) and closed states. Pores then irreversibly open into a second stage wherein conductances vary widely, from as little as a few nS to as much as 100 nS, and may remain relatively stable, slowly increase, or even fluctuate. After remaining in this plastic stage from seconds to minutes, pores expand to a fully enlarged phase with an initial, rapid (≈ 10 ms), step-like rise in conductance, followed by slower increases to the final conductance. These electrophysiological attributes are similar to pores of cell-cell fusion and exocytosis. The early structures of fusion are thus reconstituted with a purely lipidic target membrane. Supported by NIH GM27367 and AI21924.

Tu-Pos315

RATE PROCESSES IN MEMBRANE FUSION REACTIONS ((W. D. Niles)) Department of Physiology, Rush University, Chicago, IL 60612 (Sponsored by P. De Lanerolle).

Physical chemical reactions are increasingly being described empirically as processes with a state space of reaction intermediates and a mapping of reaction paths. When individual membrane fusion events can be detected and timed, these models provide a useful description of the underlying reaction, because transition probabilities (instead of state probabilities) are measured directly in the experiment. For a Markov scheme, these are independent of the initial distribution. The validity of any model and subsequent physical interpretation of its transition rates is tested by time course predictions. They are useful in determining classes of models to be used in describing fusion reactions. For example, dependencies on conditions that are obvious in the kinetics of initiation-synchronized single events can be masked by time inhomogeneities in macroscopic experiments. This is clear from the effect of surface-bound receptor on the kinetics of hemagglutinin-mediated fusion of influenza virions. Alternatively, the invariance of the synaptic delay to Ca^{2+} indicates that Ca^{2+} gates the synaptic vesicle into a queue of exocytic reactions with Ca^{2+}-independent transition rate constants. Outstanding issues include: 1) When rate constants are so large compared to the time resolution of the experiment that they are not "rate-limiting", 2) when errors of measurement overcome small differences in rate constants, and 3) whether molecular details of a reaction do or do not influence interpretation of a model's validity.

Tu-Pos316

FUSION KINETICS OF INFLUENZA VIRUS:DIFFERENTIAL pH REQUIREMENTS FOR FUSION AND INACTIVATION.
((J. Ramalho-Santos[1],S. Nir[2],N. Düzgünes[3] and M.C. Pedroso de Lima[1])) [1]Univ. of Coimbra,Portugal, [2]Hebrew Univ.,Israel, [3]Univ. of Pacific,USA.

The fusion of influenza virus (A/PR/8/34) with PC-12 cells was monitored by a fluorescence assay,and the results were analysed with a mass action model which could explain and predict the kinetics of fusion.The model accounted explicitly for the reduction in the fusion rate constant upon exposure of the virus to low pH,either for the virus alone in suspension or for the virus bound to the cells.When the pH was lowered without previous viral attachment to cells an optimal fusion activity was detected at pH 5.2.When the virus was prebound to the cells,however,reduction of pH below 5.2 resulted in enhanced fusion activity at the initial stages. These results were explained by the fact that both the rate constants of fusion and inactivation increased several-fold at pH 4.5 or 4,compared to those at pH 5.2.At pH 5.2 lowering the temperature from 37°C to 20°C or 4°C resulted in a decrease in the fusion rate constant by more than 30- or 1000-fold,respectively.Inactivation of the virus when preincubated in the absence of target membranes at pH 5 was found to be rapid and extensive at 37°C,but was also detected at 0°C.Our results indicate a strong correlation between fusion and inactivation rate constants,suggesting that the rate limiting step in viral hemagglutinin (HA)-mediated fusion,that is,rearrangement of viral glycoproteins at the contact points with the target membrane,is similar to that involved in fusion inactivation.(Supported by JNICT,Portugal and NATO Research Grant CRG 900333).

Tu-Pos317

HEMAGGLUTININ CONFORMATIONAL CHANGE IS RATE-LIMITING FOR PR/8 INFLUENZA-ERYTHROCYTE FUSION. ((C. C. Pak, M. Krumbiegel, and R. Blumenthal)) Section of Membrane Structure and Function, Laboratory of Mathematical Biology, NCI, NIH, Bethesda, MD 20892.

Fusion of influenza A virus with target membranes requires a low pH induced conformational change of the hemagglutinin (HA) fusion protein. The fusion kinetics with red blood cells (RBC) ghosts of two influenza A strains, A/Aichi/2/68 (X31) and A/PR/8/34 (PR/8) were compared and correlated with the kinetics of HA conformational change. Fusion of virus with RBC ghosts, monitored by the dequenching of octadecylrhodamine (R18), was pH dependent, although X31 fused more rapidly at sub-optimal pH. Fusion also exhibited a temperature dependence, with the rate and extent of fusion decreasing as the temperature was lowered. Unlike X31, PR/8 displayed no fusion at 4°C. Exposure of the fusion peptide and subsequent conformational change, as measured by liposome binding and proteinase K digestion, was non-existent at 4°C and slow at higher temperatures for PR/8, whereas changes in HA structure occurred rapidly prior to the onset of fusion for X31. The coincidence of fusion kinetics and HA conformational change rates suggested the latter was the rate-limiting step for PR/8 fusion. Inactivation of viral fusion and commitment to fusion (both HA conformation dependent processes) were limited in PR/8 but not affected in X31.

Tu-Pos318

INFLUENZA VIRUS MACROMOLECULAR REDISTRIBUTION OBSERVED BY VIDEO AND ELECTRON MICROSCOPY DURING LOW PH-INDUCED FUSION. ((R.J. Lowy, M.H. Whitnall, and R. Blumenthal)) AFRRI & NCI, Bethesda, MD 20889 (Spon. by D.R. Livengood)

Digitally enhanced video microscopy was used to observe the kinetics and distribution patterns of a lipid analogue, envelope proteins and RNA staining during low-pH induced influenza virus-human red blood cell (RBC) fusion. The results suggested that persistent virally derived structures might exist containing both envelope proteins and nucleocapsids subsequent to fusion junction/pore formation (J. Cell. Biochem. Suppl. 16c:131, 1992). Electron microscopic immunostaining of envelope protein distribution 30 min post pH 4.9 induced fusion confirmed light-level observations that envelope proteins were dispersed in the RBC membrane at 37° but restricted to patches at 16 °C. The patched proteins were in broad based RBC membrane evaginations several times larger than the unfused virus particles and without apparent nucleocapsids. Preliminary light-level microscopy immunochemical localization of matrix protein indicates its dispersal is extensive and more rapid than envelope protein redistribution and has a threshold similar to lipid redistribution between pH 6.0 and 5.6. The results are consistent with a rapid disassembly of the nucleocapsid below pH 6.0, allowing RNA and matrix protein dispersal, likely via a fusion pore, prior to complete disassembly of structures formed by the envelope proteins.

Tu-Pos319

FORMATION OF MULTIPLE SMALL PORES AND LIPID FLOW IN INFLUENZA HA-MEDIATED MEMBRANE FUSION. J. Zimmerberg, R. Blumenthal, D. Sarkar, M. Curran, & S.J. Morris. LTPB, NICHD & LMB, NCI, NIH, Bethesda, MD; Mol. Biol. & Bioch., UMKC, Kansas City, MO. HA is the best characterized fusion protein. Cells expressing HA fuse to red blood cells (rbc); fusion can be measured as membrane mixing (dequenching and redistribution of hydrophobic dye from the membrane of rbc to both cells), cytoplasmic mixing (dequenching and redistribution of aqueous dye from rbc to both cells), and by an increase in cell capacitance, which yields fusion pore conductance. We have measured pairs of these three parameters simultaneously, using different aqueous dyes. In each double-labelled rbc, membrane dye (DiI or R18) redistribution preceeded redistribution of any cytoplasmic dyes. The lag between lipid and cytoplasmic movement increased with increasing molecular weight of the aqueous dye for 6-carboxyfluorescein, BCECF, and Calcein. Lucifer yellow dextran (10,000 MW) did not move in 10 minutes even though membrane mixing was complete. Reversible fusion and fusion pore formation was detected prior to either membrane or cytoplasmic redistribution, with steps in conductance. We conclude that the steps in junctional conductance represent multiple small pores which impede the flux of lipid and aqueous dyes rather than a single pore widening is steps.

Tu-Pos320

A SIMPLE EXPRESSION FOR THE TIME-DEPENDENT LOCAL DENSITY OF LIPID FLUOROPHORES IN THE MEMBRANES OF A CELL-CELL FUSION COMPLEX. Robert J. Rubin and Yi-der Chen. Laboratory of Chemical Physics, NIDDK, NIH, Bethesda, MD 20892.

In a recent paper (Rubin and Chen, Biophys. J. 58, 1157-1167(1990)), the kinetics of redistribution of lipid markers between the membranes of two fused cells was studied by solving the diffusion equation for the compound system consisting of two coalesced spherical shells. Both the local density and the total number of lipid molecules on each cell were derived as a function of time after fusion. The analytic expressions for both quantities contain complicated hypergeometric functions. Recently, we have shown that the total number of lipid molecules on each cell membrane can be expressed accurately by a one-term exponential in time with a time constant that depends on the dimension of the fusion complex in a simple way. In this report we show that the local density of particles on each cell surface can also be expressed as a one-term exponential with a simple time constant. The difference between the exact and the approximate density functions is found to be small except in vicinity of the junction. The expression for local density derived here should be very useful for studying the local fluorescence change in a fusion system.

Tu-Pos321

DIRECT MEASUREMENT OF HERPES SIMPLEX VIRUS - CELL FUSION KINETICS

J.E. Fisher, D.R. Alford, T. Shangguan, M. Ponce de Leon *, R.J. Eisenberg *,#, GH Cohen * and J Bentz

Dept. of Bioscience and Biotechnology, Drexel University, 19104, *Dept. Microbiology and Center for Oral Health Research and #Dept. Pathobiology, University of Pennsylvania, Philadelphia, PA 19104

Herpes Simplex Viruses (HSV) enter cells by fusion of the viral envelope with the cell plasma membrane. Among the ten identified envelope glycoproteins, three have essential roles in infectivity: gB, gD and gH (and possibly gL). However, precise assignment of their functions in this multi - step process has been elusive. To determine which proteins are specifically involved in the membrane fusion step of viral entry, we have developed a direct assay. In this system HSV-1 envelopes were labeled with self-quenching concentrations of the fluorescence probe octadecylrhodamine. Labeled virus was incubated with mouse L-cells, in suspension, at 4° C to permit binding. After removal of unbound virus the cells were incubated at 37 ° C to monitor fusion. Increases in fluorescence, indicative of fusion - dependent relief of self - quenching were observed over 150 minutes. Over this time period 30 - 50% of bound virus had fused. These kinetics are similar to those derived from previous studies using electron microscopy or plaque assays. Fusion neutralization studies employing monoclonal antibodies against envelope glycoproteins gD and gH are underway.

Tu-Pos322

HIGH EXTRACELLULAR K^+ INHIBITS VESICULAR STOMATITIS VIRUS INFECTION OF BHK CELLS AT A STEP BETWEEN PRIMARY AND SECONDARY TRANSCRIPTION. M. Akeson, K. Rigaut, C. Sharp, and D.M. Neville, Jr. Laboratory of Molecular Biology, NIMH, Bethesda, MD. 20892.

In a previous report (Akeson et al.,1992) we showed that high extracellular K^+ inhibits production of infectious VSV by 100-fold in BHK and MDCK cells. This inhibition correlates with plasma membrane depolarization and is due, at least in part, to blockade of a very early step in infection. Recently, we tested if the K^+-sensitive step involves delivery of the viral nucleocapsid from the endosomal lumen to the cytosol as reported for Semliki Forest virus (Helenius et al.,1985). Two separate tests exclude this possibility for VSV. First, release of input VSV matrix protein into cytosol was unaffected by high K^+ administration. Because matrix protein release coincides with nucleocapsid translocation, we infer that nucleocapsid delivery is equal in control and high K^+-treated cells. Second, we measured the effect of high K^+ upon primary transcription of the VSV genome. This process is linearly dependent upon nucleocapsid content of the cytosol, therefore inhibition of translocation would result in a measurable reduction in the viral mRNA pool. However, ^{32}P-labelled probes against the VSV N protein mRNA revealed no significant difference between control and high K^+ treatments whereas 15 mM NH_4Cl resulted in a four-fold reduction in the N mRNA pool. Thus, no step in VSV infection prior to primary transcription (e.g. virus-endosome membrane fusion, nucleocapsid translocation, uncoating) appears to be altered by high K^+ application to BHK cells. In contrast, in the presence of high K^+, secondary transcription associated with newly synthesized nucleocapsids is significantly reduced and is correlated with reduced levels of newly synthesized viral G, M, and N proteins.We postulate, therefore, that the early K^+-dependent block of VSV infection involves failure to synthesize and assemble a stable pool of progeny nucleocapsids.

Tu-Pos323

MECHANISM OF INHIBITION OF CELL-CELL FUSION BETWEEN GP120/41 AND CD4 EXPRESSING CELLS BY CD4 BEARING PLASMA MEMBRANE VESICLES. ((A. Puri[1], C.C. Pak[1], D.S. Dimitrov[1], C.C. Broder[2] & R. Blumenthal[1])) [1]NCI, [2]NIAID, NIH, Bethesda, MD 20892. (spon. by H. A. Saroff)

Plasma membrane vesicles (PMV) prepared by hypotonic lysis of CD4 bearing HeLa cells were highly efficient as compared to soluble CD4 (sCD4) for inhibition of syncytia formation between gp120/41 and CD4 expressing cells and blocked infection of HIV to permissive cells. We further analysed the mechanism of inhibition of PMVs using a fluorescent chloramphenicol acetyltransferase (CAT) assay. We found that PMVs derived from human and monkey cells were 10-20 fold more effective in inhibition of cell-cell fusion as compared to sCD4. Preincubation of HeLa PMV (0.5 μg/ml CD4) with HL2/3 cells for 5 min at 37°C resulted in complete inhibition of fusion whereas complete inhibition by non-human PMVs required higher dose (1 μg/ml) and longer preincubation at 37°C (30 min). The inhibitory effect of PMVs from HeLa cells was irreversible while inhibition by non-human PMVs was reversible. Our results show that membrane anchored CD4 is 10-20 fold more effective in inhibiting fusion as compared to sCD4 which is due to multivalent binding. We also conclude that there are further steps involved for inhibition by human PMVs leading to irreversible effects.

Tu-Pos324

CALCIUM-TRIGGERED FUSION OF SEA URCHIN EGG CORTICAL GRANULES REQUIRES PROTEINS IN ONLY ONE MEMBRANE. ((S. S. Vogel, L. V. Chernomordik and J. Zimmerberg)) LTPB, NICHD, NIH, Bethesda MD 20892.

Models for calcium triggered exocytosis have been proposed requiring cytoplasmic proteins, or gap-junction like protein complexes. Fusion of sea urchin cortical granules does not require cytoplasmic proteins. While it is thought that proteins do mediate these fusion reactions, it is not known if they are required in both fusing membranes. Using light scattering assays and video microscopy we find that exocytotic granules, isolated from sea urchin eggs, do not fuse with other granules if pre-treated with either trypsin (n=24 trials) or N-ethylmaleimide (NEM; n=14) but do fuse when mixed with untreated granules (trypsin/wild type - 25 out of 26 trials; NEM/wild type - 32 out of 37 trials). Using fluorescent microscopy we find that granules can fuse with liposomes prepared from lipids extracted from sea urchin egg cortices (in 12 out of 20 trials), and with liposomes containing cholesterol and either DPPC (in 8 out of 8 trials) or PI (in 8 out of 9 trials). Granules did not fuse with liposomes containing only DPPC (n=5) or a mixture of PI & egg-PC (2:1; n=5). Granule-liposome fusion did not require added cytoplasmic proteins, was inhibited by NEM treatment (n=10), and was triggered with 59 μM calcium (in 16 out of 17 trials). Our data suggests that calcium triggered exocytosis, as does viral fusion, requires proteins which initially reside in only one of the two fusing membranes. Thus models for exocytosis requiring proteins originally residing in both membranes are not applicable to the calcium-triggered membrane fusion observed in sea urchin eggs.

Tu-Pos325

SECRETION AS WELL AS THE SUPPLY OF RELEASE-READY GRANULES IS CALCIUM DEPENDENT. ((L. v. Rüden and E. Neher)). Max Planck Institut für biophysikalische Chemie, Am Faßberg, D-3400 Göttingen, Germany.

In bovine adrenal chromaffin cells, two pools of secretory vesicles can be distinguished by combining patch-clamp capacitance measurements with Ca^{2+} monitoring using Fura-2. A small but readily releasable pool can be depleted by both a caffeine evoked Ca^{2+} transient and by a train of 5 depolarising pulses (100 to 200 ms from -60 to +10 mV at 1 second intervals). After 50 to 100 seconds of recovery, exocytosis can again be evoked by depolarising stimuli. Recovery is stronger, if calcium is elevated between stimuli by slight steady state depolarisation (see illustration below). This is taken as evidence for a calcium-dependent replenishment of a pool of readily releasable granules. This effect is more prominent in perforated patch recordings. In 7 cells, 23 out of 27 paired pulse trains showed responses augmented by 10 to 400 % in response to prior enhancement of cytosolic calcium.

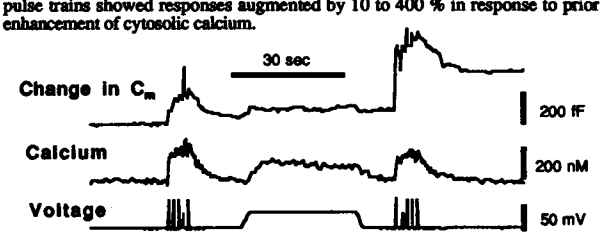

Tu-Pos326

FACTORS AFFECTING SINGLE-VESICLE AMPEROMMETRIC SIGNALS: A THEORETICAL STUDY. ((Chow, R.H. and Ch. Heinemann)) Max Planck Inst. für biophysikalische. Chemie, Am Faßberg, D-3400 Göttingen, Germany.

Recently carbon-fiber microelectrodes have been used for electrochemical detection of catecholamine release from single vesicles of adrenal chromaffin cells (Wightman et al, 1991, PNAS 88:10754-10758; Chow et al, 1992, Nature 356:60-63). Using Monte Carlo simulations incorporating realistic geometry, we have analysed some of the factors influencing the shape of the oxidation current transient: the diffusion constant D, the distance x from the release site to the detecting surface, and the time course of release. The main part of experimental traces were readily fit assuming instantaneous release of molecules from the cell surface, but required either that $x \geq 1$ μm (larger than expected) or that $D >> 5.5 \times 10^{-6}$ cm^2/s (D of freely diffusing catecholamine). This observation points to either 1) irregular carbon fiber sufaces or cell infoldings, 2) retarded diffusion, perhaps due to a slowly diffusing complex, or 3) non-instanteous release, perhaps reflecting the kinetics of dilation of the fusion pore or escape from a matrix. When D was adjusted to 3×10^{-7} cm^2/s to fit the main part of the data traces, the simulations still did not show the slow initial onset seen in many of the experimental traces. This slow "foot" signal was previously suggested to be due to the slow leak of molecules out of the narrow fusion pore that initially connects the vesicle lumen with the outside, and that later dilates to complete exocytosis. Simulations of altered time courses for release of molecules confirmed that details of the release time course are best appreciated near the detector, with the shape of the rising phase being most informative.

Tu-Pos327

WHAT HAPPENS TO A FUSION ZONE AFTER FUSION PORES ARE CREATED IN IT? ((Y.K Wu, R.A. Sjodin, K.Foster+, and A.E. Sowers)) Dept. Biophys. Univ. Maryland Sch Med, Baltimore, MD 21201, and +Dept. Bioengineering, Univ. Penn., Philadelphia, PA 19104.

We have shown by thin section electron microscopy (BJ 60:1026-1037) that in a contact zone induced between erythrocyte ghosts by dielectrophoresis, the use of an electrofusion protocol converts the contact zone into a fusion zone (FZ) containing from 1-225 fusion pores per μm^2. Also, after creation, both the i) FZ stability, and ii) the time-dependent diameter expansion rates of the fusion zone are strongly dependent on an intact spectrin network. Using computer-assisted analysis on video-recorded phase optics images of fusion zone diameters, we have found that the FZ diameter vs. time dynamics has two, or three, distinct phases (I-III) in erythrocyte ghosts with an intact or heat-disrupted (42 oC, 20 min), respectively, spectrin network. These phases, revealed by FZ diameter vs. time measurements under some combinations of various electric pulse parameters, temperatures (4-33 °C) during measurements, heat treatment temperatures (39-50 °C), and dielectrophoretic force (E_{ac} = 3.25, 4.25, & 5.25 V/mm), and under certain conditions, were remarkably *independent* from one another, yet the durations of Phase I (1.0-1.2 sec) and Phase II (4.0 sec) were remarkably *invariant* regardless of the variable studied. This suggested the existence of a complex but dissectable interplay of biomechanical factors (see also other abstract by Sowers, et al.). Supported by ONR and NSF.

Tu-Pos328

VOLTAGE-DEPENDENT SWELLING OF A SECRETORY GRANULE MATRIX. ((Chaya Nanavati and Julio M. Fernandez)) Dept. of Physiol. and Biophys., Mayo Clinic, Rochester, MN 55905.

Nature has designed the secretory granule matrix for the rapid delivery of biologically active peptides and transmitters. This matrix is a miniature biopolymer consisting of a polyanionic polymer network which traps peptides and transmitters when condensed, and releases them upon exocytotic decondensation. The physical mechanisms that trigger matrix swelling and secretory product release are, however, still unknown. Upon exocytotic fusion the secretory granule matrix is transiently subjected to strong electric fields. Therefore, we designed experiments to study the effects of an electric field on the polymer matrix from the mast cell secretory granule and discovered a host of novel, unexpected properties. The matrix responded to positive and negative voltages by condensing or swelling. These condensing and swelling cycles were reversible and could be repeated several hundred times. The swelling was accompanied by a large increase in conductance. Thus, electrically, the matrix resembled a diode with a conductance which was at least a hundredfold higher at negative potentials. This conductance was super-Ohmic, and up to six times greater than that predicted by simple electrodiffusion. In addition to passing a current, a swollen matrix exerted pressures on the order of a hundred pounds per square inch. All these responses took place within a few milliseconds of application of the electric field. We propose that this voltage-dependent swelling of the secretory granule matrix may play a role in the exocytotic release of secretory products.

Tu-Pos329

COMPARTMENTALIZATION OF ATP WITHIN CHOLINERGIC NERVE TERMINALS. ((Dixon J. Woodbury and Marie Kelly)) Department of Physiology, Wayne State University School of Medicine, Detroit, MI 48201.

Within nerve terminals of the electric organ of *Torpedo*, acetylcholine (ACh) is distributed between at least two compartments. About 60% is "bound", i.e., trapped within sub-cellular organelles such as synaptic vesicles, and 40% is "free." The free ACh is generally believed to be cytosolic ACh. Solsona et al. have shown that the distribution of ATP within nerve terminals is similar to that of ACh [Solsona, Salto, and Ymbern, 1991, *BBA* **1095**:57-62]. In synaptosomes, the bound population is distinguished from free because it is not released into solution following a freeze and thaw (F/T) cycle. The F/T cycle fractures cell membranes but, synaptic vesicles (SVs) are thought to be too small for rupture. Nevertheless, free ATP and ACh represent cytosolic amounts only if SVs do not release ATP or ACh during the freeze/thaw cycle.

We have found that synaptic vesicles, isolated from electric organ of *Torpedo*, release significant amounts of ATP (and presumably ACh) following F/T. In solutions low in Ca^{++} and high in sucrose about 15% of the ATP is released following each initial F/T cycle, but about 50% of the total trapped ATP is not released even after 8 F/T cycles. When SVs are re-suspended in *torpedo* ringer, about 30% of the trapped ATP is released after each F/T cycle, with less than 15% remaining after 8 F/T cycles. Based on these data, previous estimates of cytosolic ATP and ACh should be decreased from about half of the total pool to less than a fourth.

INTERCELLULAR COMMUNICATION

Tu-Pos330

NOVEL EFFECTS OF DEUTERIUM OXIDE ON NITRIC-OXIDE RELATED VASODILATION AND $[CA]^{2+}$ IN VASCULAR ENDOTHELIAL CELLS. ((R. Wang, L. Oster, J. de Champlain and R. Sauvé)) GRSNA and GRTM, Département de Physiologie, Université de Montréal, Montréal, Québec, Canada H3C 3J7. (Spon. by G. Roy)

Intake of deuterium oxide (D_2O) in drinking water has been reported to prevent or attenuate the development of hypertension in spontaneously hypertensive rats. The possibility that D_2O might alter $[Ca^{2+}]_i$ in vascular endothelial cells, which in turn could modulate the release of nitric oxide (NO), was investigated in the present study. It was observed that D_2O relaxed pre-contracted rat mesenteric arterial beds in an endothelium-dependent manner. This effect of D_2O could be inhibited by a NO synthase inhibitor, L-NAME. In cultured bovine aortic endothelial cells, D_2O induced a biphasic increase in $[Ca^{2+}]_i$ with a characteristic initial transient increase followed by various patterns of sustained $[Ca^{2+}]_i$ increase. The sustained phase was entirely dependent on the extracellular calcium entry. These data demonstrated a direct effect of D_2O on $[Ca^{2+}]_i$ in vascular endothelial cells, which may be responsible for the endothelium-dependent, presumably NO mediated, vasodilatation induced by D_2O in precontracted vessels. A putative use of D_2O as a novel tool for the functional study of the endothelium-dependent regulation of the vascular tone can be envisioned since the D_2O effect would be independent of receptor binding mechanisms at the cell membrane level.

Tu-Pos331

CAGED NITRIC OXIDE (NO): RUTHENIUM NITROSYL TRICHLORIDE AS A PHOTOSENSITIVE PRECURSOR OF NO AND ITS BIOLOGICAL APPLICATIONS.

Nadir Bettache, John E. T. Corrie, Tom Carter, John Williams, David Ogden, Tim V. P. Bliss and David R. Trentham. ***National Institute for Medical Research, Mill Hill, London, NW7 1AA, U.K.***

Ruthenium nitrosyl trichloride ($Ru[NO]Cl_3$) is a photosensitive precursor of nitric oxide (NO), an important mediator in several physiological processes. Hemoglobin (Hb[Fe(II)]) was used to monitor spectrophotometrically the release of NO from $Ru[NO]Cl_3$ after illumination at pH 7 and 21°C. As shown in the figure, repetitive exposure of 'caged NO' to light (λ=300-350 nm) converted deoxy Hb to nitrosyl Hb. Following a laser pulse, NO bound to deoxy Hb within 5 ms. The NO product quantum yield was estimated to be 0.012 at 320 nm. Photorelease of 10-25 nM NO from 5-10 μM caged NO induced half-maximal relaxation of rabbit aorta. The rat hippocampal slice was also used to study the effect of NO. Photorelease of NO from 100 μM $Ru[NO]Cl_3$ produced a depression of NMDA receptor-mediated synaptic responses but did not induce long-term potentiation.